UNIVERSITY OF CALIFORNIA
SANTA CRUZ

A TOP PREDATOR IN HOT WATER: EFFECTS OF A MARINE HEATWAVE ON FORAGING AND REPRODUCTION IN THE NORTHERN ELEPHANT SEAL

A dissertation submitted in partial satisfaction
of the requirements for the degree of

DOCTOR OF PHILOSOPHY

in

ECOLOGY AND EVOLUTIONARY BIOLOGY

By

Rachel R. Holser

December 2020

The Dissertation of Rachel R. Holser is approved:

_____
Professor Daniel P. Costa, Chair

_____
Professor Suzanne Alonzo

_____
Professor Chris Edwards

_____
Professor Birgitte McDonald

_____
Quentin Williams
Acting Vice Provost and Dean of Graduate Studies

Table of Contents

List of Tables

List of Figures

Abstract

A Top Predator in Hot Water: Effects of a Marine Heatwave on Foraging and Reproduction in the Northern Elephant Seal

By

Rachel R. Holser

All organisms face resource limitations that will ultimately restrict population growth, but the controlling mechanisms vary across ecosystems, taxa, and reproductive strategies. As climate change continues to alter ecosystem processes across the globe, organisms are confronted with new challenges to their ability to survive. Marine heatwaves are prolonged warm water events that are increasing in frequency and magnitude due to rising global temperatures. The Northeast Pacific Blob was a multi-year marine heatwave that affected ecosystems across the Northeast Pacific, from producers to top predators. The northern elephant seal (*Mirounga angustirostris*) is a top predator that forages on the abundant biomass of the mesopelagic Northeast Pacific Ocean. Northern elephant seals are both generalist predators and capital breeders, which may buffer the effect of environmental changes on their population.

The goal of my research was to quantify the subsurface extent of the Blob and assess its effect on the foraging and reproductive success of adult female northern elephant seals. I used a combination of telemetry data collected by instrumented elephant seals (temperature, salinity, location, depth), body composition and energy gain metrics, and pup weaning mass to examine the population-level effects of the Blob. I found that there were significant warm anomalies throughout the top 1000m of the water column

during the Blob, and that northward advection of warm, salty water at the base of the pycnocline likely played an important role in the sustained accumulation of warm water. Comparing foraging behavior during 2014 and 2015 to our 15-year tracking time series, I found evidence of a plastic behavioral response. Females increased their use of the Alaska Gyre, increased their daytime foraging effort, and increase their use of deep water (>800m depth) during the summer months, all suggesting that the prey field changed relative to previous years. Using a four-decade weaning mass time-series, we observed density-dependent effects on both weaning mass and male offspring-biased allocation of resources. Furthermore, maternal age was more important than oceanographic conditions or maternal mass in determining offspring weaning mass. While elephant seals did show reduced reproductive output during the Blob, they did not experience the mass mortality or reproductive failures that were seen in other species in the region, suggesting that they are more resilient to environmental change.

Acknowledgements

The studies completed in this dissertation were made possible by a long-term data set collected under the supervision of Daniel Costa, and before that Burney Le Boeuf, at UCSC. I would like to thank my committee members and coauthors for their support and advice in completing these chapters, as well as all of those who have contributed to this dataset. The data were collected by hundreds of graduate and undergraduate students over the last forty years, and the effort has been financially supported by numerous funding agencies, including the Office of Naval Research, and the Sloan, Packard, and Moore Foundations. The ongoing partnership between Año Nuevo State Park, the Año Nuevo UC Reserve, the Costa Lab, and other research groups has generated an enormous volume of scientific work, in addition to outstanding public education and outreach.

A graduate thesis represents the culmination of an incredible amount of effort, time, and thought (which is to say, blood, sweat, and tears) on the part of the student. That student's path is always influenced by a small army of people in their lives: coworkers, mentors, friends, and family (these subsets are often not mutually exclusive). The support and help we receive may come in the form of instruction in techniques, advise on how to write a paper, a sympathetic ear when one wants to throw one's computer through a window, or cookies at the end of a long day in the field. I am incredibly grateful for all of the opportunities, encouragement, laughter, constructive criticism, good food, shenanigans, and hugs that have sustained me over the last 6.25 years.

First, to my adviser, Daniel Costa, thank you for trusting me with so much responsibility and giving me the freedom and opportunity to explore and grow as a scientist. I did not realize that I was coming to UCSC to become a professional seal poker, but that seems to be what has happened, and I love every minute of it. Even the worst day in the field is one I am grateful for (maybe not immediately, but once I'm warm, dry, have gotten all the sand out of my teeth, and am munching on a Whale City croissant). You expend an inordinate amount of time and effort on the endless task of finding financial support to keep this work going, and I am most grateful for that.

Our lab in many ways resembles an extensive but strangely inbred family, with all of the associated quirks, benefits, and difficulties. I am grateful for every member of the lab with whom I have had the privilege of interacting: they are all extraordinary people in their own way, and each of them has influenced my experience and helped me grow as a scientist and as a person. Patrick Robinson, you did your best to teach me how to be a seal Jedi, and I continue to be amazed by your ability to read, move, and handle the animals with such intuition and care. Dan Crocker and Gitte McDonald, you have each been both friends and mentors, and I value all the time that you've each given me. I have done my best to absorb and pass on all of the information you've each given to me - physiological mechanisms, field techniques, data processing, lab stories and history, mistakes and the corresponding lessons, and how to cope in a constantly demanding and difficult field – the list seems endless, and I am so glad that we're all in this next endeavor together.

Sarah and Mike Peterson, Liz McHuron, Kim Goetz, Chandra Goetsch, Mel Conners, Sarah Kienle, Stella Villegas, Jen Maresh – you all welcomed me with open arms and taught me The Ways of the Costa Lab, field work, and marine mammal science. Luis

Hückstädt, while your arms were slightly less open in welcoming me (I didn't realize cheerfully saying "Hi! How was your ride?" to someone entering a room with a bike was a cause for suspicion, confusion, and sass), I cannot imagine what the last 6 years would have been like without you, you are an amazing scientist and a kind and selfless person. I am sure that you will deny it for the rest of our lives, but you are one of my best friends and you've taught me more than I can say. And fired me more times than any of us can count. And I really didn't drop you on purpose. And I am NOT "full of lies." Also, it is your fault that Caitie and I became friends, so you have no one but yourself for the result. Caitlin, my precious feline baby-dragon, what would I do without you? Your friendship, laughter, sass, and co-commiserating about all things science are a constant, **irreplaceable** joy. Thank you for your faith in me and for being my touchstone with reality when I am unsure if my reactions or handling of a situation/people are normal.

Theresa Keates, Ana Valenzuela, Logan Pallin, Jessie Kendall-Bar, and Arina Favilla, as the elephant seal "younglings" who entered the lab 2-3 years after I began, you have all been a treasured part of my experience. While I have done my best to teach you about our work and study system, you have all also taught me about science, about mentoring, and about life. More than that, you have shared in many of the trials and tribulations that is elephant seal fieldwork. That shared laughter is what makes the hardest days manageable, whether it is an adrenaline-fueled I-can't-believe-that-just-happened-and-we-all-survived laughter (Type II Fun) or a Logan-screamed-because-there-are-quail laughter (Type I Fun for us, Type II Fun for Logan). Theresa, you are like a little sister to me, and the time we have spent together working, baking, and talking has been precious. Ana, your enthusiasm for dead things is delightful and infectious, thank you for opening my eyes to new concepts and areas of study. Logan, your immaculate

organization and generally ridiculous ways help me maintain my sanity. I still have hopes for our traveling research van/bakery. Jessie and Arina, you are both talented, brilliant, and have learned so much in the last few years. It is a privilege to watch you both grow.

Similarly, there have been quite a crew of volunteers (undergraduates and grad students from other institutions) who have spent countless hours out at the colony with me, and their help and company always made the days brighter. James Bachellier, Adam Taylor, Lora Johansen, Trevor Barclay, Heather Barrett, Jenni Johnson, Mason Cole, Shawn Hannah, Amanda Hooper, Cameron Cooper, Jamie Grover, Lauren Cooley: thank you all for your time, your patience, your energy, and your enthusiasm. I hope you all enjoyed our time together half as much as I did.

The importance of friends and family who have listened with bewildered amusement to endless stories about difficult seals or problematic data cannot be understated. Eric Phillips, Jason Snyder, Kristina Koenig, Kit, Vic, Garrett Fielding, Antonio Romero: you have all been patient and understanding when I have been busy, and encouraging and supportive when I have felt frustrated and tired. Thank you all for what you have given me for the years (and in some cases decades) we have known each other. I hope I am able to repay your kindness and affection. Joe Ritter, you have been my friend and mentor for almost twenty years now (hard to believe). Thank you for... just everything. There is a piece of wisdom regarding graduate school that was passed to you, you passed to me, and I have passed on to as many as will listen: earning a Ph.D. makes one better than exactly one other person – who they were when they started. Luke Keehan, thank you for laughing with me and at me, as appropriate. Thank you for challenging me, for reading and editing introductions, conclusions, abstracts, whatever I

sent your way. Thank you for your affection and encouragement, it means the world to me.

My family has always been a rock, a strong foundation - they have lovingly encouraged and supported my path towards biology since I was a child running around on the Oregon coast. Auntie Karin helped me get my first opportunities to work in the field with pinnipeds and other marine vertebrates up on the Pribilof Islands in Alaska, giving me early fieldwork experience and opening doors to other opportunities. Her selflessness, strength, and determination have touched the lives of the many researchers with whom she has crossed paths, including me. Brother has been teasing me, in the way older brothers do, about earning my doctorate studying blubber since we visited the Alaska Sea Life Center in 2003...turns out he was more right than not. He has always believed in my capability and has encouraged me with a healthy mixture of mockery and affection my whole life. If I am struggling or confused, I know that I can turn to him for insight, honesty, and reassurance. Finally, my parents have been unwavering in their practical and emotional support since the beginning. Their commitment to my education from day one, and the sacrifices they made to support me growing up, are a significant part of the reason I entered graduate school to begin with. They are my first phone call when something is wrong (or right). Their love, patience, and wisdom are an example and inspiration to me and to everyone whose lives they touch. I cannot express the depth of my gratitude for what they have given and continue to give to me.

Thank you all,

Rachel Rose

Dedication

To Erica

Forever my partner in crime. We always intended to do this together, and you are still with me, reminding me what it means to be strong, to be kind, and to be selfless, whatever we might face.

Introduction

Broad Context

The planet is facing rapid warming because of anthropogenic greenhouse gas emissions. The consequences of climate change are predicted to be dramatic and far-reaching and include an increase in the frequency and severity of extreme climate events (ECEs) such as heatwaves, droughts, wildfires, and extreme precipitation [1-3]. These events can result in ecosystem-level restructuring due to changes in the distribution and composition of species. ECEs can have direct impacts on life-history traits (e.g. mortality caused by heat stress), but they can also affect vital rates through ecological processes, with fitness consequences resulting from changes in trophic dynamics [4-6]. Understanding how populations will respond to this type of disruption to their environment is a significant challenge facing both scientists and natural resource managers, but is crucial for predicting future ecosystem structure [2, 7, 8].

A marine heatwave (MHW) is a type of ECE defined as a "prolonged discrete anomalously warm water event" [9]. Like other ECEs, the frequency and intensity of MHWs has been increasing over the last century [10] and are predicted to continue to increase as a result of global warming [11-13]. Extreme events are rare by nature, giving the scientific community limited opportunity to understand the physical processes involved or assess the ecological consequences [14]. Currently, we lack knowledge of the subsurface structure of MHWs and how it contributes to their development, as subsurface observations are both sparse and more temporally restricted than surface records [15, 16]. Without sufficient subsurface characterization, our ability to predict MHWs or fully assess ecosystem effects is limited [9, 16].

The occurrence of several significant MHWs in the last decade has provoked investigation into the biological response to these extreme events [10, 14-18]. Changes in distribution, phenology, and foraging behavior are all expected responses to ongoing warming [19, 20], but the sudden and extreme nature of MHWs has the potential to cause more dramatic effects [14, 18]. Studies to date show that MHWs significantly alter biological systems due to both extrinsic physical forcing (e.g., altered circulation, reduced mixing, etc.) and intrinsic physiological limitations (e.g., increased metabolic rate in ectotherms), and generally the results are ecologically and economically detrimental [14, 16, 18, 21, 22]. The magnitude of the effect on a particular system (or organism) is dependent on the characteristics of the heatwave (duration, intensity) and the ability of the system (or organism) to tolerate or adjust to the extreme conditions [7, 17]. For example, populations on the warm edge of their range are particularly vulnerable to MHWs, but taxa that are highly mobile are more likely to be able to adjust to new conditions [17, 22]. Furthermore, while some species are likely to suffer due to MHWs and warming in general, other species are predicted to benefit [20, 22]. Forecasting the ecological consequences of MWHs requires a better understanding of the physical dynamics and the potential response of taxa at all trophic levels.

The Northeast Pacific Ocean (NEP) is a dynamic and biologically productive system that has recently experienced a severe MHW. The region is typically characterized by cool, nutrient-rich water that fuels high levels of productivity while physical features (fronts, eddies, etc.) create concentrated regions of foraging habitat with sufficient biomass to sustain large, complex populations of apex predators [23, 24]. The Transition Zone Chlorophyll Front (TZCF), located between the subarctic and subtropical gyres in the

central North Pacific, is of particular ecological relevance, providing reliable foraging habitat for large predators, including seabirds, pinnipeds, turtles, and predatory fish [25, 26]. These dynamic oceanographic features are subject to fluctuations caused in part by ocean-climate oscillations such as the El Niño-Southern Oscillation (ENSO), Pacific Decadal Oscillation (PDO), and North Pacific Gyre Oscillation (NPGO) [27, 28], which, in addition to MHWs, can impact the biological community and have consequences for the foraging success of top predators [29, 30].

The Northeast Pacific Blob 2015 (the Blob) was the largest MHW on record and was categorized as "severe" and a "once-in-a-century" event based on a combination of magnitude, extent, and duration of the anomalies observed [15, 31, 32]. Anomalously warm sea surface temperatures (SST) developed in the NEP, during the winter of 2013/2014 as a result of unusual winds and high sea level pressure anomalies that suppressed heat loss from the surface ocean and weakened cold-water advection [33, 34]. Surface temperature anomalies persisted through winter 2015/2016 and sub-surface anomalies lasted into 2017 [32]. This multi-year warm event appears to have resulted in part from coupling between the NPGO and PDO, the two dominant modes of variability in winter SST in the NEP [12]. The 2014-2015 warming may also have influenced the development of the 2015/2016 El Niño [35, 36]. Model forecasts indicate that multi-year warm anomalies are consistent with climate change projections for the NEP and that these events will become larger in scale (+ 18%) and warmer (+ 0.3-0.5°C) [12].

These projections are alarming because warming associated with the Blob had extensive ecological consequences in both the Gulf of Alaska (GOA) and California Current System (CCS), spanning all trophic levels [22]. Reduced water column mixing resulted in overall

suppressed productivity [37, 38]. In the Northern California Current, the expression of upwelling in 2014-2016 was weak despite unusually strong upwelling-favorable winds [39]. Altered plankton assemblages were seen throughout the NEP, generally favoring smaller, warmer-water species [39-42]. Low biomass and smaller prey species can reduce the efficiency of energy transfer to higher trophic levels, causing reductions in body condition, reproductive success, and survival in predator species [43-50]. Furthermore, shifts in species distribution were seen throughout the region and at all trophic levels [33, 51, 52].

Warm water conditions also supported massive harmful algal blooms resulting in domoic acid buildup in shellfish along the west coast of North America [53-56]. These algal blooms caused the closure of several fisheries, resulting in substantial economic losses in those communities [57]. Experiments indicate that *Psuedo-nitzschia spp*., the group responsible for these blooms, become both more competitively successful and more toxic at higher water temperatures. This suggests that continued warming and/or a higher frequency of marine heatwaves like the Blob will may also result in an increasing prevalence of harmful algal blooms and the resulting domoic acid poisoning that can devastate both fisheries and wildlife [54].

Understanding the response of predators to disturbance provides insight into both species-level and ecosystem-level changes. Predators integrate lower trophic levels; disturbances that impact primary producers or low-level consumers can cause dietary shifts, habitat use changes, reductions in reproductive success, or even reduced survival in predator populations [58-60]. These types of effects have been documented in some pinniped species [30, 61-65], but we are just beginning to understand how different

populations respond. Simultaneously, reductions of top predator populations can have cascading effects down the trophic web, causing shifts in lower trophic levels and loss of diversity within ecosystems [66, 67]. Continuing to advance our understanding of the functional roles these predators play within ecosystems and how they respond to environmental disturbances will illuminate current ecosystem dynamics and how those dynamics may change with ongoing anthropogenic forcing.

Study System

Elephant seals (*Mirounga sp.*) are generalist mesopelagic predators and are the largest, deepest diving pinnipeds [68, 69]. They are also highly polygynous, sexually dimorphic capital breeders [70]. This combination of behavioral and life history traits makes them excellent study organisms for understanding the connections between three-dimensional, subsurface environmental variability (e.g., MHWs), behavior, and reproductive success [30, 62, 71-77]. The northern elephant seal (*M. angustirostris*; NES) has breeding colonies ranging from Baja California, Mexico to British Columbia, Canada, and their foraging range extends throughout the NEP. The colony at Año Nuevo State Park, CA, has been studied continuously for nearly 60 years, providing a wealth of information on the behavior, physiology, and ecology of this species both on shore and at sea [62, 78, 79]. This dissertation work will focus exclusively on adult female NES due to the long-term data available for that demographic group and their importance to sustaining a healthy population.

NES spend up to ten months of the year foraging, building up the necessary body stores to sustain themselves during the time spent on shore to breed and molt [73, 79]. Each of these life-history events require extended fasting after which animals return to sea to

recover body condition and prepare for the next phase of their annual cycle. An adult female typically fasts for 5 weeks during the breeding season, losing up to 45% of her body mass [80, 81]. She will then spend 2-3 months at sea recovering body condition in preparation for the 6-week molting fast. NES exhibit embryonic diapause and do not implant their fertilized egg until sometime during the molt, assuming their physiological state (i.e. body condition, allostatic load) will support pregnancy. Gestation occurs during the 7-8 month trip to sea following the molt. Simultaneously, the female must acquire sufficient body reserves to sustain herself and nurse her pup during the following breeding season. Weaning mass of pups is an important factor for survival and largely depends on the energy stores a female has available to mobilize into milk [81, 82]. Therefore, her ability to produce successful offspring hinges on her foraging success during the post-breeding and post-molt foraging trips.

Adult female NES generally exhibit a continuous, deep-diving pattern while foraging at sea, typically spending 20-30 minutes at depth with 2 minute post-dive recovery intervals and foraging between 400-700 m (although they regularly dive to over 1000 m depth) [79, 83, 84]. Most individuals also exhibit diel diving behavior, with deep daytime dives and shallow nighttime dives that follow the daily vertical migration of prey species in the deep scattering layer [68, 79]. Despite this consistent diving behavior, adult female NES do exhibit multiple foraging strategies, the clearest of which is the use of coastal rather than pelagic habitat by ~15% of the population [79]. Quantitative fatty acid analysis and video recordings show that the adult female NES diet is composed primarily of mesopelagic fishes (67.3%), with squid species making up the remainder of the diet [85,

86]. They have a generalist diet at both species and individual levels, although a few individuals show some dietary specialization [68].

Northern elephant seals have exhibited remarkable resilience, as demonstrated by their rapid recovery from near extinction due to hunting in the early 1900's [87], and may be better suited to coping with the effects of climate change than other top predators. Both their life history and foraging strategy provide buffers to acute environmental changes by allowing for a plastic behavioral response. Capital breeding allows individuals to gradually accrue resources over large temporal and spatial scales rather than requiring rich, local food resources that income breeding species depend on [88, 89]. This life history strategy may have evolved to reduce sensitivity to environmental variability [88, 90, 91]. Similarly, the combination of an expansive foraging habitat and generalist diet provide more potential for adaptive behavior in the face of environmental disruption in their foraging habitat [19, 20]. Changes in elephant seal behaviour may serve as an early indicator of changes in the mesopelagic that impact other, more vulnerable species.

Dissertation Summary

In my dissertation I examine the development of a marine heatwave and how it affected the behavior and reproductive success of a top marine predator, the northern elephant seal. My first chapter leverages oceanographic data collected by northern elephant seals from 2014-2017 to examine the distribution, magnitude, and evolution of the Northeast Pacific Blob 2015, with a focus on subsurface structure and dynamics. In the second chapter, I use long-term (2004-2019) tracking, diving, and body condition data sets to evaluate the foraging behavior and success of the population during the peak of this marine heatwave. Finally, my third chapter examines the relationship between weaning

mass, ocean conditions, maternal traits, and population density across multiple decades (1984-2018). This work helps to fill identified knowledge gaps in our understanding of marine heatwaves, the behavioral response of organisms to these extreme climate events, and the population-level consequences of a significant ecological disturbance.

References

1. Jentsch A. 2007 A new generation of climate-change experiments: events, not trends. *Frontiers in Ecology and the Environment* **5**(7), 365-374.

2. Ummenhofer C.C., Meehl G.A. 2017 Extreme weather and climate events with ecological relevance: a review. *Philosophical transactions of the Royal Society of London Series B, Biological sciences* **372**(1723). (doi:10.1098/rstb.2016.0135).

3. Diffenbaugh N.S., Singh D., Mankin J.S., Horton D.E., Swain D.L., Touma D., Charland A., Liu Y., Haugen M., Tsiang M., et al. 2017 Quantifying the influence of global warming on unprecedented extreme climate events. *Proceedings of the National Academy of Sciences of the United States of America* **114**(19), 4881-4886. (doi:10.1073/pnas.1618082114).

4. Lea M.A., Johnson D., Ream R., Sterling J.T., Melin S., Gelatt T. 2009 Extreme weather events influence dispersal of naive northern fur seals.

5. Jenouvrier S., Peron C., Weimerskirch H. 2015 Extreme climate events and individual heterogeneity shape life-history traits and population dynamics. *Ecological Monographs* **85**(4), 605-624. (doi:10.1890/14-1834.1).

6. Harris R.M.B., Beaumont L.J., Vance T.R., Tozer C.R., Remenyi T.A., Perkins-Kirkpatrick S.E., Mitchell P.J., Nicotra A.B., McGregor S., Andrew N.R., et al. 2018 Biological responses to the press and pulse of climate trends and extreme events. *Nature Climate Change* **8**(7), 579-587. (doi:10.1038/s41558-018-0187-9).

7. Wernberg T., Smale D.A., Tuya F., Thomsen M.S., Langlois T.J., de Bettignies T., Bennett S., Rousseaux C.S. 2013 An extreme climatic event alters marine ecosystem structure in a global biodiversity hotspot. *Nature Climate Change* **3**(1), 78-82. (doi:10.1038/Nclimate1627).

8. Harris R.M.B., Loeffler F., Rumm A., Fischer C., Horchler P., Scholz M., Foeckler F., Henle K. 2020 Biological responses to extreme weather events are detectable but difficult to formally attribute to anthropogenic climate change. *Sci Rep* **10**(1), 14067. (doi:10.1038/s41598-020-70901-6).

9. Hobday A.J., Alexander L.V., Perkins S.E., Smale D.A., Straub S.C., Oliver E.C.J., Benthuysen J.A., Burrows M.T., Donat M.G., Feng M., et al. 2016 A hierarchical approach to defining marine heatwaves. *Progress in Oceanography* **141**, 227-238. (doi:10.1016/j.pocean.2015.12.014).

10. Oliver E.C.J., Donat M.G., Burrows M.T., Moore P.J., Smale D.A., Alexander L.V., Benthuysen J.A., Feng M., Sen Gupta A., Hobday A.J., et al. 2018 Longer and more frequent marine heatwaves over the past century. *Nature communications* **9**(1), 1324. (doi:10.1038/s41467-018-03732-9).

11. Oliver E.C.J. 2019 Mean warming not variability drives marine heatwave trends. *Climate Dynamics*. (doi:10.1007/s00382-019-04707-2).

12. Joh Y., Di Lorenzo E. 2017 Increasing Coupling Between NPGO and PDO Leads to Prolonged Marine Heatwaves in the Northeast Pacific. *Geophysical Research Letters*.

13. Frolicher T.L., Fischer E.M., Gruber N. 2018 Marine heatwaves under global warming. *Nature* **560**(7718), 360-364. (doi:10.1038/s41586-018-0383-9).

14. Frolicher T.L., Laufkotter C. 2018 Emerging risks from marine heat waves. *Nature communications* **9**(1), 650. (doi:10.1038/s41467-018-03163-6).

15. Holbrook N.J., Scannell H.A., Sen Gupta A., Benthuysen J.A., Feng M., Oliver E.C.J., Alexander L.V., Burrows M.T., Donat M.G., Hobday A.J., et al. 2019 A global assessment of marine heatwaves and their drivers. *Nature communications* **10**(1), 2624. (doi:10.1038/s41467-019-10206-z).

16. Holbrook N.J., Sen Gupta A., Oliver E.C.J., Hobday A.J., Benthuysen J.A., Scannell H.A., Smale D.A., Wernberg T. 2020 Keeping pace with marine heatwaves. *Nature Reviews Earth & Environment*. (doi:10.1038/s43017-020-0068-4).

17. Smale D.A., Wernberg T., Oliver E.C.J., Thomsen M., Harvey B.P., Straub S.C., Burrows M.T., Alexander L.V., Benthuysen J.A., Donat M.G., et al. 2019 Marine heatwaves threaten global biodiversity and the provision of ecosystem services. *Nature Climate Change* **9**(4), 306-312. (doi:10.1038/s41558-019-0412-1).

18. Jacox M.G., Alexander M.A., Bograd S.J., Scott J.D. 2020 Thermal displacement by marine heatwaves. *Nature* **584**(7819), 82-86. (doi:10.1038/s41586-020-2534-z).

19. Evans M.R., Moustakas A. 2018 Plasticity in foraging behaviour as a possible response to climate change. *Ecological Informatics* **47**, 61-66. (doi:10.1016/j.ecoinf.2017.08.001).

20. Hazen E.L., Jorgensen S., Rykaczewski R.R., Bograd S.J., Foley D.G., Jonsen I.D., Shaffer S.A., Dunne J.P., Costa D.P., Crowder L.B., et al. 2012 Predicted habitat shifts of Pacific top predators in a changing climate. *Nature Climate Change* **3**(3), 234-238. (doi:10.1038/nclimate1686).

21. Jacox M.G. 2019 Marine heatwaves in a changing climate. *Nature* **571**(7766), 485-487. (doi:10.1038/d41586-019-02196-1).

22. Cavole L., Demko A., Diner R., Giddings A., Koester I., Pagniello C., Paulsen M.-L., Ramirez-Valdez A., Schwenck S., Yen N., et al. 2016 Biological Impacts of the 2013–2015 Warm-Water Anomaly in the Northeast Pacific: Winners, Losers, and the Future. *Oceanography* **29**(2). (doi:10.5670/oceanog.2016.32).

23. Palacios D.M., Bograd S.J., Foley D.G., Schwing F.B. 2006 Oceanographic characteristics of biological hot spots in the North Pacific: a remote sensing

perspective. *Deep Sea Research Part II: Topical Studies in Oceanography* **53**(3), 250-269.

24. Whitney F.A., Crawford W.R., Harrison P.J. 2005 Physical processes that enhance nutrient transport and primary productivity in the coastal and open ocean of the subarctic NE Pacific. *Deep Sea Research Part II: Topical Studies in Oceanography* **52**(5–6), 681-706. (doi:http://dx.doi.org/10.1016/j.dsr2.2004.12.023).

25. Block B.A., Jonsen I.D., Jorgensen S.J., Winship A.J., Shaffer S.A., Bograd S.J., Hazen E.L., Foley D.G., Breed G.A., Harrison A.L., et al. 2011 Tracking apex marine predator movements in a dynamic ocean. *Nature* **475**(7354), 86-90. (doi:http://www.nature.com/nature/journal/v475/n7354/abs/nature10082-f1.2.html#supplementary-information).

26. Polovina J.J., Howell E., Kobayashi D.R., Seki M.P. 2001 The transition zone chlorophyll front, a dynamic global feature defining migration and forage habitat for marine resources. *Progress in Oceanography* **49**(1), 469-483.

27. Etnoyer P., Canny D., Mate B., Morgan L. 2004 Persistent pelagic habitats in the Baja California to Bering Sea (B2B) ecoregion. *OCEANOGRAPHY-WASHINGTON DC-OCEANOGRAPHY SOCIETY-* **17**(1), 90-101.

28. Polovina J.J., Howell E.A., Kobayashi D.R., Seki M.P. 2015 The Transition Zone Chlorophyll Front updated: Advances from a decade of research. *Progress in Oceanography*. (doi:10.1016/j.pocean.2015.01.006).

29. Costa D., Antonelis G., DeLong R. 1991 Effects of El Niño on the foraging energetics of the California sea lion. In *Pinnipeds and El Nino* (pp. 156-165, Springer.

30. Crocker D.E., Costa D.P., Le Boeuf B.J., Webb P.M., Houser D.S. 2006 Impact of El Niño on the foraging behavior of female northern elephant seals. *Marine Ecology-Progress Series* **309**.

31. Hobday A., Oliver E., Sen Gupta A., Benthuysen J., Burrows M., Donat M., Holbrook N., Moore P., Thomsen M., Wernberg T., et al. 2018 Categorizing and Naming Marine Heatwaves. *Oceanography* **31**(2). (doi:10.5670/oceanog.2018.205).

32. Freeland H., Ross T. 2019 'The Blob' - or, how unusual were ocean temperatures in the Northeast Pacific during 2014-2018? *Deep Sea Research Part I: Oceanographic Research Papers* **150**. (doi:10.1016/j.dsr.2019.06.007).

33. Bond N.A., Cronin M.F., Freeland H., Mantua N. 2015 Causes and impacts of the 2014 warm anomaly in the NE Pacific. *Geophysical Research Letters* **42**(9), 3414-3420. (doi:10.1002/2015gl063306).

34. Whitney F.A. 2015 Anomalous winter winds decrease 2014 transition zone productivity in the NE Pacific. *Geophysical Research Letters* **42**(2), 428-431. (doi:10.1002/2014GL062634).

35. Di Lorenzo E., Mantua N. 2016 Multi-year persistence of the 2014/15 North Pacific marine heatwave. *Nature Climate Change*. (doi:10.1038/nclimate3082).

36. Jacox M.G., Hazen E.L., Zaba K.D., Rudnick D.L., Edwards C.A., Moore A.M., Bograd S.J. 2016 Impacts of the 2015-2016 El Niño on the California Current System: Early assessment and comparison to past events. *Geophysical Research Letters* **43**(13), 7072-7080. (doi:10.1002/2016gl069716).

37. Kahru M., Jacox M.G., Ohman M.D. 2018 CCE1: Decrease in the frequency of oceanic fronts and surface chlorophyll concentration in the California Current System during the 2014–2016 northeast Pacific warm anomalies. *Deep Sea Research Part I: Oceanographic Research Papers*. (doi:10.1016/j.dsr.2018.04.007).

38. Peña M.A., Nemcek N., Robert M. 2018 Phytoplankton responses to the 2014-2016 warming anomaly in the northeast subarctic Pacific Ocean. *Limnology and Oceanography*. (doi:10.1002/lno.11056).

39. Peterson W.T., Fisher J.L., Strub P.T., Du X., Risien C., Peterson J., Shaw C.T. 2017 The pelagic ecosystem in the Northern California Current off Oregon during the 2014-2016 warm anomalies within the context of the past 20 years. *Journal of Geophysical Research: Oceans* **122**(9), 7267-7290. (doi:10.1002/2017jc012952).

40. Batten S.D., Raitsos D.E., Danielson S., Hopcroft R., Coyle K., McQuatters-Gollop A. 2017 Interannual variability in lower trophic levels on the Alaskan Shelf. *Deep Sea Research Part II: Topical Studies in Oceanography*. (doi:10.1016/j.dsr2.2017.04.023).

41. Jiménez-Quiroz M.d.C., Cervantes-Duarte R., Funes-Rodríguez R., Barón-Campis S.A., García-Romero F.d.J., Hernández-Trujillo S., Hernández-Becerril D.U., González-Armas R., Martell-Dubois R., Cerdeira-Estrada S., et al. 2019 Impact of "The Blob" and "El Niño" in the SW Baja California Peninsula: Plankton and Environmental Variability of Bahia Magdalena. *Frontiers in Marine Science* **6**. (doi:10.3389/fmars.2019.00025).

42. Irigoien X., Duffy-Anderson J.T., Kimmel D.G. 2020 Zooplankton abundance trends and patterns in Shelikof Strait, western Gulf of Alaska, USA, 1990–2017. *Journal of Plankton Research*. (doi:10.1093/plankt/fbaa019).

43. Jones T., Parrish J.K., Peterson W.T., Bjorkstedt E.P., Bond N.A., Ballance L.T., Bowes V., Hipfner J.M., Burgess H.K., Dolliver J.E., et al. 2018 Massive Mortality of a Planktivorous Seabird in Response to a Marine Heatwave. *Geophysical Research Letters* **45**(7), 3193-3202. (doi:10.1002/2017gl076164).

44. Piatt J.F., Parrish J.K., Renner H.M., Schoen S.K., Jones T.T., Arimitsu M.L., Kuletz K.J., Bodenstein B., Garcia-Reyes M., Duerr R.S., et al. 2020 Extreme mortality and reproductive failure of common murres resulting from the northeast Pacific marine heatwave of 2014-2016. *PLoS One* **15**(1), e0226087. (doi:10.1371/journal.pone.0226087).

45. von Biela V.R., Arimitsu M.L., Piatt J.F., Heflin B., Schoen Sk Trowbridge J.L., Clawson C.M. 2019 Extreme reduction in nutritional value of a key forage fish during the Pacific marine heatwave of 2014-2016. *Marine Ecology Progress Series* **613**, 171-182. (doi:10.3354/meps12891).

46. Basilio A., Searcy S., Thompson A.R. 2017 Effects of the Blob on settlement of spotted sand bass, Paralabrax maculatofasciatus, to Mission Bay, San Diego, CA. *PLoS One* **12**(11), e0188449. (doi:10.1371/journal.pone.0188449).

47. Thompson A.R., Harvey C.J., Sydeman W.J., Barceló C., Bograd S.J., Brodeur R.D., Fiechter J., Field J.C., Garfield N., Good T.P., et al. 2019 Indicators of pelagic forage community shifts in the California Current Large Marine Ecosystem, 1998–2016. *Ecological Indicators* **105**, 215-228. (doi:10.1016/j.ecolind.2019.05.057).

48. Gálvez C., Pardo M.A., Elorriaga-Verplancken F.R. 2020 Impacts of extreme ocean warming on the early development of a marine top predator: The Guadalupe fur seal. *Progress in Oceanography* **180**. (doi:10.1016/j.pocean.2019.102220).

49. Thalmann H.L., Daly E.A., Brodeur R.D. 2020 Two anomalously warm years in the northern California Current: impacts on early marine Steelhead diet composition, morphology, and potential survival. *Transactions of the American Fisheries Society*. (doi:10.1002/tafs.10244).

50. Osborne O.E., O'Hara P.D., Whelan S., Zandbergen P., Hatch S.A., Elliott K.H. 2020 Breeding seabirds increase foraging range in response to an extreme marine heatwave. *Marine Ecology Progress Series* **646**, 161-173. (doi:10.3354/meps13392).

51. Sanford E., Sones J.L., Garcia-Reyes M., Goddard J.H.R., Largier J.L. 2019 Widespread shifts in the coastal biota of northern California during the 2014-2016 marine heatwaves. *Sci Rep* **9**(1), 4216. (doi:10.1038/s41598-019-40784-3).

52. Lonhart S.I., Jeppesen R., Beas-Luna R., Crooks J.A., Lorda J. 2019 Shifts in the distribution and abundance of coastal marine species along the eastern Pacific Ocean during marine heatwaves from 2013 to 2018. *Marine Biodiversity Records* **12**(1). (doi:10.1186/s41200-019-0171-8).

53. McCabe R.M., Hickey B.M., Kudela R.M., Lefebvre K.A., Adams N.G., Bill B.D., Gulland F.M., Thomson R.E., Cochlan W.P., Trainer V.L. 2016 An unprecedented coastwide toxic algal bloom linked to anomalous ocean conditions. *Geophys Res Lett* **43**(19), 10366-10376. (doi:10.1002/2016GL070023).

54. Zhu Z., Qu P., Fu F., Tennenbaum N., Tatters A.O., Hutchins D.A. 2017 Understanding the blob bloom: Warming increases toxicity and abundance of the harmful bloom diatom Pseudo-nitzschia in California coastal waters. *Harmful algae* **67**, 36-43. (doi:10.1016/j.hal.2017.06.004).

55. Ryan J.P., Kudela R.M., Birch J.M., Blum M., Bowers H.A., Chavez F.P., Doucette G.J., Hayashi K., Marin R., Mikulski C.M., et al. 2017 Causality of an extreme harmful algal

bloom in Monterey Bay, California, during the 2014-2016 northeast Pacific warm anomaly. *Geophysical Research Letters* **44**(11), 5571-5579. (doi:10.1002/2017gl072637).

56. Trainer V.L. 2017 Conditions Promoting Extreme Pseudo-nitzschia Events in the Eastern Pacific but not the Western Pacific. *PICES Scientific Report*.

57. Ritzman J., Brodbeck A., Brostrom S., McGrew S., Dreyer S., Klinger T., Moore S.K. 2018 Economic and sociocultural impacts of fisheries closures in two fishing-dependent communities following the massive 2015 U.S. West Coast harmful algal bloom. *Harmful algae* **80**, 35-45. (doi:10.1016/j.hal.2018.09.002).

58. Scherber C., Eisenhauer N., Weisser W.W., Schmid B., Voigt W., Fischer M., Schulze E.D., Roscher C., Weigelt A., Allan E., et al. 2010 Bottom-up effects of plant diversity on multitrophic interactions in a biodiversity experiment. *Nature* **468**(7323), 553-556. (doi:10.1038/nature09492).

59. Lindeman R.L. 1942 The trophic-dynamic aspect of ecology. *Ecology* **23**(4), 399-417.

60. Fretwell S.D. 1987 Food chain dynamics: the central theory of ecology? *Oikos*, 291-301.

61. Arthur B., Hindell M., Bester M., Trathan P., Jonsen I., Staniland I., Oosthuizen W.C., Wege M., Lea M.A. 2015 Return customers: foraging site fidelity and the effect of environmental variability in wide-ranging antarctic fur seals. *PLoS One* **10**(3), e0120888. (doi:10.1371/journal.pone.0120888).

62. Le Boeuf B.J., Crocker D.E. 2005 Ocean climate and seal condition. *BMC biology* **3**, 9. (doi:10.1186/1741-7007-3-9).

63. McIntyre T., Ansorge I.J., Bornemann H., Plotz J., Tosh C.A., Bester M.N. 2011 Elephant seal dive behaviour is influenced by ocean temperature: implications for climate change impacts on an ocean predator. *Marine Ecology Progress Series* **441**, 257-272. (doi:10.3354/meps09383).

64. Hückstädt L.A., Burns J.M., Koch P.L., McDonald B.I., Crocker D.E., Costa D.P. 2012 Diet of a specialist in a changing environment: the crabeater seal along the western Antarctic Peninsula. *Marine Ecology Progress Series* **455**, 287-301. (doi:10.3354/meps09601).

65. Bost C.A., Cotte C., Terray P., Barbraud C., Bon C., Delord K., Gimenez O., Handrich Y., Naito Y., Guinet C., et al. 2015 Large-scale climatic anomalies affect marine predator foraging behaviour and demography. *Nature communications* **6**, 8220. (doi:10.1038/ncomms9220).

66. Estes J.A., Terborgh J., Brashares J.S., Power M.E., Berger J., Bond W.J., Carpenter S.R., Essington T.E., Holt R.D., Jackson J.B. 2011 Trophic downgrading of planet Earth. *science* **333**(6040), 301-306.

67. Estes J.A., Heithaus M., McCauley D.J., Rasher D.B., Worm B. 2016 Megafaunal Impacts on Structure and Function of Ocean Ecosystems. *Annual Review of Environment and Resources* **41**(1), 83-116. (doi:10.1146/annurev-environ-110615-085622).

68. Goetsch C. 2018 lluminating the Twilight Zone: Diet and Foraging Strategies of a Deep-Sea Predator, the Northern Elephant Seal, University of California, Santa Cruz.

69. Green D.B., Bestley S., Trebilco R., Corney S.P., Lehodey P., McMahon C.R., Guinet C., Hindell M.A. 2020 Modelled mid-trophic pelagic prey fields improve understanding of marine predator foraging behaviour. *Ecography*. (doi:10.1111/ecog.04939).

70. Le Boeuf B.J. 1972 Sexual behavior of the northern elephant seal Mirounga angustirostris. *Behaviour* **41**, 1-26.

71. Abrahms B., Hazen E.L., Bograd S.J., Brashares J.S., Robinson P.W., Scales K.L., Crocker D.E., Costa D.P. 2018 Climate mediates the success of migration strategies in a marine predator. *Ecol Lett* **21**(1), 63-71. (doi:10.1111/ele.12871).

72. Abrahms B., Scales K.L., Hazen E.L., Bograd S.J., Schick R.S., Robinson P.W., Costa D.P. 2018 Mesoscale activity facilitates energy gain in a top predator. *Proceedings Biological sciences / The Royal Society* **285**(1885). (doi:10.1098/rspb.2018.1101).

73. Biuw M., Boehme L., Guinet C., Hindell M., Costa D., Charrassin J.B., Roquet F., Bailleul F., Meredith M., Thorpe S., et al. 2007 Variations in behavior and condition of a Southern Ocean top predator in relation to in situ oceanographic conditions. *Proceedings of the National Academy of Sciences of the United States of America* **104**(34), 13705-13710. (doi:10.1073/pnas.0701121104).

74. Bradshaw C.J.A., Hindell M.A., Sumner M.D., Michael K.J. 2004 Loyalty pays: potential life history consequences of fidelity to marine foraging regions by southern elephant seals. *Animal Behaviour* **68**(6), 1349-1360. (doi:10.1016/j.anbehav.2003.12.013).

75. Clausius E., McMahon C.R., Harcourt R., Hindell M.A. 2017 Effect of climate variability on weaning mass in a declining population of southern elephant seals Mirounga leonina. *Marine Ecology Progress Series* **568**, 249-260. (doi:10.3354/meps12085).

76. Clausius E., McMahon C.R., Hindell M.A. 2017 Five decades on: Use of historical weaning size data reveals that a decrease in maternal foraging success underpins the long-term decline in population of southern elephant seals (Mirounga leonina). *PLoS One* **12**(3), e0173427. (doi:10.1371/journal.pone.0173427).

77. Mestre J., Authier M., Cherel Y., Harcourt R., McMahon C.R., Hindell M.A., Charrassin J.B., Guinet C. 2020 Decadal changes in blood delta(13)C values, at-sea distribution, and weaning mass of southern elephant seals from Kerguelen Islands. *Proceedings Biological sciences / The Royal Society* **287**(1933), 20201544. (doi:10.1098/rspb.2020.1544).

78. Le Boeuf B.J., Condit R., Reiter J. 2019 Lifetime reproductive success of northern elephant seals, Mirounga angustirostris . *Canadian Journal of Zoology*. (doi:10.1139/cjz-2019-0104).

79. Robinson P.W., Costa D.P., Crocker D.E., Gallo-Reynoso J.P., Champagne C.D., Fowler M.A., Goetsch C., Goetz K.T., Hassrick J.L., Hückstädt L.A. 2012 Foraging behavior and success of a mesopelagic predator in the northeast Pacific Ocean: insights from a data-rich species, the northern elephant seal. *PLoS One* **7**(5), e36728.

80. Costa D.P., Leboeuf B.J., Huntley A.C., Ortiz C.L. 1986 The Energetics of Lactation in the Northern Elephant Seal, Mirounga-Angustirostris. *Journal of Zoology* **209**, 21-33.

81. Crocker D.E., Williams J.D., Costa D.P., Le Boeuf B.J. 2001 Maternal traits and reproductive effort in northern elephant seals. *Ecology* **82**(12), 3541-3555. (doi:10.1890/0012-9658(2001)082[3541:Mtarei]2.0.Co;2).

82. Reiter J., Stinson N.L., Le Boeuf B.J. 1978 Northern Elephant Seal Development: The Transition from Weaning to Nutritional Independence. *Behavioral Ecology and Sociobiology* **3**(4), 337-367.

83. Le Boeuf B.J., Costa D.P., Huntley A.C., Feldkamp S.D. 1988 Continuous, Deep Diving in Female Northern Elephant Seals, Mirounga-Angustirostris. *Canadian Journal of Zoology* **66**(2), 446-458.

84. Le Boeuf B.J., Crocker D.E., Costa D.P., Blackwell S.B., Webb P.M., Houser D.S. 2000 Foraging Ecology of Northern Elephant Seals. *Ecological Monographs* **70**(3), 353-382. (doi:10.1890/0012-9615(2000)070[0353:feones]2.0.co;2).

85. Goetsch C., Conners M.G., Budge S.M., Mitani Y., Walker W.A., Bromaghin J.F., Simmons S.E., Reichmuth C., Costa D.P. 2018 Energy-Rich Mesopelagic Fishes Revealed as a Critical Prey Resource for a Deep-Diving Predator Using Quantitative Fatty Acid Signature Analysis. *Frontiers in Marine Science* **5**. (doi:10.3389/fmars.2018.00430).

86. Yoshino K., Takahashi A., Adachi T., Costa D.P., Robinson P.W., Peterson S.H., Huckstadt L.A., Holser R.R., Naito Y. 2020 Acceleration-triggered animal-borne videos show a dominance of fish in the diet of female northern elephant seals. *The Journal of experimental biology* **223**(Pt 5). (doi:10.1242/jeb.212936).

87. Lowry M.S., Condit R., Hatfield B., Allen S.G., Berger R., Morris P.A., Le Boeuf B.J., Reiter J. 2014 Abundance, Distribution, and Population Growth of the Northern Elephant Seal (Mirounga angustirostris) in the United States from 1991 to 2010. *Aquatic Mammals* **40**(1), 20-31. (doi:10.1578/Am.40.1.2014.20).

88. Boyd I.L. 2000 State-dependent fertility in pinnipeds: contrasting capital and income breeders. *Functional Ecology* **14**(5), 623-630. (doi:10.1046/j.1365-2435.2000.t01-1-00463.x).

89. Costa D.P., Maresh J.L. in press Reproductive Energetics of Phocids. In *Ethology of Earless or True Seals, the Phocids* (eds. Costa D.P., McHuron E.). Heidelberg, Germany, Springer-Verlag.

90. Stephens P.A., Boyd I.L., McNamara J.M., Houston A.I. 2009 Capital breeding and income breeding: their meaning, measurement, and worth. *Ecology* **90**(8), 2057-2067. (doi:10.1890/08-1369.1).

91. McHuron E.A., Costa D.P., Schwarz L., Mangel M., Matthiopoulos J. 2017 State-dependent behavioural theory for assessing the fitness consequences of anthropogenic disturbance on capital and income breeders. *Methods in Ecology and Evolution* **8**(5), 552-560. (doi:10.1111/2041-210x.12701).

Chapter 1: Extent and Magnitude of Subsurface Anomalies During the Northeast Pacific Blob, 2014-2017

Rachel R. Holser, Theresa R. Keates, Daniel P. Costa, Chris A. Edwards

1.1 Abstract

Marine heatwaves (MHWs) are prolonged warm water events that are increasing in frequency and magnitude due to rising global temperatures. The Northeast Pacific Blob was an unusually widespread MHW that affected ecosystems across the Northeast Pacific, from producers to top predators. Temperature and salinity data collected by northern elephant seals (*Mirounga angustirostris*) from 2014-2017 and show significant (>2 sd) warm anomalies throughout the top 1000 m of the water column, with peak warming in late 2015. Using temperature and salinity as a tracer on layers of constant density, we looked at how lateral advection may have contributed to the development of the Blob. Temperature and salinity anomalies and the expansion of the water column at the base of the pycnocline both indicate that northward advection of warm, salty water played an important role in the observed accumulation of warm water, in addition to surface warming. These findings contribute to our understanding of the physical dynamics of the Blob, especially the thermal content and structure of the water column, and offer mechanisms for its formation and maintenance, which are crucial to assessing the ecological effects of MHWs now and in the future.

1.2 Background

Extreme climate events (ECEs) are increasing in frequency and magnitude across the globe [1]. An ECE is the occurrence of a weather or climate variable (i.e. - temperature, rainfall) that is outside of the historical range for that variable and location [1]. ECEs can result in ecosystem-level perturbations, changing the distribution and abundance of

species which can have cascading trophic effects. Knowing the magnitude, duration, and spatial extent of ECEs is crucial to understanding future species distributions and ecosystem structure [2]. Marine heatwaves (MHWs) are discrete, prolonged, anomalously warm water events [3]. MHWs are a type of ECE that are poorly understood, largely due to a lack of observation at adequate temporal and spatial scales. The mechanisms underlying the build-up, persistence, and decay of these phenomena are not well understood, nor is the ecological response, which requires knowing the magnitude and duration of a disturbance in addition to the sensitivity and adaptive capacity of the biological system [4, 5]. MHWs can impact all levels of the trophic web, from productivity [6-8] to top predator survival and reproduction [9-12], and consequently can also have economic effects on local communities that depend on fisheries [13-15]. Like other ECEs, MHWs are expected to increase in frequency, magnitude, and duration in the future and are a growing threat to vulnerable ecosystems [5, 16, 17].

The Northeast Pacific Blob 2015 (the Blob) was the largest marine heatwave on record and was categorized as "severe" based on a combination of magnitude, extent, and duration of the anomalies observed [18, 19]. Anomalously warm sea surface temperatures (SST) developed in the Northeast Pacific (NEP), during the boreal winter of 2013/2014 as a result of reduced winds and high sea level pressure anomalies that suppressed heat loss from the surface ocean and weakened cold-water advection [6, 20]. Surface temperature anomalies persisted through winter 2015/2016 and sub-surface anomalies lasted into 2017 [21]. This multi-year warm event appears to result in part from coupling between the North Pacific Gyre Oscillation (NPGO) and Pacific Decadal Oscillation (PDO), the two dominant modes of variability in winter SST in the NEP [22].

The 2014-2015 warming may also have influenced the development of the 2015/2016 El Niño Southern Oscillation (ENSO) event [23, 24].

The warming associated with the Blob had extensive ecological consequences in both the Gulf of Alaska (GOA) and California Current System (CCS), spanning all trophic levels [25]. Reduced nutrient mixing resulted in overall suppressed productivity [7, 8]. Altered plankton assemblages were seen throughout the NEP, generally favoring smaller, warmer-water species [26-29]. Low biomass and smaller prey species can reduce the efficiency of energy transfer to higher trophic levels, causing reductions in body condition, reproductive success, and survival in predator species [10-12, 30-34]. Species distribution shifts were seen throughout the region [35, 36], and warm water conditions supported massive harmful algal blooms resulting in domoic acid buildup in shellfish along the west coast of North America [37-40]. The effects observed are the result of organisms responding to both extrinsic physical forcing (i.e. - altered circulation, reduced mixing, etc.) and intrinsic physiological limitations associated with warmer water temperatures (i.e. - increased metabolic rate in ectotherms).

A clear understanding of the physical dynamics of these events, especially the thermal content and structure of the water column, is crucial to assessing the ecological effects of MHWs now and in the future. The primary mechanisms for collecting data on sub-surface water properties are the Argo float network, gliders, and oceanographic cruises that target specific regions [20, 21, 41-44]. Advances in tagging technology have enabled the use of animals as ocean-sensing platforms, facilitating the collection of additional temperature and salinity data from the world's oceans that supplements and complements traditional oceanographic methods. CTD-SRDLs (Conductivity

Temperature Depth-Satellite Relay Data Loggers) allow us to collect data at biologically relevant temporal and spatial scales, enhancing our understanding of the physical ocean [45-52]. To date, studies examining the sub-surface evolution and physical dynamics of the Blob have depended on data available from the Argo float network, moorings, and ship-based surveys [21, 41-43, 53]. These data are sparser in time, horizontal space, and vertical resolution than those available from animal borne CTDs.

In this study, we examine temperature and salinity data collected by 71 northern elephant seals (*Mirounga angustirostris*) across the NEP in 2014-2017. Elephant seals dive continuously throughout their 3,000-12,000 km migrations, regularly reaching depths over 800 m. The data collected from these animals significantly enhance our understanding of the subsurface dynamics, particularly in the region of the gyre-gyre boundary which is heavily travelled by this species. Data collection and processing are described in Section 1.3. The depth, magnitude, and spatial extent of the anomaly are assessed in Section 1.4, and Section 1.5 examines advective dynamics that may have contributed to sustained subsurface anomalies.

1.3 Data Collection and Processing

Data were collected from the northern elephant seal colonies at Año Nuevo State Park, San Mateo County, California, U.S.A., and San Nicolas Island, Ventura County, California, U.S.A. All animal handling was conducted under NMFS permits #17952 and 19108, and with the approval and oversight of the UCSC Institutional Animal Care and Use Committee.

We deployed CTD-SRDLs (Sea Mammal Research Unit, St. Andrews, UK) on adult female northern elephant seals at Año Nuevo State Park (37.11°N, 237.67°E) during the post-breeding (PB: March-May) and post-molting (PM: June-January) foraging trips from 2014 - 2017, and at San Nicolas Island (33.25°N, 240.5°E) during PM 2015. Animals were sedated and instruments attached following established protocols [54]. CTD-SRDLs collect CTD profiles every 4-6 hours throughout deployment and data are collected and stored at a 1Hz sampling rate. Profiles are collected on the ascent phase of the dive, after animals have spent ~15 minutes at depth. Subsets of these data are transmitted through the Argos satellite system throughout the animal's trip [51]. Whenever possible, instruments were recovered upon the animals' return and downloaded the full-resolution stored data. When animals did not return or were not accessible, transmitted data were used instead. A summary of the number of deployments and data used can be found in Table 1.1.

All CTD data were processed following established methods. Temperature and salinity were corrected for thermal mass effects and salinity was adjusted for spiking and density inversions [47]. All measurements are quality controlled following ARGO quality criteria [55]. For this study, included data qualities 1-3 were included. Six instruments were found to have conductivity sensor drift resulting in unrealistic salinity values across their deployment. All measurements for those instruments were removed from the data set. CTD-SRDLs also provide locations via the Argos system. Locations were Kalman filtered and then passed through a speed filter to eliminate unrealistic movement. Resulting locations were linearly interpolated and matched to CTD data based on timestamps to assign locations to temperature and salinity data (Fig. 1.1) [48].

Potential density (σ_θ) and conservative temperature (Θ) were calculated using the Gibbs Sea Water toolbox [56]. Then CTD data were vertically averaged at the depth resolution of climatology data: 5 m bins from 0-100 m depth, 25 m bins from 100-500 m, and 50 m bins below 500 m depth. We extracted World Ocean Atlas 2018 (WOA18) monthly climatology temperature and salinity values (1981-2010 climatology, 1x1° grid) [57, 58] that were the nearest match in space and time to each CTD cast collected along the animals' satellite tracks and calculated temperature and salinity anomalies from both modelled (an; $\Theta_{Clim_{an}}$, $S_{Clim_{an}}$) and measured (mn; $\Theta_{Clim_{mn}}$, $S_{Clim_{mn}}$) climatologies (i.e. $\Theta_{Anom_{an}} = \Theta_{Data} - \Theta_{Clim_{an}}$). Data were separated into surface (<100 m), mid (100-500 m), and deep (500-1000 m) subsets, means and standard deviations (sd) of both temperature and salinity anomaly were calculated for each depth range, and outliers, defined as values ± 8 sd from the mean, were removed. Sigma for each temperature anomaly value was calculated (where possible) using: $sd_{\Theta_{Anom}} = \sqrt{sd_{\Theta_{Tag}}^2 + sd_{\Theta_{Clim}}^2}$ where $sd_{\Theta_{Tag}} = 0.02$ [47] and $sd_{\Theta_{Clim}}$ is provided for all measured climatologies (t_mn). The same process was followed for salinity anomalies with $sd_{S_{Tag}} = 0.03$ [47]. The resulting distribution of temperature and salinity anomalies, standardized to $sd_{\Theta_{Anom}}$ and $sd_{S_{Anom}}$, respectively, are shown in Fig. 1.2 and summarized in Table 1.2. To assess the error in modelled climatology values relative to measured climatology values, we calculated linear regressions of $\Theta_{Clim_{an}} \sim \Theta_{Clim_{mn}}$ and $S_{Clim_{an}} \sim S_{Clim_{mn}}$ (Fig. 1.2) and the standard deviation of the difference in an and mn anomaly fields for both Θ and S (Table 1.2).

1.4 Anomaly Magnitude and Extent

1.4.1 Distribution of Anomalies

The distributions of standardized anomalies of both temperature and salinity had means > 0 across all depth categories, with the strongest anomalies (both absolute anomaly and standardized) in surface water (Table 1.2). Histograms of standardized anomalies (Fig. 1.2) illustrate the non-Gaussian distribution of temperature anomalies, with high peaks around the mean and significant right skewness (Table 1.2), resulting in high frequency of anomalies between 2 and 5sd and very few below -2sd at all depths. These distributions illustrate how ubiquitous the warm anomaly was throughout the geographic range and time period sampled here.

T-S diagrams were generated on a 2x2° grid across the full range of data collected. Selected locations (see Fig. 1.1B) are shown in Figs. 3 and 4. Surface temperature anomalies were most pronounced in the core region of the Blob in 2015 and 2016 and were not always accompanied by density-compensating salinity anomalies (Fig. 1.3). This warm, low-density water would increase stratification and further enhance the surface warm anomaly due to reduced mixing. In offshore profiles (e.g. Fig. 1.3 g - l) there are see consistent warm anomalies and corresponding salt anomalies across isopycnals to the base of the main pycnocline at $\sim \sigma_\theta = 26.5$. Nearshore profiles in the region show warm, fresh anomalies that are more isolated to the surface, especially in 2015 and 2016 (e.g. Fig. 1.3 e & f). Looking at profiles from the periphery of the region with most intense warming, there is still some surface warming, but much more notable variability in salinity anomalies, with pronounced freshening in 2016, particularly around the $\sigma_\theta = 26.0$ isopycnal (Fig. 1.4). Zhi et al. [59] and Liu and Huang [60] suggest that subduction north of the Kuroshio Extension region induces subsurface fresh anomalies that then propagate

eastward towards the dateline and into the North Pacific Current (NPC). This process may account for the fresh anomalies seen in Fig. 1.4.

1.4.2 Temporal and Spatial Development

To examine the development of the warm anomaly both spatially and temporally, we generated seasonal zonal sections (40-44°N x 180-240°E) across the sampling period. Within each season, data were averaged by depth at 1° longitude intervals. To account for the varying number of data points contributing to each interval, we calculated error propagation for each mean as follows: $sd^2_{\bar{\Theta}_{Anom}} = \frac{1}{N^2}(sd^2_{\Theta_{Anom_1}} + sd^2_{\Theta_{Anom_2}} + \cdots + sd^2_{\Theta_{Anom_N}})$. For $\overline{\Theta}_{Anom} < 2 * sd_{\overline{\Theta}_{Anom}}$ the anomaly was considered not significant and assumed to be 0. Profiles with a consistent vertical resolution (5 m intervals) were then generated using linear interpolation. The same process was used to create sections of $\bar{S}_{Anom}$, $\overline{\sigma_\theta}$, and $\bar{\sigma}_{\theta\mathrm{Anom}}$ (Fig. 1.5 & 1.6). Similarly, we calculated monthly average temperature anomalies ($\overline{\Theta}_{Anom}$) by depth for all data within the core Blob region (40-50°N x 210-230°E), and used the same method to determine significance as described for the zonal sections. These data were used to create contour plots of $\overline{\Theta}_{Anom}$ and $\overline{\Theta}_{Anom} / sd_{\overline{\Theta}_{Anom}}$ (Fig. 1.7).

We found significant warming throughout the zonal section, both in surface and subsurface water, although the most pronounced and sustained warming occurred east of 200°E (Fig. 1.5a). While surface anomalies peak in late 2015, the subsurface anomaly at 200-400m is sustained through the end of 2017. The bands of positive salinity anomalies seen ~100 m in 2014-2015 may be due to reduction in the mixed layer depth because of the profound surface warming (and negative density anomalies – Fig. 1.6b)

occurring at that time. Work by Zhi et al. shows that fresh anomalies (<-0.2) in the upper 100 m preceded the onset of the marine heatwave (2012-2013) and contributed to shallowing of the mixed layer depth, which then would have inhibited heat penetration at depth, and enhanced the development of surface warm anomalies [59]. We cannot directly corroborate this pre-conditioning here, but there are fresh anomalies in 2014 at around 200 m depth, underneath areas with stronger surface warming at that time, which may be a remnant of the eastward-propagating fresh anomaly they reported.

The circulation and SST dynamics of the NEP is influenced by the expression of several large-scale phenomena, especially the PDO [61], NPGO [62], and ENSO [63]. We included monthly values of all three of these indices (MEIv2 for ENSO) in our time series figure for context of these additional large-scale phenomena (Fig. 1.7). Positive (or warm-phase) PDO is associated with a SST pattern characterized by warming in the NEP and a large pool of cool water in the central Pacific [61]. Warm-phase PDO is also associated with a stronger Alaska Gyre and a southward shift of the zero geostrophic flow contour separating the Alaska and subtropical gyres (~1° in 2014-2016) [43]. The initial development of the Blob and maintenance of the anomaly has been attributed in part to coupled NPGO/PDO dynamics and a transition between NPGO-expression (2014) to PDO-expression (2015) [22].

Peak warm anomalies co-occurred with the 2015/16 ENSO event (Fig. 1.7), which was an extreme, mixed Central and Eastern Pacific El Niño [64]. While past El Niño events have been linked to sustained warming in the GOA [65], the expression of the 2015/16 event did not match previous observations, particularly compared to prior strong El Niños (1983/84 and 1997/98) [24, 64, 66]. Because of the Blob, the GOA and CCS were both in

an unusually warm state prior to the onset of El Niño, which likely influenced the difference in observed effects. For example, the CCS experienced upwelling favorable winds and shoaling of the 26.0 isopycnal, whereas the opposite was true in prior events [24]. Both positive PDO and ENSO can result in surface cooling in the central north Pacific. The intrusion of cool, fresh water in the second half of 2016 may be related to these dynamics (Figs. 1.5-1.7). Although the cooling coincides with the end of the 2015-2016 ENSO event in the tropics, generally there is a 2-3 month lag in expression in the NEP [64].

Within the core region of the Blob, the warm temperature anomaly was initially concentrated in the top ~100 m of the water column, but by late summer 2014 anomalies extended down to 300 m depth (Fig. 1.7). Surface warming became most pronounced in late 2015, with normalized temperature anomalies >5 sd from climatology in the top 100 m. Subsurface anomalies were high throughout 2015-2017. Between 100-500 m depth range, Θ_{Anom} of 0.4-1.5°C (2-5 sd) occurred throughout the event. Below 500 m, the maximum anomaly occurred in late 2015 at around 800 m depth (+ 0.21°C, 4.2 sd). This maximum is both earlier in the event and deeper in the water column than predicted or observed in previous studies [21, 41, 42].

1.5 Isopycnal Variability and Advection

1.5.1 Vertical Displacement

Isopycnal variability in the GOA from 2004-2018 was examined by Cummins and Masson [53] and they found that downward pycnocline displacement through the top 1000 m in this region was associated with strengthening of the gyre circulation and positive PDO values (warmer regional SST). Given the strong positive PDO signal during the Blob, this

relationship implies downward movement of isopycnals in 2014-2017. They found that a model driven by Ekman pumping generally had good agreement with vertical displacement of the base of the pycnocline starting in 2004, however this relationship broke down during the Blob (2015-2017), suggesting different mechanisms driving vertical variability during the MHW [53].

We calculated mean Θ, S, and depth (d) in a 1x1° grid for each year from elephant seal observations and from annual WOA18 climatology on the σ_θ = 26.5 and σ_θ = 27.0 isopycnals (Figs. 8 & 9). North of 45°N, the σ_θ = 26.5 surface is near the base of the main pycnocline while σ_θ = 27.0 is well below the pycnocline but still has high density elephant seal data coverage. We subtracted climatological isopycnal depth from observed depth to find depth anomalies of both isopycnals (Fig. 1.10). The depth anomalies on the σ_θ = 26.5 are mixed, and notably the regions with the greatest warming in 2014 and 2015 show 10-20 m shallowing of the isopycnal, as was seen by Cummins and Masson [53]. However, the σ_θ = 27.0 isopycnal is less variable and generally shows deepening, as would normally be expected with positive PDO and a strengthened Alaska Gyre [43, 53].

To quantify expansion (or compression) of the water column between the σ_θ = 26.5 and σ_θ = 27.0 isopycnals, we calculated the difference in depth anomalies between the two density surfaces in each year, which may indicate net advection of water into (or out of) the region (Fig. 1.11). In 2014 and 2015, we see clear spreading between isopycnals (~ +20-30 m) throughout the core region of the Blob and in surrounding water, suggesting net transport of water into the region on these density surfaces. In 2016, we see vertical expansion between isopycnals on the western edge of the core Blob region, where we begin to see cold, fresh anomalies in our zonal section in the second half of that year (Fig.

1.5). This could be the result of increased southward transport from the Alaskan Stream or from the eastward propagation of a water mass subducted near the Kuroshio Extension into the NPC, and we consider possible advective transport further in section 1.5.2. In 2017, there is significant deepening of the σ_θ = 26.5 layer, especially west of 220°E, and compression of the distance between the two isopycnals (Fig. 1.11). At that time, there were still significant sub-surface warm anomalies (100-500 m depth), but the top 100 m was dominated by cold anomalies until the last quarter of the year. These characteristics may be related to changes in the climate mode and large-scale circulation, as both PDO and ENSO had transitioned to near neutral in the second half of 2017. The shift of the zero meridional flow contour and transport anomalies across the bifurcation region also returned to ~0 at that time.

1.5.2 Lateral Advection

The potential contribution of lateral advection along subsurface isopycnals to maintaining the warm anomaly in the NEP has been assessed in two studies using Argo data. Hristova et al. [43] quantified geostrophic advection anomalies across the southern and northern boundaries of the NPC bifurcation region (40-50°N x 205-240°E) and found northward transport anomalies in 0-300 m at both boundary latitudes from 2014-2016. Geostrophic transport in this region exhibits seasonal variability, with greatest northward transport during winter months when the Alaska Gyre is at its largest and strongest [43]. The authors suggest that this advection contributed to warming given the covariation of northward transport with temperature and salinity anomalies in the GOA [43]. However, Cummins and Mason [53] suggest that anomalous advection likely

contributed to anomalies in the last half of 2016, but that heat was transported downward through isopycnals during the first two years of the heatwave.

To quantify the lateral movement required to account for spice anomalies (density compensating temperature and salinity variations on an isopycnal surface) across each isopycnal through advection, we calculated a cost function for each climatology grid cell within 5° of our data and found the location and value of the minimum $J_{i,j}$ for each data cell ($Data_{k,l}$):

$$J_{i,j}^{k,l} = \left[\frac{\left(\Theta_{Data_{k,l}} - \Theta_{Clim_{i,j}}\right)}{\overline{sd}_{\Theta_{Clim}}}\right]^2 + \left[\frac{\left(S_{Data_{k,l}} - S_{Clim_{i,j}}\right)}{\overline{sd}_{S_{Clim}}}\right]^2$$

where $\overline{sd}_{\Theta_{Clim}}$ and $\overline{sd}_{S_{Clim}}$ were calculated for each density surface from the area where seal-collected data were present (σ_θ = 26.5: $\overline{sd}_{\Theta_{Clim}} = 0.7048°$ and $\overline{sd}_{S_{Clim}} = 0.1851$; σ_θ = 27.0, : $\overline{sd}_{\Theta_{Clim}} = 0.5643°$ and $\overline{sd}_{S_{Clim}} = 0.1313$; Fig. 1.12). To account for error in both measured and climatology fields, we repeated these calculations 10000 times while adding a random, zero-centered normally distributed perturbation to both $\Theta_{Data_{k,l}}$ and $S_{Data_{k,l}}$ on each iteration. We found the mean location of the resulting minimum $J_{i,j}$ value for each grid cell. Density surface maps of temperature anomaly with overlaid arrows indicate the direction and distance of lateral movement required to account for the temperature and salinity values seen in each year compared to climatology (Fig. 1.13). The anomalies were sustained over multiple years, so we also calculated the difference in lateral advection from one year to the next to examine the cumulative movement required to account for year-to-year spice anomalies in the region (Fig. 1.14). Given

differences in data coverage from year to year, we used average values on a 3x3° grid for these calculations.

Both density surfaces show significant, coherent northward movement into the core region of the Blob in 2014-2016 (Fig. 1.13). Looking at year-to-year cumulative movement, the strongest advection is seen in 2015, at the peak of the heatwave, with very comparatively little additional cohesive movement in 2016 to maintain the spice signatures. Hristova et al. [43] saw the strongest northward transport anomalies from late 2014 through mid-2016. The expansion seen between these density surfaces in 2015 (Fig. 1.11) further supports the likelihood that lateral movement near the base of the pycnocline contributed to the development and maintenance of subsurface warming. To assess the relative contributions of temperature and salinity to the cost function calculations, we completed the calculations as described above using only the temperature or salinity terms. Looking at 2015 as an example (Fig. 1.15), within the core warming region both salinity and temperature anomalies are explained by consistent northward advection, although the salinity signature requires much greater movement than temperature alone does.

In addition to the region of core warming, there is a notable cool, fresh water sub-surface anomaly seen on both density surfaces in 2016 (and was also evident in the zonal sections – Fig. 1.5). Our calculations here indicate southward transport from the Alaska Stream as potential source water for those anomalies (Fig. 1.13, 1.14). The Alaska Gyre was both larger and stronger throughout the Blob, with peak gyre strength (maximum transport) at the start of 2016 [43]. Increased overall transport combined with the southward shift

of the zero meridional transport contour could have resulted in an influx of cool fresh water to that region in 2016.

1.6 Conclusion

In this study we analyzed a rich dataset that contributes to our understanding of the 3-dimensional extent, magnitude, and physical dynamics of the Northeast Pacific Blob 2015. CTD casts collected by northern elephant seals provide temperature and salinity data for the top 1000 m of the water column at higher temporal and spatial resolution than can be achieved with more conventional means. We found standardized temperature anomalies >2 sd at all depths throughout the heatwave, with peak deep anomalies of 4.2 sd at 800 m in 2015 (Fig. 1.7). These anomalies were deeper and greater than those previously reported for the subsurface [41, 42], and occurred earlier in the event than predicted [21]. Lateral advection at the base of the pycnocline likely contributed to the subsurface structure we observed. Spice anomalies in the core region of the Blob suggest northward advection of warm, salty water (Fig. 1.13), and corresponding expansion of the water column (Fig. 1.11) also supports net influx of water into the region as a mechanism driving subsurface warming.

MHWs are expected to increase in frequency, magnitude, and duration as global temperatures continue to rise [16, 17, 67, 68]. These events have significant ecological consequences for the affected systems, as well as economic consequences for the local communities that rely on those systems [4, 5, 13-15]. The Blob reduced energy transfer through the trophic web resulting in profound consequences for many top predator species, who serve as sentinels for the overall health of the ecosystem [11, 12, 30, 31]. The warm conditions of the Blob also fostered an extreme harmful algae bloom [37-39]

that forced shellfish fisheries to close along the West Coast of the U.S. In addition to lost catch, there were substantial costs to related industries and impacts on overall community health and vitality [15]. Understanding the physical mechanisms and associated climate drivers that cause and maintain MHWs is essential to predicting the onset and development of these events in the future, and will help us anticipate and mitigate their ecological and economic consequences [5, 14, 19].

1.7 References

1. Ummenhofer C.C., Meehl G.A. 2017 Extreme weather and climate events with ecological relevance: a review. *Philosophical transactions of the Royal Society of London Series B, Biological sciences* **372**(1723). (doi:10.1098/rstb.2016.0135).

2. Wernberg T., Smale D.A., Tuya F., Thomsen M.S., Langlois T.J., de Bettignies T., Bennett S., Rousseaux C.S. 2013 An extreme climatic event alters marine ecosystem structure in a global biodiversity hotspot. *Nature Climate Change* **3**(1), 78-82. (doi:10.1038/Nclimate1627).

3. Hobday A.J., Alexander L.V., Perkins S.E., Smale D.A., Straub S.C., Oliver E.C.J., Benthuysen J.A., Burrows M.T., Donat M.G., Feng M., et al. 2016 A hierarchical approach to defining marine heatwaves. *Progress in Oceanography* **141**, 227-238. (doi:10.1016/j.pocean.2015.12.014).

4. Frolicher T.L., Laufkotter C. 2018 Emerging risks from marine heat waves. *Nature communications* **9**(1), 650. (doi:10.1038/s41467-018-03163-6).

5. Smale D.A., Wernberg T., Oliver E.C.J., Thomsen M., Harvey B.P., Straub S.C., Burrows M.T., Alexander L.V., Benthuysen J.A., Donat M.G., et al. 2019 Marine heatwaves threaten global biodiversity and the provision of ecosystem services. *Nature Climate Change* **9**(4), 306-312. (doi:10.1038/s41558-019-0412-1).

6. Whitney F.A. 2015 Anomalous winter winds decrease 2014 transition zone productivity in the NE Pacific. *Geophysical Research Letters* **42**(2), 428-431. (doi:10.1002/2014GL062634).

7. Peña M.A., Nemcek N., Robert M. 2018 Phytoplankton responses to the 2014-2016 warming anomaly in the northeast subarctic Pacific Ocean. *Limnology and Oceanography*. (doi:10.1002/lno.11056).

8. Kahru M., Jacox M.G., Ohman M.D. 2018 CCE1: Decrease in the frequency of oceanic fronts and surface chlorophyll concentration in the California Current System during the 2014–2016 northeast Pacific warm anomalies. *Deep Sea Research Part I: Oceanographic Research Papers*. (doi:10.1016/j.dsr.2018.04.007).

9. Wild S., Krutzen M., Rankin R.W., Hoppitt W.J.E., Gerber L., Allen S.J. 2019 Long-term decline in survival and reproduction of dolphins following a marine heatwave. *Curr Biol* **29**(7), R239-R240. (doi:10.1016/j.cub.2019.02.047).

10. Jones T., Parrish J.K., Peterson W.T., Bjorkstedt E.P., Bond N.A., Ballance L.T., Bowes V., Hipfner J.M., Burgess H.K., Dolliver J.E., et al. 2018 Massive Mortality of a Planktivorous Seabird in Response to a Marine Heatwave. *Geophysical Research Letters* **45**(7), 3193-3202. (doi:10.1002/2017gl076164).

11. Gálvez C., Pardo M.A., Elorriaga-Verplancken F.R. 2020 Impacts of extreme ocean warming on the early development of a marine top predator: The Guadalupe fur seal. *Progress in Oceanography* **180**. (doi:10.1016/j.pocean.2019.102220).

12. Osborne O.E., O'Hara P.D., Whelan S., Zandbergen P., Hatch S.A., Elliott K.H. 2020 Breeding seabirds increase foraging range in response to an extreme marine heatwave. *Marine Ecology Progress Series* **646**, 161-173. (doi:10.3354/meps13392).

13. Richerson K., Leonard J., Holland D.S. 2018 Predicting the economic impacts of the 2017 West Coast salmon troll ocean fishery closure. *Marine Policy*. (doi:10.1016/j.marpol.2018.03.005).

14. Bograd S.J., Kang S., Di Lorenzo E., Horii T., Katugin O.N., King J.R., Lobanov V.B., Makino M., Na G., Perry R.I., et al. 2019 Developing a Social–Ecological–Environmental System Framework to Address Climate Change Impacts in the North Pacific. *Frontiers in Marine Science* **6**. (doi:10.3389/fmars.2019.00333).

15. Ritzman J., Brodbeck A., Brostrom S., McGrew S., Dreyer S., Klinger T., Moore S.K. 2018 Economic and sociocultural impacts of fisheries closures in two fishing-dependent communities following the massive 2015 U.S. West Coast harmful algal bloom. *Harmful algae* **80**, 35-45. (doi:10.1016/j.hal.2018.09.002).

16. Oliver E.C.J., Donat M.G., Burrows M.T., Moore P.J., Smale D.A., Alexander L.V., Benthuysen J.A., Feng M., Sen Gupta A., Hobday A.J., et al. 2018 Longer and more frequent marine heatwaves over the past century. *Nature communications* **9**(1), 1324. (doi:10.1038/s41467-018-03732-9).

17. Frolicher T.L., Fischer E.M., Gruber N. 2018 Marine heatwaves under global warming. *Nature* **560**(7718), 360-364. (doi:10.1038/s41586-018-0383-9).

18. Hobday A., Oliver E., Sen Gupta A., Benthuysen J., Burrows M., Donat M., Holbrook N., Moore P., Thomsen M., Wernberg T., et al. 2018 Categorizing and Naming Marine Heatwaves. *Oceanography* **31**(2). (doi:10.5670/oceanog.2018.205).

19. Holbrook N.J., Scannell H.A., Sen Gupta A., Benthuysen J.A., Feng M., Oliver E.C.J., Alexander L.V., Burrows M.T., Donat M.G., Hobday A.J., et al. 2019 A global assessment of marine heatwaves and their drivers. *Nature communications* **10**(1), 2624. (doi:10.1038/s41467-019-10206-z).

20. Bond N.A., Cronin M.F., Freeland H., Mantua N. 2015 Causes and impacts of the 2014 warm anomaly in the NE Pacific. *Geophysical Research Letters* **42**(9), 3414-3420. (doi:10.1002/2015gl063306).

21. Freeland H., Ross T. 2019 'The Blob' - or, how unusual were ocean temperatures in the Northeast Pacific during 2014-2018? *Deep Sea Research Part I: Oceanographic Research Papers* **150**. (doi:10.1016/j.dsr.2019.06.007).

22. Joh Y., Di Lorenzo E. 2017 Increasing Coupling Between NPGO and PDO Leads to Prolonged Marine Heatwaves in the Northeast Pacific. *Geophysical Research Letters*.

23. Di Lorenzo E., Mantua N. 2016 Multi-year persistence of the 2014/15 North Pacific marine heatwave. *Nature Climate Change*. (doi:10.1038/nclimate3082).

24. Jacox M.G., Hazen E.L., Zaba K.D., Rudnick D.L., Edwards C.A., Moore A.M., Bograd S.J. 2016 Impacts of the 2015-2016 El Niño on the California Current System: Early assessment and comparison to past events. *Geophysical Research Letters* **43**(13), 7072-7080. (doi:10.1002/2016gl069716).

25. Cavole L., Demko A., Diner R., Giddings A., Koester I., Pagniello C., Paulsen M.-L., Ramirez-Valdez A., Schwenck S., Yen N., et al. 2016 Biological Impacts of the 2013–2015 Warm-Water Anomaly in the Northeast Pacific: Winners, Losers, and the Future. *Oceanography* **29**(2). (doi:10.5670/oceanog.2016.32).

26. Peterson W.T., Fisher J.L., Strub P.T., Du X., Risien C., Peterson J., Shaw C.T. 2017 The pelagic ecosystem in the Northern California Current off Oregon during the 2014-2016 warm anomalies within the context of the past 20 years. *Journal of Geophysical Research: Oceans* **122**(9), 7267-7290. (doi:10.1002/2017jc012952).

27. Batten S.D., Raitsos D.E., Danielson S., Hopcroft R., Coyle K., McQuatters-Gollop A. 2017 Interannual variability in lower trophic levels on the Alaskan Shelf. *Deep Sea Research Part II: Topical Studies in Oceanography*. (doi:10.1016/j.dsr2.2017.04.023).

28. Jiménez-Quiroz M.d.C., Cervantes-Duarte R., Funes-Rodríguez R., Barón-Campis S.A., García-Romero F.d.J., Hernández-Trujillo S., Hernández-Becerril D.U., González-Armas R., Martell-Dubois R., Cerdeira-Estrada S., et al. 2019 Impact of "The Blob" and "El Niño" in the SW Baja California Peninsula: Plankton and Environmental Variability of Bahia Magdalena. *Frontiers in Marine Science* **6**. (doi:10.3389/fmars.2019.00025).

29. Irigoien X., Duffy-Anderson J.T., Kimmel D.G. 2020 Zooplankton abundance trends and patterns in Shelikof Strait, western Gulf of Alaska, USA, 1990–2017. *Journal of Plankton Research*. (doi:10.1093/plankt/fbaa019).

30. Piatt J.F., Parrish J.K., Renner H.M., Schoen S.K., Jones T.T., Arimitsu M.L., Kuletz K.J., Bodenstein B., Garcia-Reyes M., Duerr R.S., et al. 2020 Extreme mortality and reproductive failure of common murres resulting from the northeast Pacific marine heatwave of 2014-2016. *PLoS One* **15**(1), e0226087. (doi:10.1371/journal.pone.0226087).

31. von Biela V.R., Arimitsu M.L., Piatt J.F., Heflin B., Schoen Sk Trowbridge J.L., Clawson C.M. 2019 Extreme reduction in nutritional value of a key forage fish during the Pacific marine heatwave of 2014-2016. *Marine Ecology Progress Series* **613**, 171-182. (doi:10.3354/meps12891).

32. Basilio A., Searcy S., Thompson A.R. 2017 Effects of the Blob on settlement of spotted sand bass, Paralabrax maculatofasciatus, to Mission Bay, San Diego, CA. *PLoS One* **12**(11), e0188449. (doi:10.1371/journal.pone.0188449).

33. Thompson A.R., Harvey C.J., Sydeman W.J., Barceló C., Bograd S.J., Brodeur R.D., Fiechter J., Field J.C., Garfield N., Good T.P., et al. 2019 Indicators of pelagic forage community shifts in the California Current Large Marine Ecosystem, 1998–2016. *Ecological Indicators* **105**, 215-228. (doi:10.1016/j.ecolind.2019.05.057).

34. Thalmann H.L., Daly E.A., Brodeur R.D. 2020 Two anomalously warm years in the northern California Current: impacts on early marine Steelhead diet composition, morphology, and potential survival. *Transactions of the American Fisheries Society*. (doi:10.1002/tafs.10244).

35. Sanford E., Sones J.L., Garcia-Reyes M., Goddard J.H.R., Largier J.L. 2019 Widespread shifts in the coastal biota of northern California during the 2014-2016 marine heatwaves. *Sci Rep* **9**(1), 4216. (doi:10.1038/s41598-019-40784-3).

36. Lonhart S.I., Jeppesen R., Beas-Luna R., Crooks J.A., Lorda J. 2019 Shifts in the distribution and abundance of coastal marine species along the eastern Pacific Ocean during marine heatwaves from 2013 to 2018. *Marine Biodiversity Records* **12**(1). (doi:10.1186/s41200-019-0171-8).

37. McCabe R.M., Hickey B.M., Kudela R.M., Lefebvre K.A., Adams N.G., Bill B.D., Gulland F.M., Thomson R.E., Cochlan W.P., Trainer V.L. 2016 An unprecedented coastwide toxic algal bloom linked to anomalous ocean conditions. *Geophys Res Lett* **43**(19), 10366-10376. (doi:10.1002/2016GL070023).

38. Zhu Z., Qu P., Fu F., Tennenbaum N., Tatters A.O., Hutchins D.A. 2017 Understanding the blob bloom: Warming increases toxicity and abundance of the harmful bloom diatom Pseudo-nitzschia in California coastal waters. *Harmful algae* **67**, 36-43. (doi:10.1016/j.hal.2017.06.004).

39. Ryan J.P., Kudela R.M., Birch J.M., Blum M., Bowers H.A., Chavez F.P., Doucette G.J., Hayashi K., Marin R., Mikulski C.M., et al. 2017 Causality of an extreme harmful algal bloom in Monterey Bay, California, during the 2014-2016 northeast Pacific warm anomaly. *Geophysical Research Letters* **44**(11), 5571-5579. (doi:10.1002/2017gl072637).

40. Trainer V.L. 2017 Conditions Promoting Extreme Pseudo-nitzschia Events in the Eastern Pacific but not the Western Pacific. *PICES Scientific Report*.

41. Hu Z.-Z., Kumar A., Jha B., Zhu J., Huang B. 2017 Persistence and Predictions of the Remarkable Warm Anomaly in the Northeastern Pacific Ocean during 2014–16. *Journal of Climate* **30**(2), 689-702. (doi:10.1175/jcli-d-16-0348.1).

42. Chao Y., Farrara J.D., Bjorkstedt E., Chai F., Chavez F., Rudnick D.L., Enright W., Fisher J.L., Peterson W.T., Welch G.F., et al. 2017 The origins of the anomalous warming in

the California coastal ocean and San Francisco Bay during 2014-2016. *Journal of Geophysical Research: Oceans* **122**(9), 7537-7557. (doi:10.1002/2017jc013120).

43. Hristova H.G., Ladd C., Stabeno P.J. 2019 Variability and Trends of the Alaska Gyre From Argo and Satellite Altimetry. *Journal of Geophysical Research: Oceans* **124**(8), 5870-5887. (doi:10.1029/2019jc015231).

44. Zaba K.D., Rudnick D.L. 2016 The 2014-2015 warming anomaly in the Southern California Current System observed by underwater gliders. *Geophysical Research Letters* **43**(3), 1241-1248. (doi:10.1002/2015gl067550).

45. Boehlert G.W., Costa D.P., Crocker D.E., Green P., O'Brien T., Levitus S., Le Boeuf B.J. 2001 Autonomous pinniped environmental samplers: Using instrumented animals as oceanographic data collectors. *J Atmos Ocean Tech* **18**(11), 1882-1893. (doi:Doi 10.1175/1520-0426(2001)018<1882:Apesui>2.0.Co;2).

46. Biuw M., Boehme L., Guinet C., Hindell M., Costa D., Charrassin J.B., Roquet F., Bailleul F., Meredith M., Thorpe S., et al. 2007 Variations in behavior and condition of a Southern Ocean top predator in relation to in situ oceanographic conditions. *Proceedings of the National Academy of Sciences of the United States of America* **104**(34), 13705-13710. (doi:10.1073/pnas.0701121104).

47. Siegelman L., Roquet F., Mensah V., Rivière P., Pauthenet E., Picard B., Guinet C. 2019 Correction and accuracy of high- and low-resolution CTD data from animal-borne instruments. *J Atmos Ocean Tech*. (doi:10.1175/jtech-d-18-0170.1).

48. Roquet F.G.W., Mark A. Hindell, Rob Harcourt, Clive McMahon,, Christophe Guinet J.-B.C., Gilles Reverdin, Lars Boehme,, Fedak P.L.M. 2014 A Southern Indian Ocean database of hydrographic profiles obtained with instrumented elephant seals. *Scientific Data*, 10. (doi:10.1038/sdata.2014.28).

49. Charrassin J., Roquet F., Park Y., Bailleul F., Guinet C., Meredith M., Nicholls K., Thorpe S., Tremblay Y., Costa D. 2010 New insights into Southern Ocean physical and biological processes revealed by instrumented elephant seals. *Proceedings of OceanObs 09: Sustained Ocean Observations and Information for Society (Vol 2), Venice, Italy, 21-25 September 2009, Hall, J, Harrison DE & Stammer, D, Eds, ESA Publication WPP-306*.

50. Boehme L., Kovacs K., Lydersen C., Nøst O., Biuw M., Charrassin J., Roquet F., Guinet C., Meredith M., Nicholls K. 2010 Biologging in the global ocean observing system. *Proceedings of OceanObs 09: Sustained Ocean Observations and Information for Society (Vol 2), Venice, Italy, 21-25 September 2009, Hall, J, Harrison DE & Stammer, D, Eds, ESA Publication WPP-306*.

51. Boehme L., Lovell P., Biuw M., Roquet F., Nicholson J., Thorpe S.E., Meredith M.P., Fedak M. 2009 Technical Note: Animal-borne CTD-Satellite Relay Data Loggers for real-time oceanographic data collection. *Ocean Sci* **5**(4), 685-695. (doi:10.5194/os-5-685-2009).

52. Costa D.P., Breed G.A., Robinson P.W. 2012 New insights into pelagic migrations: implications for ecology and conservation. *Annual Review of Ecology, Evolution, and Systematics* **43**, 73-96.

53. Cummins P.F., Masson D. 2018 Low-frequency isopycnal variability in the Alaska Gyre from Argo. *Progress in Oceanography* **168**, 310-324. (doi:10.1016/j.pocean.2018.09.014).

54. Robinson P.W., Costa D.P., Crocker D.E., Gallo-Reynoso J.P., Champagne C.D., Fowler M.A., Goetsch C., Goetz K.T., Hassrick J.L., Hückstädt L.A. 2012 Foraging behavior and success of a mesopelagic predator in the northeast Pacific Ocean: insights from a data-rich species, the northern elephant seal. *PLoS One* **7**(5), e36728.

55. Wong A., Keeley R., Carval T., Team A.D.M. 2018 Argo Quality Control Manual For CTD and Trajectory Data. (

56. McDougall T.J., Barker P.M. 2011 Getting started with TEOS-10 and the Gibbs Seawater (GSW) oceanographic toolbox. *SCOR/IAPSO WG* **127**, 1-28.

57. Locarnini R.A., A. V. Mishonov, O. K. Baranova, T. P. Boyer, M. M. Zweng, H. E. Garcia, J. R. Reagan, D. Seidov, K. Weathers, C. R. Paver, and I. Smolyar. 2018 World Ocean Atlas 2018, Volume 1: Temperature. (ed. Ed A.M.T.), p. 52, NOAA Atlas NESDIS 81.

58. Zweng M.M., J. R. Reagan, D. Seidov, T. P. Boyer, R. A. Locarnini, H. E. Garcia, A. V. Mishonov, O. K. Baranova, K. Weathers, C. R. Paver, and I. Smolyar. 2018 World Ocean Atlas 2018, Volume 2: Salinity. (p. 50, NOAA Atlas NESDIS.

59. Zhi H., Lin P., Zhang R.-H., Chai F., Liu H. 2019 Salinity effects on the 2014 warm "Blob" in the Northeast Pacific. *Acta Oceanologica Sinica* **38**(9), 24-34. (doi:10.1007/s13131-019-1450-2).

60. Liu L.L., Huang R.X. 2012 The Global Subduction/Obduction Rates: Their Interannual and Decadal Variability. *Journal of Climate* **25**(4), 1096-1115. (doi:10.1175/2011jcli4228.1).

61. Mantua N.J., Hare S.R. 2002 The Pacific decadal oscillation. *Journal of Oceanography* **58**(1), 35-44.

62. Di Lorenzo E., Schneider N., Cobb K., Franks P., Chhak K., Miller A., McWilliams J., Bograd S., Arango H., Curchitser E. 2008 North Pacific Gyre Oscillation links ocean climate and ecosystem change. *Geophysical Research Letters* **35**(8).

63. Wolter K. 1993 Monitoring ENSO in COADS with a seasonlly adjusted principle component index. In *Proc of the 17th Climate Diagnostics Workshop* (

64. Santoso A., McPhaden M.J., Cai W. 2017 The Defining Characteristics of ENSO Extremes and the Strong 2015/2016 El Niño. *Reviews of Geophysics* **55**(4), 1079-1129. (doi:10.1002/2017rg000560).

65. Whitney F.A., Freeland H.J. 1999 Variability in upper-ocean water properties in the NE Pacific Ocean. *Deep-Sea Research Part Ii-Topical Studies in Oceanography* **46**(11-12), 2351-2370. (doi:Doi 10.1016/S0967-0645(99)00067-3).

66. Zhong W., Cai W., Zheng X.T., Yang S. 2019 Unusual Anomaly Pattern of the 2015/2016 Extreme El Niño Induced by the 2014 Warm Condition. *Geophysical Research Letters*. (doi:10.1029/2019gl085681).

67. Oliver E.C.J. 2019 Mean warming not variability drives marine heatwave trends. *Climate Dynamics*. (doi:10.1007/s00382-019-04707-2).

68. Jacox M.G. 2019 Marine heatwaves in a changing climate. *Nature* **571**(7766), 485-487. (doi:10.1038/d41586-019-02196-1).

Table 1.1 – Summary of CTD-SRDL deployments on elephant seals from 2014-2017 and the number of casts with temperature and salinity data that reach to at least 100, 500, and 800 m of depth.

	# CTD Deployments		*#100+ m Casts*		*#500+ m Casts*		*#800+ m Casts*	
Year	Post-Breed	Post-Molt	Temp	Salinity	Temp	Salinity	Temp	Salinity
2014	11	12	7190	7190	4712	4712	553	553
2015	4	12	11945	10346	6666	5664	452	311
2016	11	11	9346	5146	4699	2763	585	152
2017	0	10	8133	5710	4240	2841	445	182
Total	**26**	**45**	**36614**	**28392**	**20317**	**15980**	**2035**	**1198**

Table 1.2 – Summary of the distributions of $\Theta_{Anom_{an}}$ and $S_{Anom_{an}}$ (standardized to $sd_{\Theta_{Anom}}$ and $sd_{S_{Anom}}$ respectively) from surface, mid, and deep water depths.

	Surface (<100 m)		**Mid (100-500 m)**		**Deep (500-1000 m)**	
	Temp	Salinity	Temp	Salinity	Temp	Salinity
Mean	0.71°C	0.06	0.29°C	0.04	0.07°C	0.03
sd	1.41°C	0.24	0.56°C	0.13	0.17°C	0.06
Standardized Mean	1.20	0.67	0.98	0.89	0.79	0.90
Standardized sd	4.20	3.29	2.86	2.44	2.10	2.96
Skewness	10.3	0.75	7.19	-0.46	1.49	0.038
Kurtosis	267.6	12.0	155.6	12.4	15.3	6.77
Mn-An sd	0.513°C	0.141	0.244°C	0.064	0.103°C	0.016

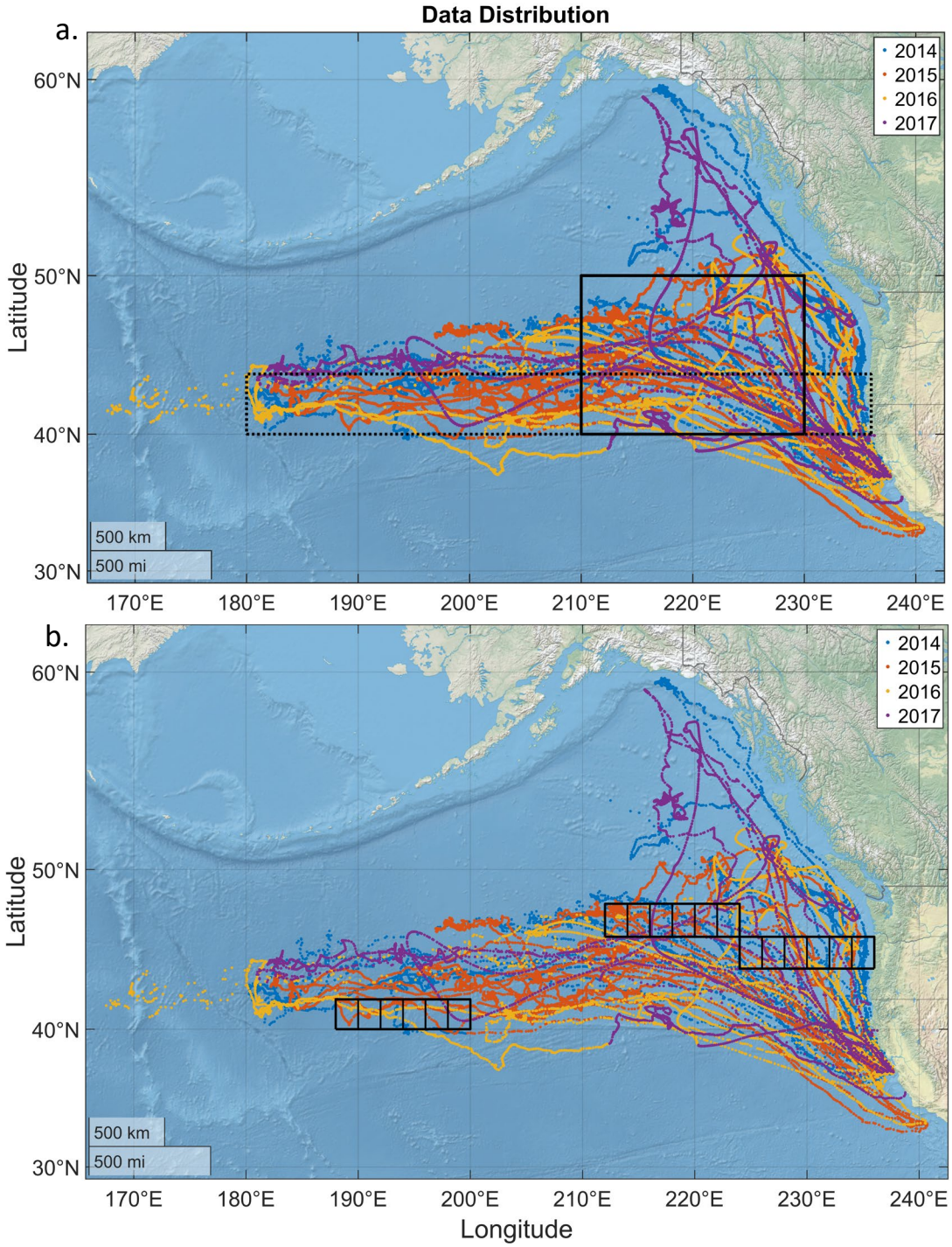

Fig. 1.1 - Distribution of CTD casts with both temperature and salinity data collected in 2014-2017, each point represents a single cast. The solid black box in a) outlines the core region, and the dashed rectangle outlines the region used to create zonal sections. Boxes in b) indicate selected locations of T-S diagrams shown in Figs. 1.4 and 1.5.

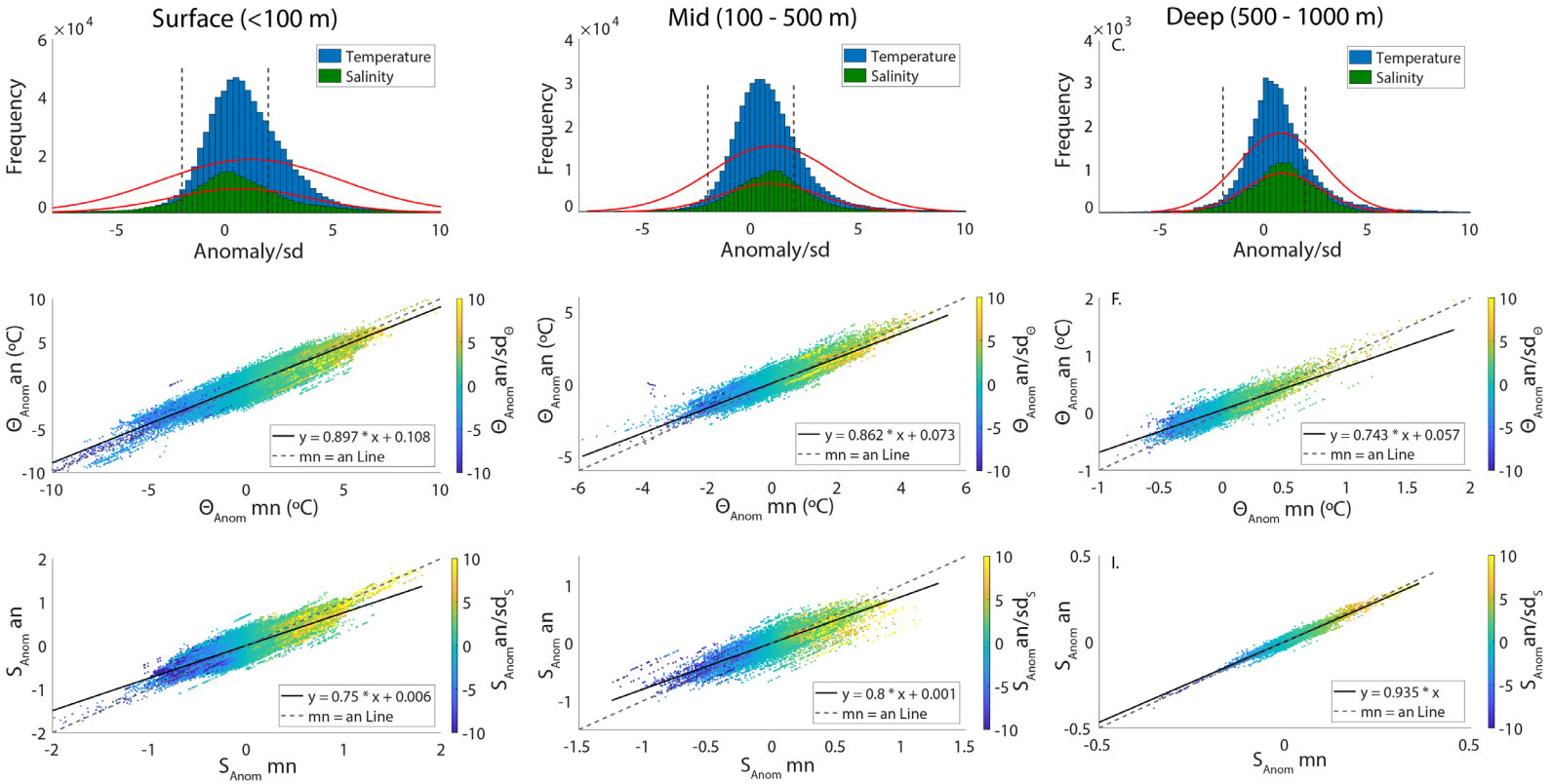

Fig. 1.2 - Distribution and scatter of all temperature and salinity anomaly data in surface (<100 m), mid (100-500 m), and deep water (500-1000m). Histograms are of temperature and salinity anomalies normalized to error with red lines indicating a normal distribution for each. Dashed vertical lines indicate ± 2sd. Lower panels show scatter in anomalies calculated by measured (mn) and modelled (an) climatology values, with linear regression (solid) and 1:1 (dashed) lines. Color scale indicates anomaly normalized to sigma, as in histograms.

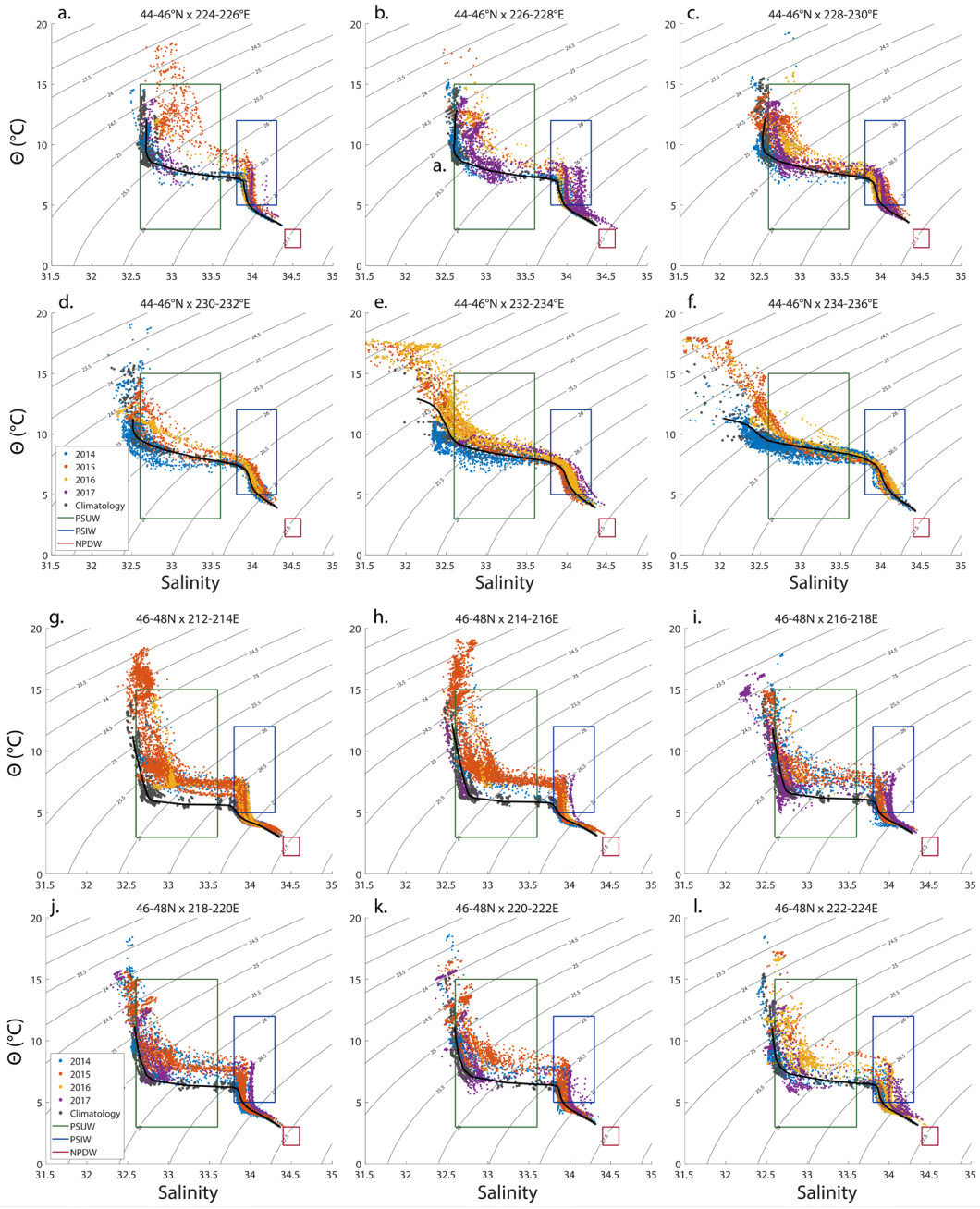

Fig. 1.3 - Temperature-salinity plots of data collected by elephant seals from 2014-2017 within core Blob region (see Fig. 1.1b). Each figure represents a 2°x2° box in which data were collected from 0-1000 m depth. Contour lines show density anomaly (σ_θ) calculated at 0 m depth. Grey dots show all climatology values corresponding to the locations and months of data collected. The black line is the mean climatology, weighted to match the distribution of observed values. Water mass T/S ranges are indicated with boxes: Pacific Subarctic Upper Water (0-500 m, green), Pacific Subarctic Intermediate Water (500-1500 m, blue), and North Pacific Deep Water (1500-3000 m, red).

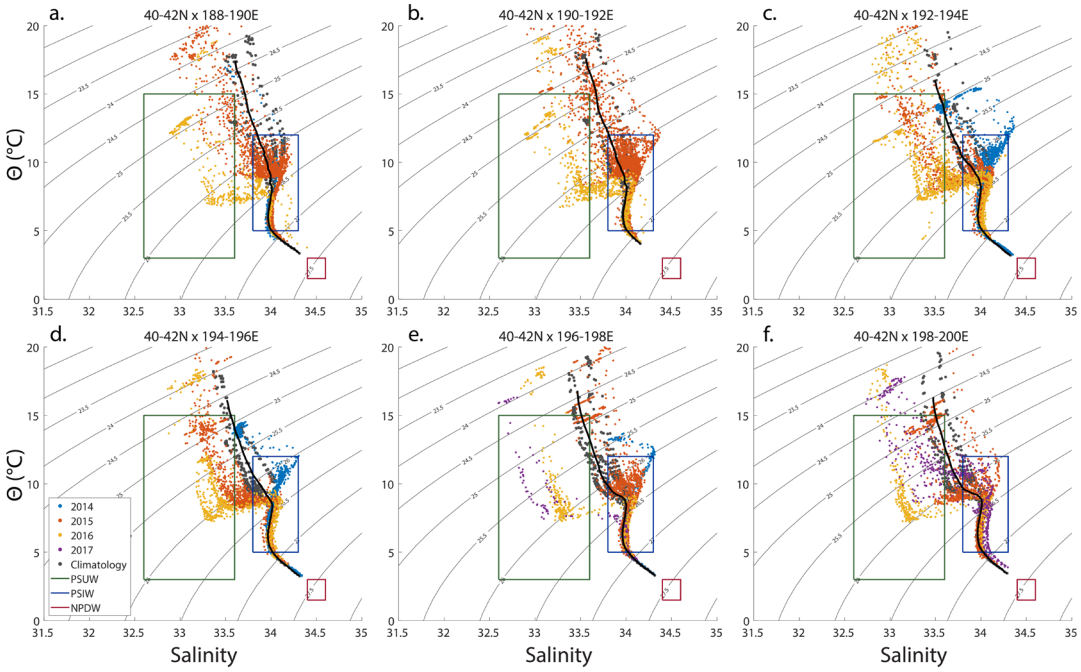

Fig. 1.4 - Temperature-salinity diagrams of data collected by elephant seals from 2014-2017 outside of core Blob region (see Fig. 1b). Each figure represents a 2° x 2° box in which data were collected from 0 - 1000 m depth. Contour lines show density anomaly (σ_θ) calculated at 0 m depth. Grey dots show all climatology values corresponding to the locations and months of data collected. The black line is the mean climatology, weighted to match the distribution of observed values. Water mass T/S ranges are indicated with boxes: Pacific Subarctic Upper Water (0-500 m, green), Pacific Subarctic Intermediate Water (500-1500 m, blue), and North Pacific Deep Water (1500-3000 m, red).

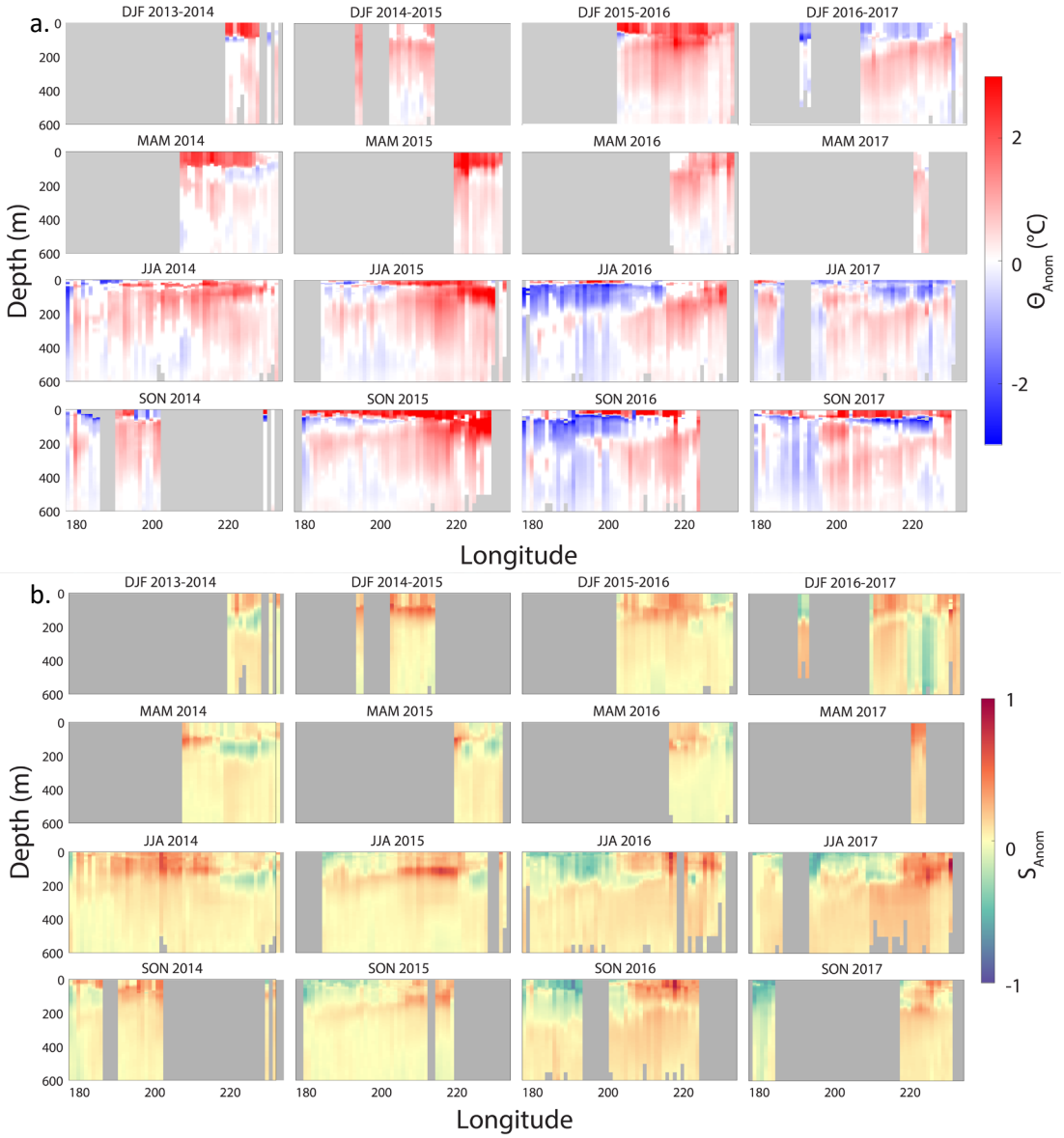

Fig. 1.5 – Depth (0-600 m) by longitude sections of conservative temperature anomaly (a) and salinity anomaly (b) averaged at 1° longitude. Each section includes all data from 40-44°N (dashed box in Fig. 1.1) during a 3-month season, starting from Dec 2013 – Nov 2017. Grey indicates data gaps.

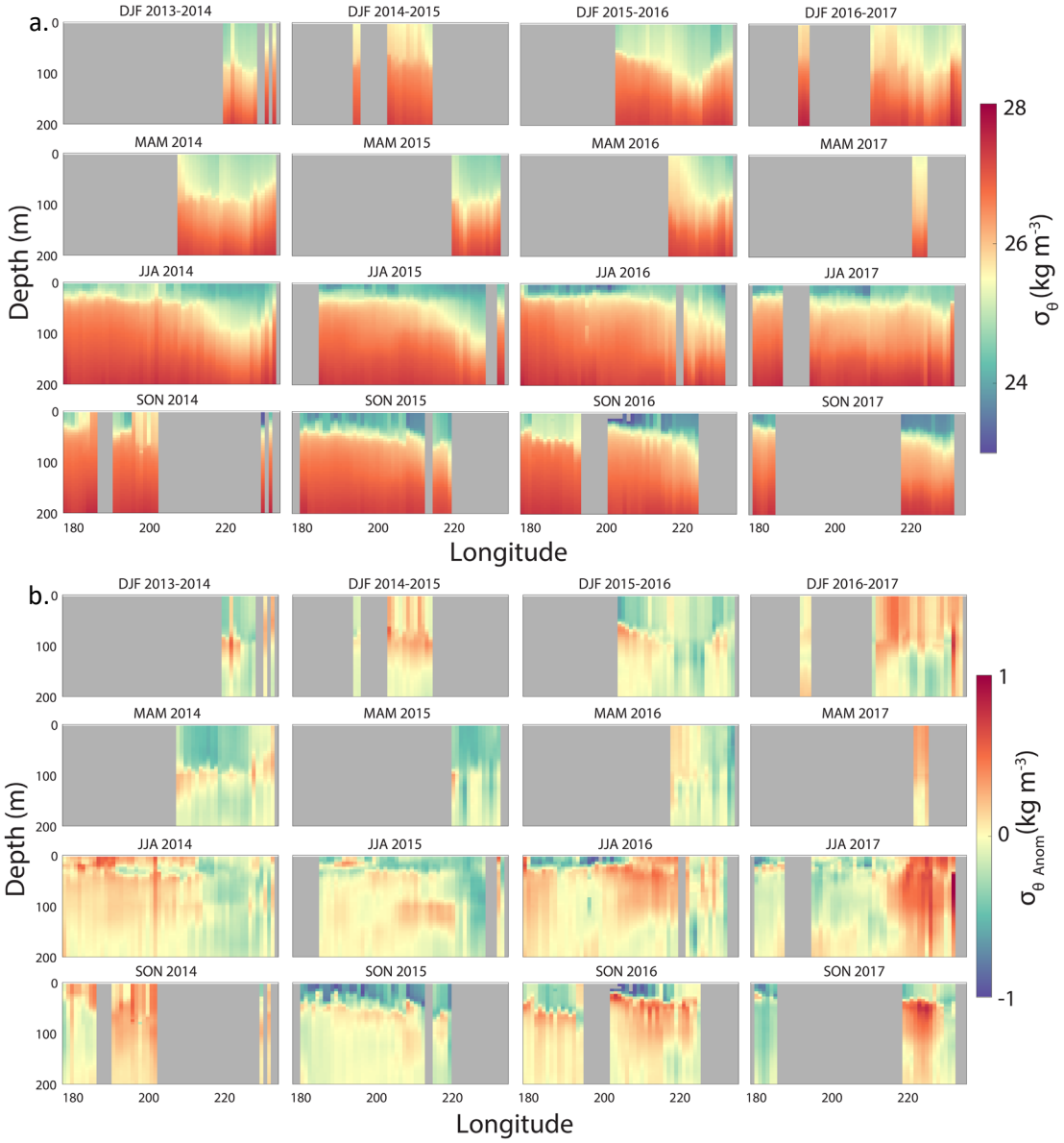

Fig. 1.6 – Depth (0-200 m) by longitude sections of (a) σ_θ and (b) σ_θ anomaly averaged at 1° longitude. Each section includes all data from 40-44°N (dashed box in Fig. 1.1) during a 3-month season, from Dec 2013 – Nov 2017. Grey indicates data gaps.

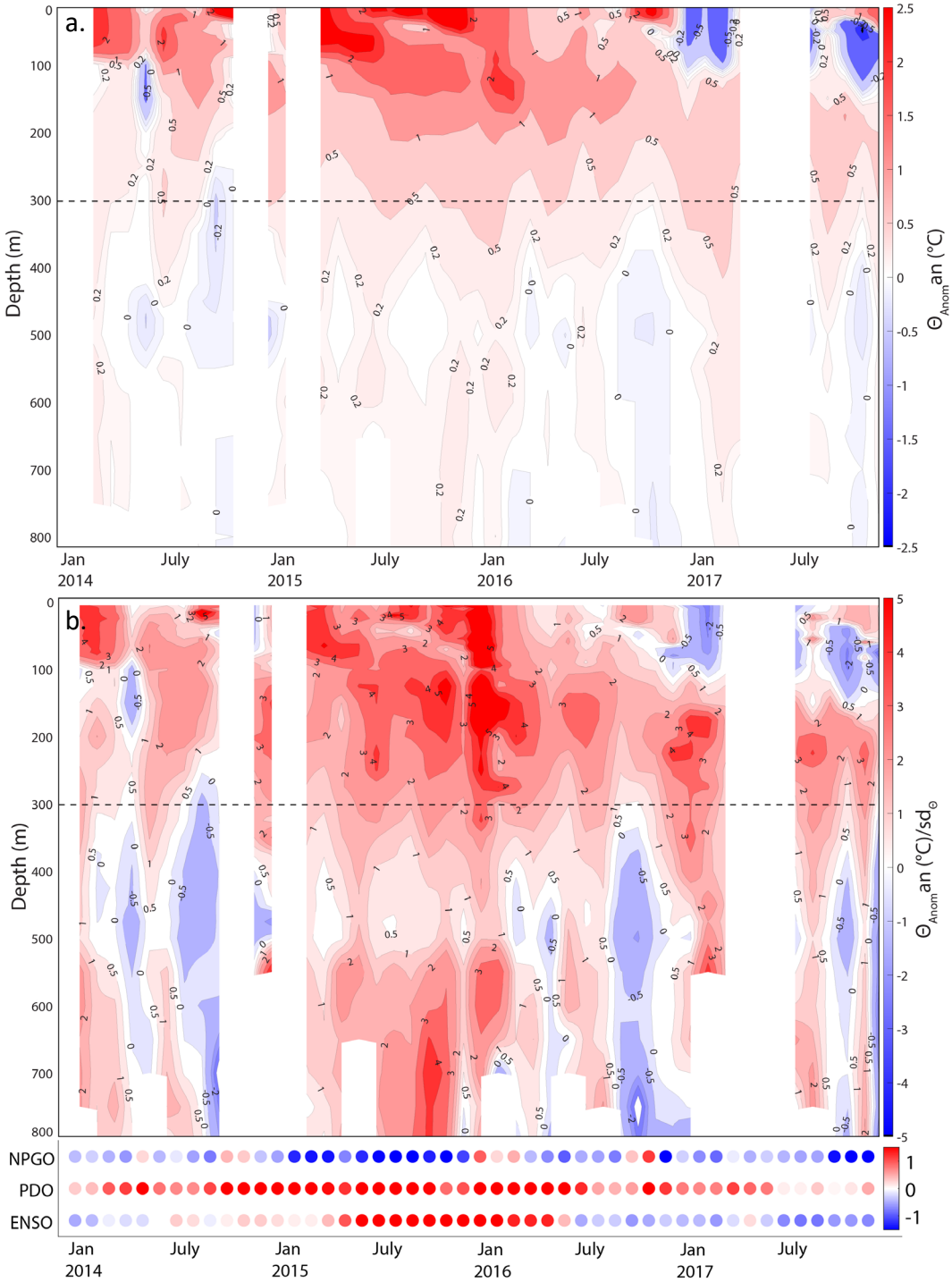

Fig. 1.7 - Monthly averaged temperature anomaly (a) and standardized anomaly (b) within the core region of the Blob (40-50°N x 150-130°W, solid box in Fig. 1) from Jan 2014-Dec 2017. Solid white sections indicate periods when no data were collected within the geographic range. Dashed black lines are 300 m depth reference. Corresponding NPGO, PDO, and ENSO indices are indicated at the bottom.

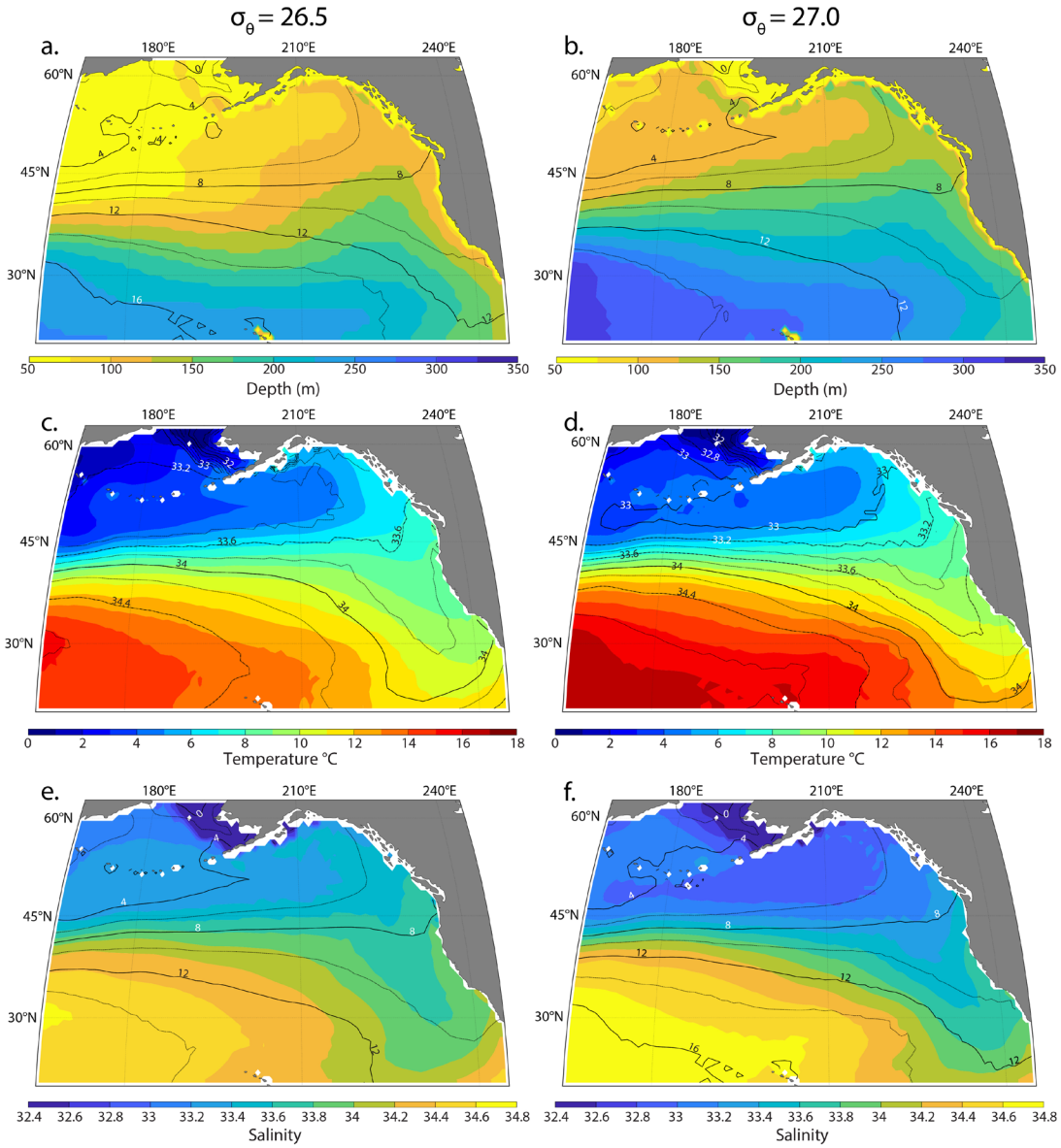

Fig. 1.8 - Distribution of climatological depth (a & b), temperature (c & d), and salinity (e & f) on isopycnal surfaces σ_θ = 26.5 (left) and σ_θ = 27.0 (right). Color shows primary variable, overlaid contour lines on depth and salinity maps show temperature, and contour lines on temperature maps show salinity.

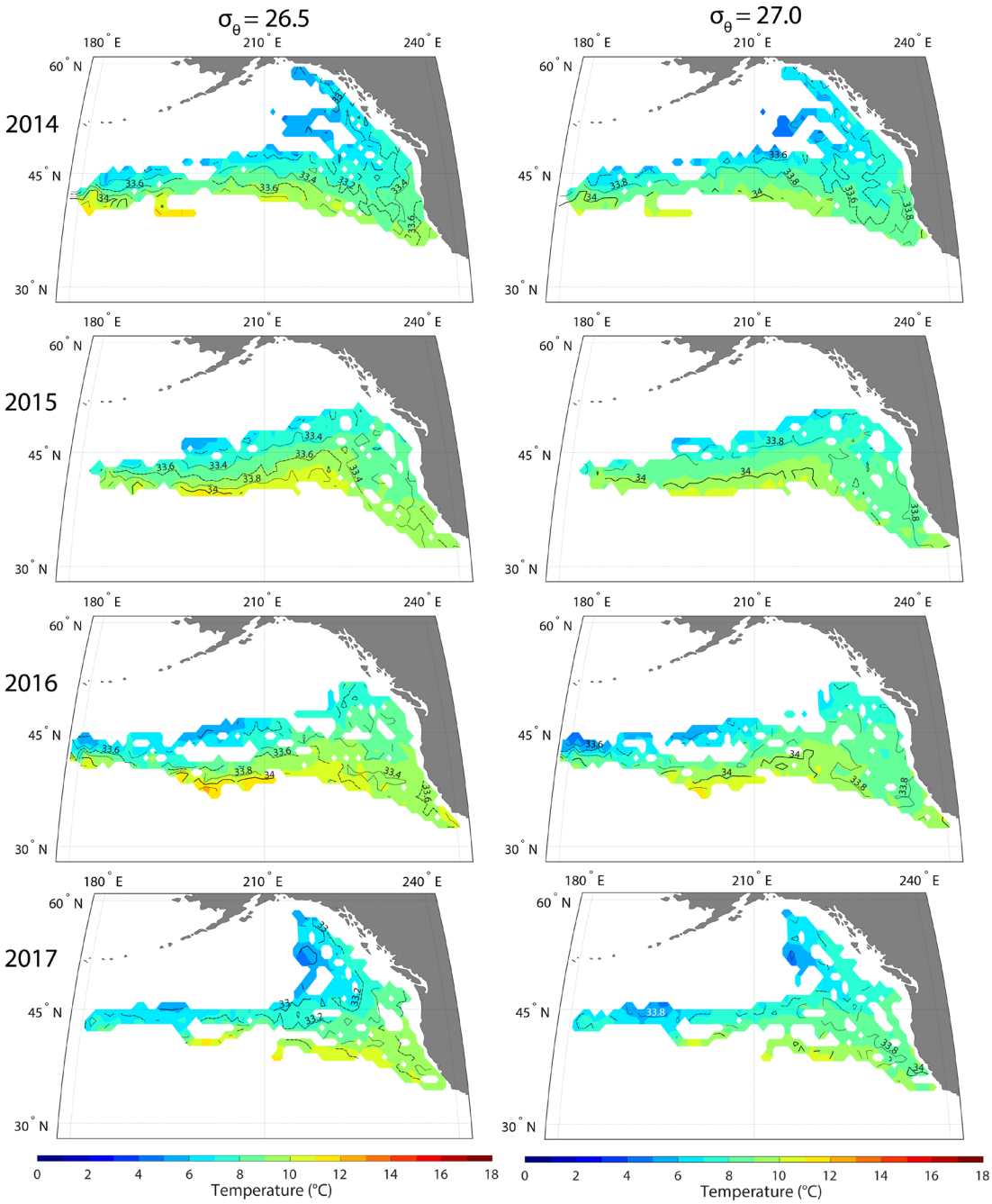

Fig. 1.9 – Temperature and salinity on isopycnal surfaces σ_θ = 26.5 (left) and σ_θ = 27.0 (right) in 2014-2017. Color contours indicate temperature, overlaid lines are salinity contours.

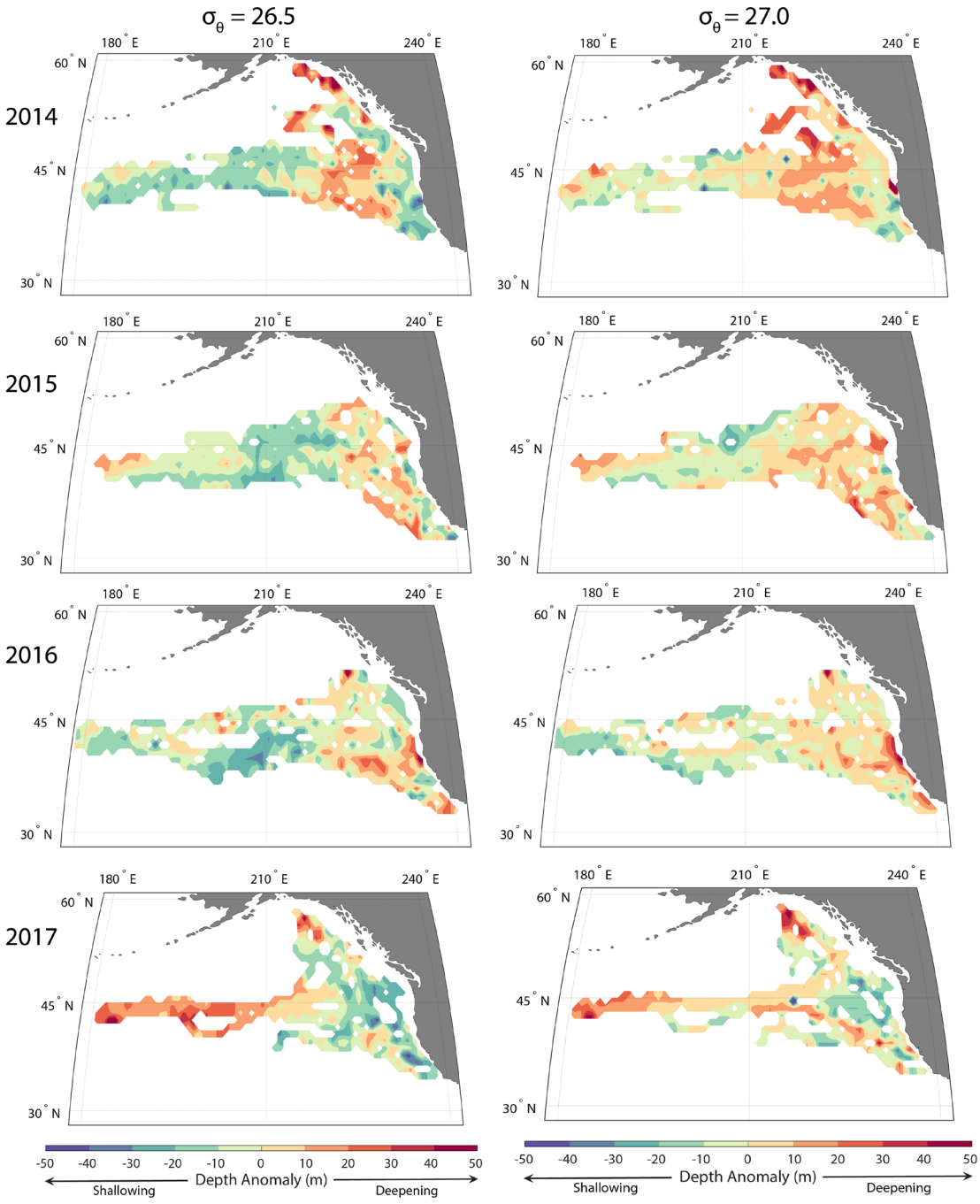

Fig. 1.10 – Depth anomaly of isopycnal surfaces $\sigma_\theta = 26.5$ (left) and $\sigma_\theta = 27.0$ (right) in 2014-2017 compared to climatology (WOA18 annual, 1981-2010).

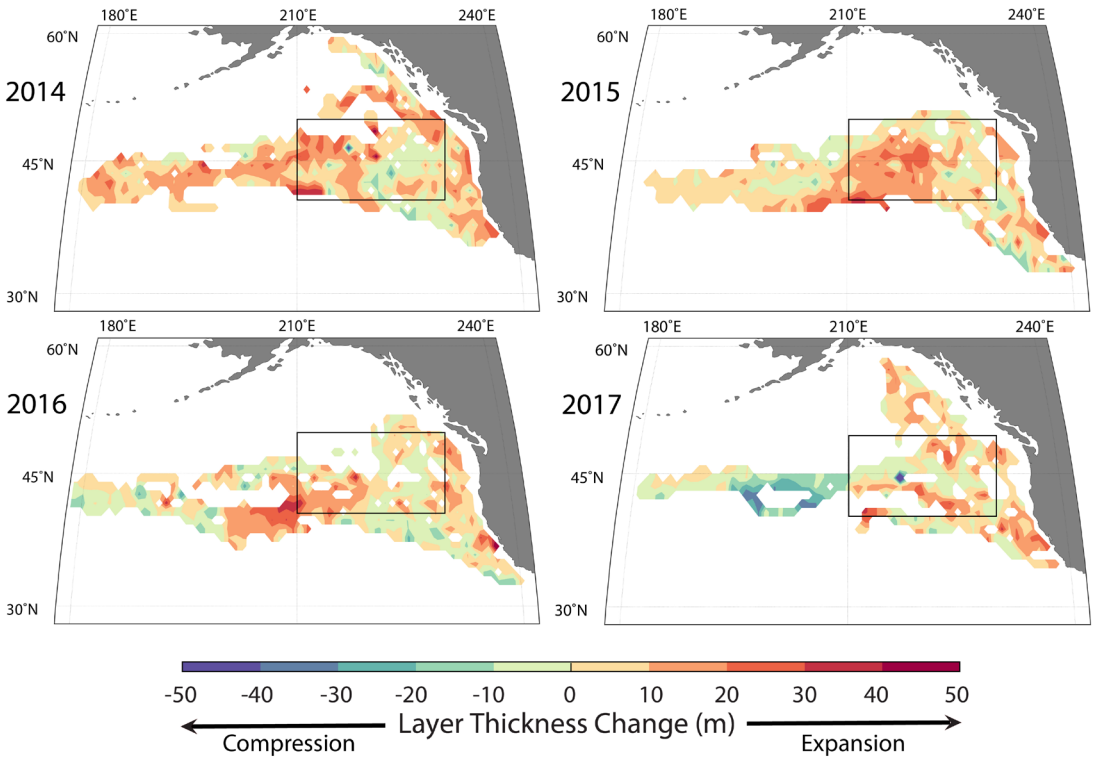

Fig. 1.11 - Spreading and compression of the water column between isopycnals $\sigma_\theta = 26.5$ and $\sigma_\theta = 27.0$ in 2014-2017 relative of climatology, calculated as the difference in depth anomalies between density surfaces, as shown in Fig. 10. Boxes indicate core Blob region.

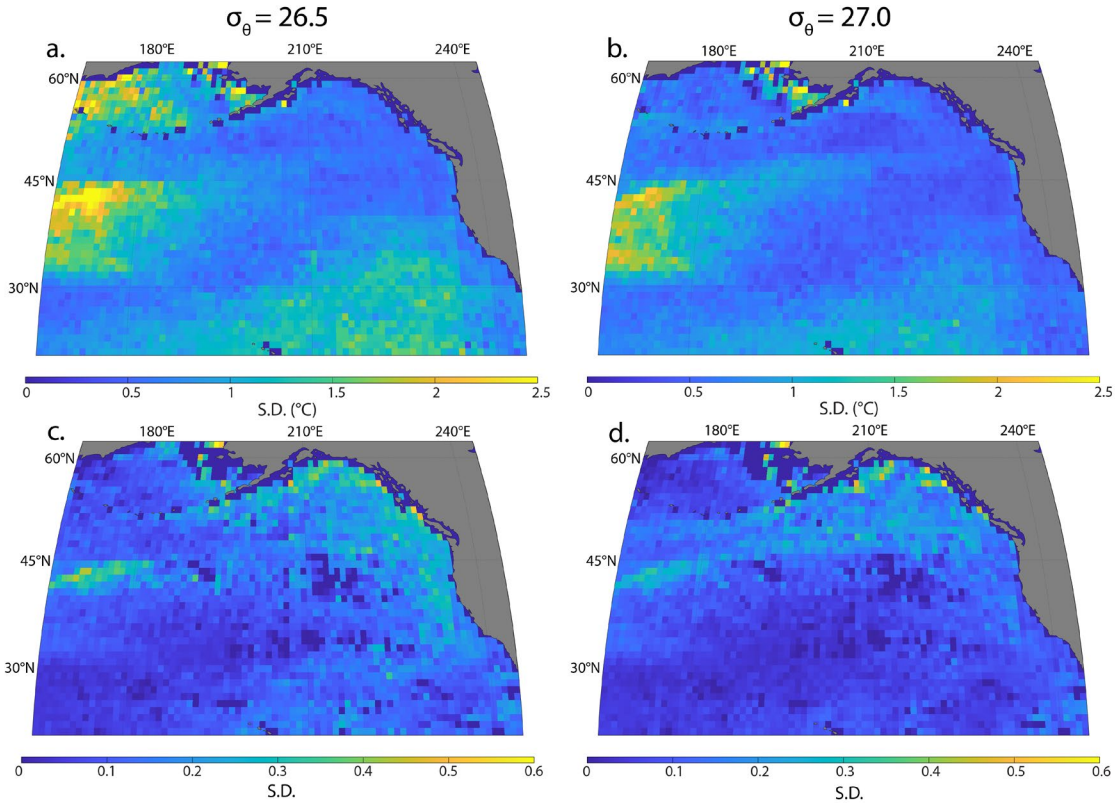

Fig. 1.12 - Distribution of climatology sd in temperature (a&b) and salinity (c&d) on isopycnal surfaces $\sigma_\theta = 26.5$ (left) and $\sigma_\theta = 27.0$ (right).

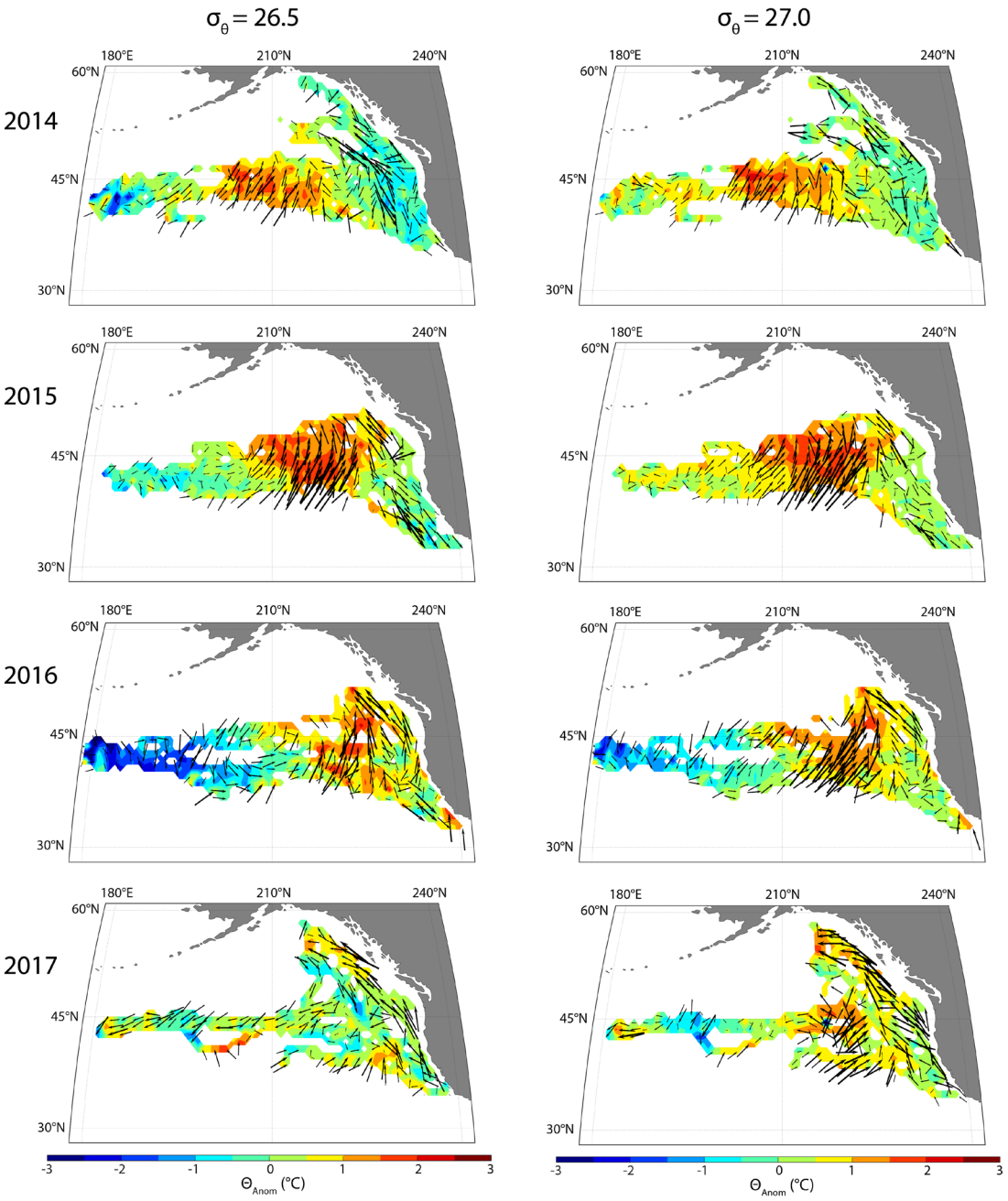

Fig. 1.13 – Mean conservative temperature anomaly on isopycnal surfaces $\sigma_\theta = 26.5$ (left) and $\sigma_\theta = 27.0$ (right) with arrows indicating advection from climatology (WOA18 annual, 1981-2010) required to account for observed spice anomalies in each year. Arrows were calculated on a 1x1° grid, but only every other longitude is displayed for visual clarity.

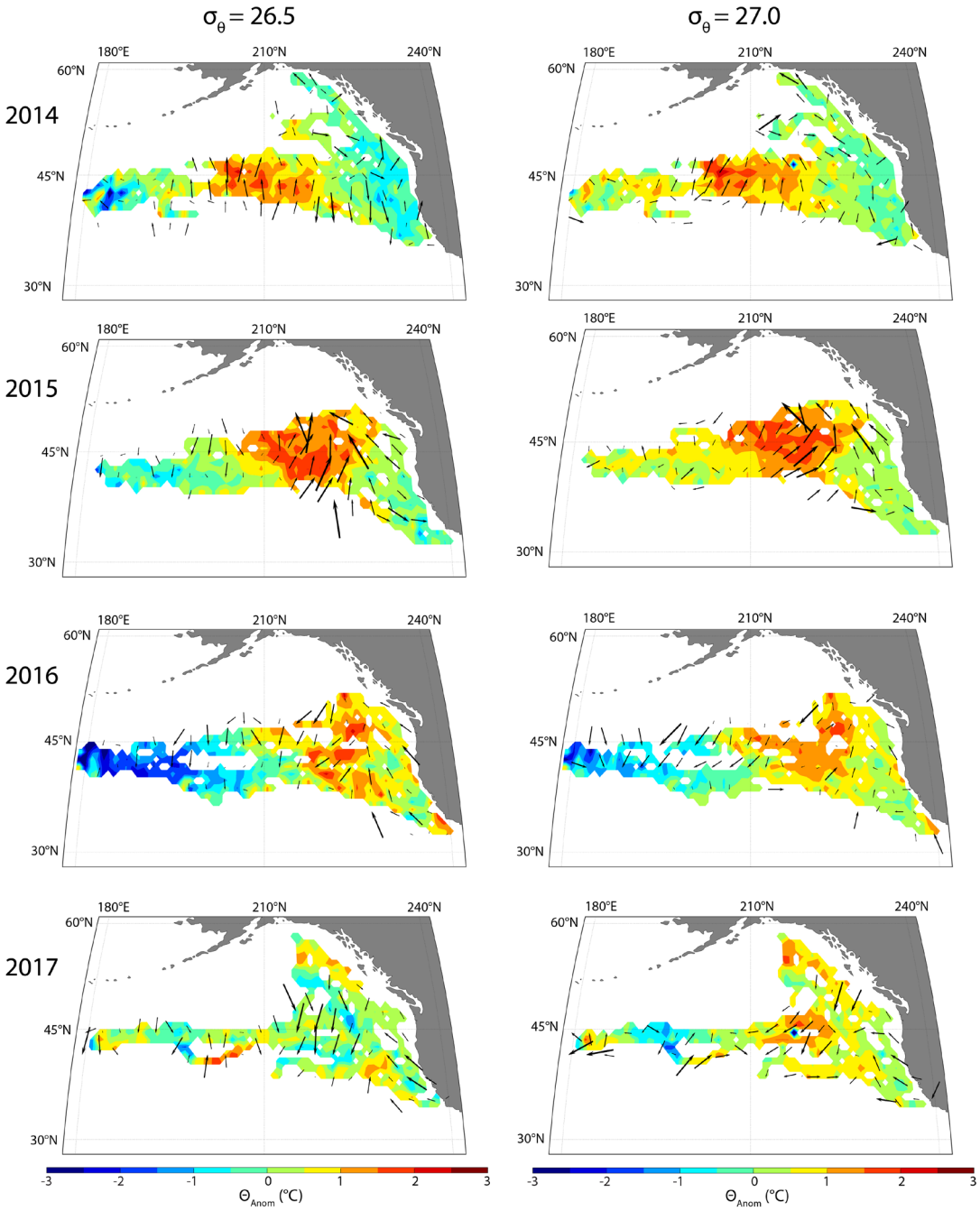

Fig. 1.14 – Mean conservative temperature anomaly on isopycnal surfaces σ_θ = 26.5 (left) and σ_θ = 27.0 (right). For 2014, arrows indicate advection from climatology (WOA18 annual, 1981-2010) required to account for observed spice anomalies. In subsequent years, arrows indicate advection from climatology minus movement from prior year, averaged to a 3x3° grid.

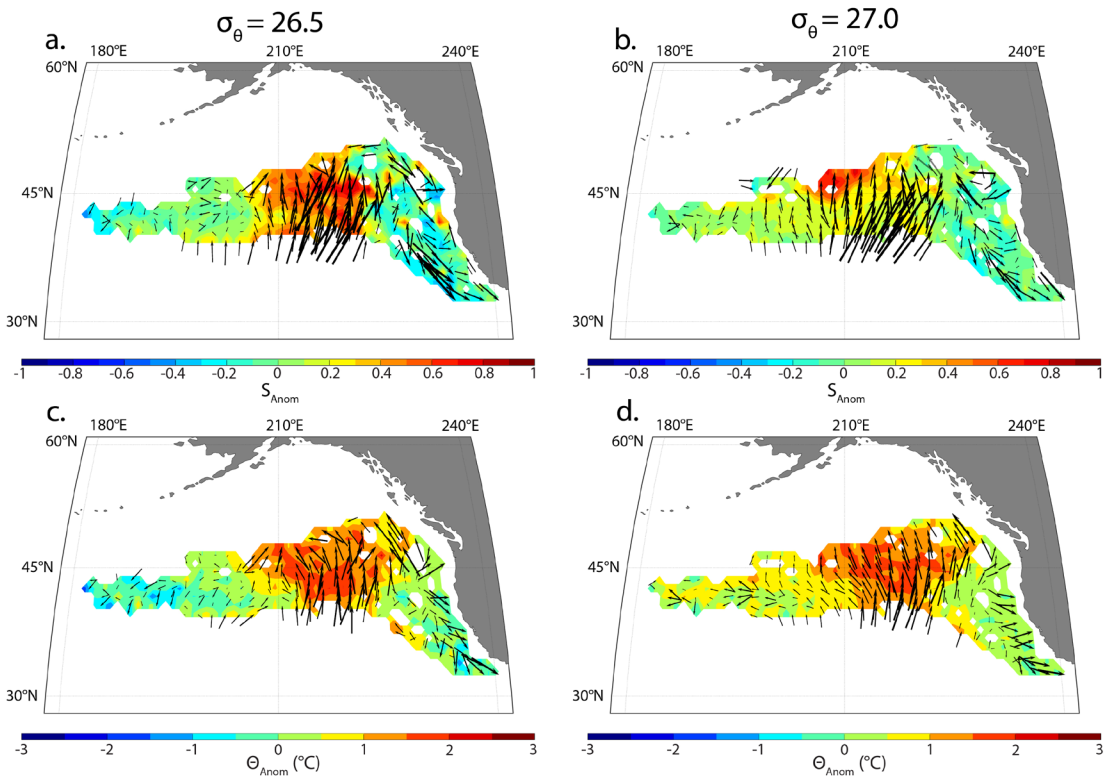

Fig. 1.15 – Arrows generated using only salinity (a & b) and only conservative temperature (c & d) on isopycnal surfaces σ_θ = 26.5 (left) and σ_θ = 27.0 (right) in 2015. Color is mean salinity anomaly (a & b) or mean conservative temperature anomaly (c & d).

Chapter 2: Response of a generalist marine predator to the Northeast Pacific Blob 2015 marine heatwave

Rachel R. Holser, Luis Hückstädt, Daniel E. Crocker, Theresa R. Keates, Chandra Goetsch, Birgitte I. McDonald, Sarah E. Peterson, Patrick W. Robinson, Daniel P. Costa

2.1 Abstract

Northern elephant seals are wide-ranging predators that forage on the abundant biomass of the mesopelagic Northeast Pacific Ocean. Their generalist strategy may buffer the effect of environmental changes on their population. Here we examine the distribution, foraging behavior, and changes in body condition of adult female elephant seals during the Northeast Pacific Blob 2015, a marine heatwave that caused extensive ecosystem disturbance. We observed a plastic behavioral response, where, surprisingly, females increased their lipid stores during both annual foraging trips compared to non-heatwave years. There was an increased use of the Alaska Gyre, increased daytime foraging effort, and a substantial increase in deep diving behavior (>800 m depth), all suggesting that the prey field changed relative to previous years. The ability to alter behavior in response to environmental change will be critically important in allowing elephant seals to adjust as the ocean climate changes. Our findings indicate that northern elephant seals may be more capable of coping with a warming ocean than some other predator species, who experienced mass mortality or reproductive failure during the same warming event. Their broad diet and extensive foraging range allow them to succeed where more specialized species do not.

2.2 Introduction

Extreme climate events, from landslides to droughts, can have ecosystem-scale effects, triggering changes in productivity, species distribution and abundance, and trophic dynamics [1,2]. The frequency, magnitude, and longevity of extreme climate events are increasing due to climate change [1,3]. Understanding how these episodic events affect species' ecology is essential for accurately forecasting ecosystem dynamics [1]. Marine heatwaves are extreme climate events that pose a great risk to marine ecosystems, as marine biogeochemical processes are particularly sensitive to changes in temperature [4-7]. Increasing water temperature alters mixing and circulation, nutrient availability, and content of dissolved gases, all of which affect the biological system [8]. Furthermore, marine organisms are often more vulnerable to warming than their terrestrial counterparts [9].

During the winter of 2013-2014, anomalously warm sea surface temperatures developed in the Northeast Pacific Ocean (NEP) and persisted at the surface through 2015 and in the sub-surface water column through 2017 [10-12]. This marine heatwave, the Northeast Pacific Blob 2015 (the Blob) [13], was the largest marine heatwave on record. It resulted from unusually high sea level pressure anomalies that resulted in suppressing heat loss and weakened cold-water advection in the surface ocean [10,12]. The Blob was categorized as a severe marine heatwave based on its duration and magnitude [13]. In 2015, anomalous surface temperatures up to 6.5°C, or 4.8σ (standard deviations) above the climatological mean, were seen [11]. Sub-surface anomalies of 0.5°C, 2.0σ above climatology for the depth, were widespread at 300-500 m depth in 2015-2017, even after the surface warming had subsided [Chapter 1].

The Blob caused ecosystem-level disturbance across the Northeast Pacific. This is a region of high productivity: where cool, nutrient-rich waters fuel high levels of productivity, while physical features (fronts, eddies, etc.) concentrate prey into regions, making them available to apex predators [14, 15]. There was an extreme depression in chlorophyll content in early 2014 [16], and the assemblage of both diatoms and copepods shifted to primarily warm-water taxa [17]. These taxa are comparatively low in lipid content, reducing the efficiency of energy transfer to mid-[18,19] and upper-[20,21] trophic levels, at times with devastating effects. Cassin's auklets (*Ptychoramphus aleuticus*) and common murres (*Uria aalge*) experienced mass mortality events from throughout the region due to lack of prey [21, 22]. In addition to trophic effects, there were record-level harmful algal blooms along the U.S. west coast [17, 23, 24], and numerous reports of shifts in distribution and abundance of various vertebrate and invertebrate species [25].

The NEP is characterized by a deep oxygen minimum zone (OMZ) that concentrates prey species in the deep scattering layer [26, 27]. The upper boundary of hypoxia levels (cat. B: [O_2] <1.4 mL/L; <30% saturation) is found between 200-800 m of depth, with shallower upper boundaries in the Pacific Subarctic Gyre and waters closer to the continental margin [28]. This layer of low-oxygen water is hundreds of meters thick, with severely hypoxic [O_2] levels (cat. C: [O_2] <0.5 mL/L; <10% saturation) at 800-1200 m depth [28], that can act as a physical barrier, preventing prey from accessing deeper water. Additionally, some prey species may use the OMZ as a refuge from larger, predatory fish that require well-oxygenated water to fuel quick movement in pursuit of prey [29]. Air-breathing predators, like elephant seals, are not physiologically limited by the oxygen content of the water, therefore prey species taking refuge in the OMZ would

be especially vulnerable to predation from these species. OMZs are expected to expand as global oceans continue to warm, causing oxygen depletion. How marine heatwaves cause short-term changes in OMZ structure because of altered mixing, water temperature, and biological activity, remains unknown, although oxygen depletion would be expected in surface waters [30].

This unusual event provides an opportunity to examine the response of populations to the changing climate, and specifically how marine heatwaves will affect organisms beyond changes resulting from baseline warming. Most taxa respond negatively to marine heatwaves, although highly mobile species are less susceptible as they can avoid unfavorable areas [4]. Similarly, generalist predators might be better able to compensate for the ecological disruptions caused by marine heatwaves due to their ability to forage opportunistically [31]. Some marine predators exhibit behavioral plasticity, modifying their foraging behavior based on the physical properties of the water they encounter (i.e., thermal structure, eddy activity, oxygen content), as these characters influence the abundance and distribution of prey [32-35]. Behavioral and physiological plasticity allows individuals to adapt to changing demands and conditions. Still, only within the constraints of their phenotype [36], and marine heatwaves may push the limits of many species' capabilities.

Elephant seals (*Mirounga sp.*) are generalist mesopelagic predators and are the largest, deepest diving pinnipeds. They spend up to ten months of the year foraging, building up the necessary body stores to sustain themselves during the time spent on shore breeding and molting [37,38]. The northern species (*M. angustirostris*) has colonies from Baja California, Mexico to British Columbia, Canada, and their foraging range extends

throughout the NEP. Adult female northern elephant seals concentrate their foraging effort around the subtropical-subarctic gyre boundary, an area characterized by converging water masses resulting in subsurface temperature inversions and chlorophyll maxima [38,39]. They are also known to use the deep OMZ as a foraging strategy [35]. Shifts in ocean conditions have caused this species to alter its foraging behavior and affect foraging and reproductive success. During the 1998 El Niño, adult females extended their foraging trips to compensate for reduced rates of energy gain, although natality during the 1999 breeding season was still unusually low [40]. Each year since 2004, 19-45 adult female elephant seals have been tracked (N=579), providing an ideal dataset to test the effect of a marine heatwave on foraging behavior.

Here, we examine how the foraging behavior of a generalist predator differed during the Blob as compared to other years. We use biologging and body composition data collected from 2004-2019 to explore differences in distribution, diving, and foraging success in adult female northern elephant seals. We hypothesize that during the Blob: (1) their distribution will shift northward to avoid the warmest region of the anomaly; (2) they will increase foraging effort to compensate for poor conditions; and (3) their foraging success will be similar or slightly reduced. Long-term movement and behavior datasets are rare, but they can provide powerful insight into a species' response in changing conditions.

2.3 Methods

2.3.1 Study Site and Ethics

This study was conducted at the northern elephant seal colony at Año Nuevo State Park, San Mateo County, California, U.S.A. All animal handling was done under NMFS permits

#786-1463, 87-143, 17952, and 19108 and with the approval and oversight of the UCSC Institutional Animal Care and Use Committee.

2.3.2 Data Collection

Adult female foraging behavior was measured using various instruments to track ~20 individuals during both the post-breeding and post-molting foraging trips from 2004 onward (Table 2.1). Each animal was sedated following standard protocols [38] and equipped with a time-depth recorder programmed to collect diving data at least every 8 sec and with a satellite tag providing Argos and/or GPS locations [41]. Upon returning to shore, individuals were sedated again for instrument recovery. Breeding animals were handled ~5 days post-partum to minimize the impact of handling on the pup.

Body composition and energy gain were calculated following the methods detailed in Robinson et al. [38]. Briefly, during both deployment and recovery sedations, morphometric measurements, including weight, blubber depths, lengths, and girths, were collected and body composition was calculated using the truncated cones technique [42]. Body mass was corrected for mass loss associated with fasting and lactation and for variation in the time spent onshore before and after measurements were taken. Mass of the pup at birth was added to female mass gain for post-molt females. Departure from and arrival at the colony was determined from instrument records, and during the breeding, season animals were resighted daily after arrival to assess whether they had given birth.

2.3.3 Data Processing

Data Processing and statistical analyses were completed in R 3.6.1 [43] and MATLAB R2019b. Raw location data were filtered and processed using the MATLAB toolbox IKNOS [38] and the R package Crawl [44] to eliminate erroneous location points and interpolate between locations, generating a realistic track of the animal's movement. For each segment of the track, the distance between locations and distance from the colony was calculated using lldistkm.

The IKNOS toolkit was used to calculate summary dive statistics (depth, duration, ascent and descent rates, bottom time, bottom wiggles, post-dive interval) and to determine dive type (foraging, benthic, transit, or drift) for each dive. All dive records were subsampled to 8-sec intervals so that statistics were comparable across all deployments. Geographic locations for each dive are determined using a linear interpolation between points of the Crawl-processed satellite track. Solar elevation was calculated for each dive using location and Julian date/time to allow the diel analysis of behavior.

Elephant seals exhibit drift dives, which can provide information on foraging success and changes in body composition throughout their foraging trips [45,46]. Drift rates were calculated using previously established methods [46]. Drift rate data are inherently noisy as the measurement is highly sensitive to an animal's orientation and drag [45], so additional filtering is needed before analysis [46]. For each foraging season, drift rates outside of 2.5σ of the grand mean were removed. Each record was then filtered using a 15-day moving window with 5-day steps. Data outside of 2σ of the window mean were flagged for removal at each step.

2.3.4 Analyses

The sample sizes for all data sets are compiled in Table 2.1. Interannual differences in foraging success metrics were evaluated using Welch's t-tests, ANOVA with post-hoc Tukey test, linear models (LMs), generalized additive mixed-effects models (GAMMs) using R packages lme4 [47], mgcv [48], and MuMIn [49]. Data presented are mean ± σ unless otherwise stated.

Spatial variation was calculated separately for the two foraging trips. We used kernel densities of all tracks from 2014 and 2015 and calculated a difference in density from the Blob to a randomly selected, equal-sized subset of tracks from all other years (2004-2013 and 2016-2018). This process was repeated 1000 times for each trip to ensure the differences seen were not the result of sampling bias between years.

To examine population shifts in foraging behavior, we calculated mean dive statistics from all records excluding 2014 and 2015 to generate a behavioral "climatology." We then used all records from 2014 and 2015 to characterize their behavior during the Blob. Statistics calculated included dive depth, duration, bottom time, bottom wiggles, total vertical distance, bottom range, and drift dive depth. Elephant seals' behavior responds to both diel and seasonal patterns in prey availability, so mean values for each hour of the day, each day of the year were calculated. For dive metrics related to foraging behavior, we excluded all drift dives as well as the first and last 100 dives from each record (cross-shelf transit when arriving/departing the colony) to eliminate clear non-foraging behavior. To characterize water column use, for each day of the year, we calculated the frequency of max depth (binned to 10 m), normalized to the total number of dives recorded that day. Lastly, we calculated daily values for mean drift rate, bottom range,

and total vertical distance, as well as the frequency of drift dives and bottom wiggles. Both drift dive and bottom wiggle frequency were normalized by the number of contributing animals, so that time periods were comparable. We excluded all values between the mean arrival and departure dates for the two foraging trips (see S1; Jan 9–Feb 16 and Apr 30–Jun 8) as these in-between periods exhibit unrealistic patterns due to the temporal overlap between arriving and departing individuals.

2.4 Results

2.4.1 Foraging Success

Estimate energy gain rate (MJ day^{-1}) was significantly higher during the Blob across both post-breeding (p=0.02) and post-molting (p=0.003; Table 2.2) foraging trips. Furthermore, females had higher adipose content at recovery during the Blob during the post-molt ($p<<0.001$).

Foraging success during post-breeding trips varied little except for 2014 (Table 2.2, Fig. 2.1). Energy gain rate and mass gain were both significantly higher in 2014 than in other years (ANOVA, $F_{14,\ 230} = 3.29$, $p<0.05$; Tukey's HSD, $p<0.05$). Foraging success, as measured by percent adipose tissue at recovery, varied over the post-molt trip (ANOVA, $F_{14,\ 213} = 8.24$, $p<<0.001$). The highest increases in adipose tissue occurring during 2009, 2014, and 2015 (Tukey's HSD, $p<0.05$), while mass gain has remained consistent (Table 2.2, Fig. 2.1). This difference held when only reproductive females were included in the analysis (S2), and therefore was not an artifact of the high number of skip breeding females in 2014. Furthermore, reproductive post-molt females in 2015 had lower lean mass gain than in other years (ANOVA, $F_{14,\ 179} = 2.64$, p=0.0016; Tukey's HSD, $p<0.05$; S2).

There was also significant variability in energy gain rate (ANOVA, $F_{14,\ 213} = 3.11$, $p<<0.001$), with 2007 significantly lower than other years (Tukey's HSD, $p<0.05$).

2.4.2 Distribution and Movement

The post-breeding movement of females in 2014 and 2015 showed a shift to the north and east of the species' range (Fig. 2.2, left panels), nearer the continent than typically observed. During the post-molt foraging trip, there was an increase in the use of areas north of 45 degrees (the sub-Arctic gyre) and at the western edge of the typical distribution (Fig. 2.2, right panels). In addition, there was a significant increase in the mean distance traveled during the post-molt trip across the time series (LM; $F_{14,223} = 5.022$, p=3.91e-08, Adjusted $R^2 = 0.144$; Table 2.2, Table 2.3, S3), although the maximum distance from the colony did not vary between years.

2.4.3 Diving Behavior

Post-Breeding (Feb-May)

Seals increased the use of shallower depths for non-drift diving during the Blob (Fig. 2.3C), which corresponded to a shoaling in overall daytime dive depth (581 ± 24 m vs. 617 ± 20 m, $p<<0.001$, Fig. 2.4C), an increase in the frequency of daytime wiggles (30.7 ± 4.4 vs. 27.9 ± 2.4, $p<<0.001$, Fig. 2.5), shallower peak depth use and higher peak intensity during both night and day (Fig. 2.6, S4, and S5), and a decrease in bottom range (103 ± 11 m vs. 111 ± 7 m, $p<<0.001$, S6). There was no significant change in dive duration (Fig. 2.7), bottom time (S7), dive efficiency (S8), the frequency or temporal distribution of drift dives (S9), or drift rate (Fig. 2.3D).

Early Post-Molt (Jun-Sept)

There was an increase in the use of both shallower and deeper depths used during non-drift diving in the early post-molt (Fig. 2.3, Fig. 2.6). Daytime diving during the marine heatwave was dominated by an increase in the use of depths greater than 800m (Fig. 2.3C, Fig. 2.6, Fig. 2.7, S4). This deep-diving behavior did not correspond with an increase in dive duration (Fig. 2.8). Consequently, there was also a reduction in daytime bottom time (8.2 ± 1.0 min vs. 9.8 ± 0.8 min, $p<<0.001$, S7), dive efficiency (0.31 ± 0.02 vs. 0.37 ± 0.01, $p<<0.001$, S8), and bottom wiggles (20.7 ± 3.3 vs. 23.4 ± 2.1, $p<<0.001$, Fig. 2.3E) during the first half of the post-molt trip during the Blob. This deep-diving strategy is visually distinct (e.g., Fig. 2.7) in individual dive records and was used by most individuals (68%) the Blob. This deep-diving ends abruptly mid-way through the foraging trip in all cases, which coincides with drift rates approaching neutral buoyancy (Fig. 2.3). Modeling shows that individuals exhibit greater deep-diving frequency when their drift rate is lower (Table 2.3).

Late Post-Molt (Oct-Jan)

Shallow depths were used more during the Blob throughout the post-molt foraging trip (Fig. 2.3C), especially at the end of the night in the latter half of the trip, when mean dive depth decreased by ~50m (Fig. 2.4C and Fig. 2.6). The intensity of the peak in daytime dive depth was higher during the Blob (Fig. 2.6, S4), indicating that daytime foraging was more concentrated within the water column. Daytime dives were significantly longer (36.3 ± 1.7 min vs. 34.5 ± 0.8 min; $p<<0.001$, Fig. 2.5C), and shallower (585 ± 49 m vs. 615 ± 34 m, $p<<0.001$, Fig. 2.4C) during the Blob. As a result, bottom time increased (18.5 ± 1.6 min vs. 17.4 ± 0.9 min; $p<<0.001$, S7) during daytime and twilight hours. There was a slight increase in the frequency of wiggles per hour during daytime in 2014-2015 (23.9 ± 3.7 vs. 22.5 ± 2.1 $p<<0.001$; Fig. 2.5B), although overall foraging effort was similar to

non-Blob foraging effort (Fig. 2.3E). The change in drift rate was consistent between the two time periods until the end of the trip when Blob drift rates were higher (Fig. 2.3D), corresponding with higher body composition at recovery (Fig. 2.1, Table 2.2).

2.5 Discussion

2.5.1 Ocean Conditions and Behavior

Many marine predators experienced profound adverse effects on reproduction and survival during the Northeast Pacific Blob 2015 [20-22,50]. Marine heatwaves can reduce productivity and exert physiological controls on all trophic levels resulting in shifts in species assemblages, abundance, distribution, and body condition [4,16,18,19,51]. Such an ecological disturbance will result in a change in behavior or a reduction in reproduction and/or survival [20-22]. Female northern elephant seals are generalists in both their diet and in their vertical foraging strategy at individual and population levels: very few individuals show high levels of dietary specialization [52]. This generalist approach, combined with a capital breeding reproductive strategy, may allow the species to adapt to changing environmental conditions and buffer them from the impact of extreme climate events.

The oceanographic implications of the Blob are not yet fully understood or documented, especially regarding how it may have affected the mesopelagic zone. What has been observed has implications for all species using the NEP, including northern elephant seals. The surface ocean experienced intense warming in the top 100 m, and moderate warming down to 500 m depth, inhibiting mixing and resulting in reduced surface productivity [10,12,16]. Shifts in phytoplankton and zooplankton assemblages were seen in multiple geographic regions, reducing the transfer of energy to higher trophic levels

[24,53,54]. Changes in the OMZ and deep scattering layer were not documented for this event but are likely to have expanded vertically because of ongoing ocean warming [27,29,30]. An expanding OMZ combined with surface warming should cause a shallower and narrower range of suitable night-time habitat for vertical migrating species, resulting in more concentrated aggregations at shallower depths [29]. Finally, there was an expansion of the Alaska Gyre due to a southward shift in the North Pacific Current gyre-gyre boundary during late 2014-2016 [55].

The spatial distribution during post-breeding trips shows a clear shift towards the western boundary of the Alaska Gyre. The OMZ in this region has a shallower upper boundary (Fig. 2.9), which likely contributes to the shallower dive depths seen post-breeding females during both the day and night (Fig. 2.4, Fig. 2.6, S4, S5). This shift in foraging location in 2014 was associated with high rates of mass and energy gain, along with an increase in relative fat content from deployment to recovery, indicating that prey were more available (Fig. 2.1). During 2015, foraging success was within the normal range despite the northward shift in foraging location. The increase in daytime dive bottom wiggles, a proxy for foraging effort [56,57], indicates a greater abundance of prey items, especially around 600 m of depth during daylight hours (Fig. 2.6), which is the upper depth of severely hypoxic ($[O_2]$ <0.5 mL/L) conditions based on oxygen climatology (Fig. 2.9). The increase in daytime foraging effort could indicate either an increased density of typical prey items or a shift in prey type. For example, smaller prey in dense patches could result in more prey capture attempts per dive. Alternately, they may have encountered prey that was more active and required more effort to capture.

The post-molt foraging trips showed a more complex shift in both behavior and foraging success, which together implies a profound change in prey distribution and/or types during the summer months when the warm anomaly was at its greatest extent and magnitude. Elephant seal spatial distribution was again more concentrated in the Alaska Gyre, although they did not show increased use of the western boundary, as was seen during post-breeding (Fig. 2.2). While there was no difference in the maximum distance traveled from the colony, there was an increase in the total horizontal distance traveled (Table 2.2, S3), implying that the animals were more nomadic, moving more within their foraging range. This increased movement was not unique to years of the Blob, however, and may indicate longer-term shifts in prey distribution in recent years. In addition to greater use of the Alaska Gyre, the animals made greater use of deep water (700+ m) than seen in non-heatwave years (Fig. 2.3, Fig. 2.6, Fig. 2.7, S4). These daytime deep dives, combined with the reduced foraging effort (bottom wiggle frequency - Fig. 2.5), are a marked departure from previous years and may indicate a shift in prey and increased use of the OMZ. The upper boundary of severely hypoxic water in July-September ranges from 700-1000 m depth in the geographic areas most heavily used by the seals (Fig. 2.9).

Foraging in the OMZ requires deeper diving and more effort over a shorter period. Deep diving is associated with larger prey, as it results in a less efficient dive – greater time spent in transit than in the bottom phase, when most foraging activity occurs [57]. Consequently, the pay-off from successful foraging should be greater to compensate for the increased cost. Mesopelagic fishes exhibit size stratification with depth, with larger individuals generally deeper within a species' vertical range. However, very little is known about the abundance or distribution of prey species below 700 m depth in the NEP

[39,58]. In southern elephant seals, deeper diving and a reduction in foraging time are predicted in areas where the mesoscale activity is expected to concentrate prey [33]. Larger animals are more efficient divers due to their reduced metabolic rate and greater oxygen stores [59]. Body mass was a significant predictor of OMZ use during the post-breeding trip in a subset of northern elephant seals previously studied [35]. The early post-molt use of deep water seen here contradicts that finding, as animals are at their lowest body mass of the year, immediately following the molt. However, we found that deep-diving frequency increases with more negative drift rates (Table 2.3), suggesting that the ability to descend quickly may be more important than size in enabling animals to use a deep-diving foraging strategy when conditions require it.

2.5.2 Dietary Implications

Drift rates, frequency of drift dives, and end-of-trip body condition all provide information about diet and energy balance. Changes in drift rate reflect shifting body composition, which controls an individual's buoyancy, and thereby can indicate day-to-day foraging success while animals are at sea [45,46]. Negative drift rates indicate a leaner, negatively buoyant, body composition. A decline in drift rate can occur either by a loss of adipose tissue due to negative energy balance (insufficient prey) or by an increase in lean tissue from building muscle and viscera tissue during protein-rich foraging.

Foraging elephant seals need to recover sufficient body stores to prepare for one of two physiologically intensive fasting periods: reproduction or molting. Both fasting periods require the turnover of large amounts of lean and fatty tissues to fuel the physiological process. Adult female elephant seals lose up to 27% of their lean tissue during the 26 days

of lactation [60] and ~24% lean tissue during the 42-day molting fast (S11). These values border on Stage III fasting (terminal starvation) in other mammal species, so lean tissue stores are likely the factor that limits elephant seal fast duration and the transfer of energy to offspring [61]. Adult females gain 44.3 ± 17.0 kg of lean tissue (~58% of mass gain) during post-breeding foraging and 184.7 ± 49.0 kg of lean tissue (~70% of mass gain) during post-molt foraging (Table 2.2). While dietary protein can either be used to build lean tissue, fuel metabolism or be converted to fats for storage, dietary fat can only be used as an energy source or be stored as adipose tissue. The balance between these tissue compartments depends on the dietary composition of the prey encountered.

Migrating myctophid fishes are one of the largest components of the elephant seal diet and are present in the greatest abundance in the diet of individuals that use the Sub-Arctic Pacific mesopelagic ecoregion [62], which generally corresponds to the Alaska Gyre [63]. These fish are small (1.0 – 8.4 g), migrate to the surface- or mid-water, and are one of the most energy-rich prey resources available in the NEP mesopelagic (12100 kJ kg^{-1}) [52]. In addition, the Sub-Arctic Pacific diet is characterized by a higher occurrence of non-migrating squid, which are less energy-dense than myctophid species (~3500 kJ kg^{-1}), but much larger (48.65 – 565.0 g), slow-moving, sit and wait predators, making them easy potential targets [52]. Adult female elephant seal field metabolic rate (FMR) while foraging is 90.1 kJ $kg^{-1}d^{-1}$ during post-breeding and 69.4 kJ $kg^{-1}d^{-1}$ during post-molt [64], meaning that an individual would need to consume 30 MJ d^{-1} and 19.6 MJ d^{-1} respectively just to maintain their departure body mass (333 ± 44 kg and 282 ± 36 kg). The small size of myctophids would necessitate capturing many individual prey to satisfy an elephant seal's energetic needs. When the 18.7 MJ d^{-1} of daily energy gain (Table 2.2) is added to

the FMR requirements, an elephant seal would need to consume 4.0 kg d^{-1} of myctophids, or 550 daily prey captures, at the start of the post-breeding trip. At the beginning of the post-molt trip, 3.2 kg d^{-1} or 450 daily prey captures would be required. These values increase across both trips, as the increasing mass of the animals would require additional energy to maintain (S12). On a diet of non-migrating squid, the animals would need to consume more mass to acquire the same energy, but as they are larger, many fewer prey captures would be required to meet that benchmark: 8.6 kg d^{-1} of squid or 43 prey captures at the start of post-breeding, and 5.6 kg d^{-1} of squid or 28 prey captures at the start of post-molt. On a per-dive basis this means elephant seals need to consume 7-15 myctophids or 1-2 squid per dive to satisfy their energy requirements (S12).

The increased use of the Sub-Arctic Pacific region, the diving characteristics seen during both foraging trips, and the unusually high %Adipose at recovery suggest a higher dependence on myctophid fish, or other small energy-dense prey, during the Blob. The elevated number of bottom wiggles (foraging effort) during post-breeding suggests densely packed, smaller prey. During post-breeding 2015-2017, seals were instrumented with video recorders, and prey captures were scored by prey type. Captures recorded by the eight individuals instrumented during 2015 were 75-90% fish species. In contrast, seal instrumented in other years showed greater variability [65]. While there was not a similar increase in bottom wiggles during post-molt trips, the increase in deep diving likely caused an underestimate of foraging effort based exclusively on dive bottom wiggles. These dives penetrate regions of severe hypoxia, inhibiting prey's ability to evade capture by a mobile, air-breathing predator, and thereby reducing the need for vertical pursuit excursion by the seals. Deep V-shaped dives can have multiple jaw motion

events on the descent without any corresponding wiggles, and video footage of prey captured at these depths shows minimal movement prior to capture [35,57].

The ability to take advantage of changing prey resources provides a buffer against stochastic environmental events, but total energy acquisition is not the only consideration when looking at dietary shifts. Being able to recoup sufficient stores in both lean and lipid tissue pools is essential, as both are vital to sustaining reproduction [61]. Reduced lean tissue gain, as seen in 2015, could result in reduced lactation time, lower weaning mass, and lower probability of offspring survival [61,66]. Furthermore, different foraging behaviors influence the accumulation of persistent organic pollutants and heavy metals in elephant seal tissue, with higher burdens of some POPs seen in individuals using more coastal and northerly foraging areas [67]. The effects of these changes also need to be examined in fully assessing the northern elephant seal response to the Blob.

2.6 Conclusion

Northern elephant seals exhibited a population-level plastic response to environmental conditions in 2014-2015. During both foraging trips, there was an increased use of the Alaska Gyre (Fig. 2.2) and a broader distribution of diving within the water column (Fig. 2.3). As a result, their foraging success was similar or better than in normal years (Fig. 2.1). Their spatial use, diving characteristics, and high adipose gain suggest that they took advantage of different prey fields during both trips and that using the OMZ for daytime foraging was an important strategy for success. These results, however, are indicative of the behavior of individuals that survived this event. Northern elephant seals did not experience an unusual mortality event like some other species in the region [20-22]. However, at-sea mortality (25%) was higher and more females did not breed (25%)

among the female seals that were tracked during the 2014 post-molt trip than during other years (Chapter 3). Additionally, not all individuals exhibited the same behavior, and a more detailed examination of individual plasticity and the behavior of individuals that did not survive will strengthen our understanding of this species' response to extreme climate events and ongoing climate change.

2.7 References

1. Ummenhofer C.C., Meehl G.A. 2017 Extreme weather and climate events with ecological relevance: a review. *Philosophical transactions of the Royal Society of London Series B, Biological sciences* **372**(1723). (doi:10.1098/rstb.2016.0135).

2. Estes J.A., Terborgh J., Brashares J.S., Power M.E., Berger J., Bond W.J., Carpenter S.R., Essington T.E., Holt R.D., Jackson J.B. 2011 Trophic downgrading of planet Earth. *science* **333**(6040), 301-306.

3. Diffenbaugh N.S., Singh D., Mankin J.S., Horton D.E., Swain D.L., Touma D., Charland A., Liu Y., Haugen M., Tsiang M., et al. 2017 Quantifying the influence of global warming on unprecedented extreme climate events. *Proceedings of the National Academy of Sciences of the United States of America* **114**(19), 4881-4886. (doi:10.1073/pnas.1618082114).

4. Smale D.A., Wernberg T., Oliver E.C.J., Thomsen M., Harvey B.P., Straub S.C., Burrows M.T., Alexander L.V., Benthuysen J.A., Donat M.G., et al. 2019 Marine heatwaves threaten global biodiversity and the provision of ecosystem services. *Nature Climate Change* **9**(4), 306-312. (doi:10.1038/s41558-019-0412-1).

5. Oliver E.C.J., Donat M.G., Burrows M.T., Moore P.J., Smale D.A., Alexander L.V., Benthuysen J.A., Feng M., Sen Gupta A., Hobday A.J., et al. 2018 Longer and more frequent marine heatwaves over the past century. *Nature communications* **9**(1), 1324. (doi:10.1038/s41467-018-03732-9).

6. Frolicher T.L., Fischer E.M., Gruber N. 2018 Marine heatwaves under global warming. *Nature* **560**(7718), 360-364. (doi:10.1038/s41586-018-0383-9).

7. Frolicher T.L., Laufkotter C. 2018 Emerging risks from marine heat waves. *Nature communications* **9**(1), 650. (doi:10.1038/s41467-018-03163-6).

8. Poloczanska E.S., Burrows M.T., Brown C.J., García Molinos J., Halpern B.S., Hoegh-Guldberg O., Kappel C.V., Moore P.J., Richardson A.J., Schoeman D.S., et al. 2016 Responses of Marine Organisms to Climate Change across Oceans. *Frontiers in Marine Science* **3**. (doi:10.3389/fmars.2016.00062).

9. Pinsky M.L., Eikeset A.M., McCauley D.J., Payne J.L., Sunday J.M. 2019 Greater vulnerability to warming of marine versus terrestrial ectotherms. *Nature* **569**(7754), 108-111. (doi:10.1038/s41586-019-1132-4).

10. Bond N.A., Cronin M.F., Freeland H., Mantua N. 2015 Causes and impacts of the 2014 warm anomaly in the NE Pacific. *Geophysical Research Letters* **42**(9), 3414-3420. (doi:10.1002/2015gl063306).

11. Freeland H., Ross T. 2019 'The Blob' - or, how unusual were ocean temperatures in the Northeast Pacific during 2014-2018? *Deep Sea Research Part I: Oceanographic Research Papers* **150**. (doi:10.1016/j.dsr.2019.06.007).

12. Di Lorenzo E., Mantua N. 2016 Multi-year persistence of the 2014/15 North Pacific marine heatwave. *Nature Climate Change*. (doi:10.1038/nclimate3082).

13. Hobday A., Oliver E., Sen Gupta A., Benthuysen J., Burrows M., Donat M., Holbrook N., Moore P., Thomsen M., Wernberg T., et al. 2018 Categorizing and Naming Marine Heatwaves. *Oceanography* **31**(2). (doi:10.5670/oceanog.2018.205).

14. Palacios D.M., Bograd S.J., Foley D.G., Schwing F.B. 2006 Oceanographic characteristics of biological hot spots in the North Pacific: a remote sensing perspective. *Deep Sea Research Part II: Topical Studies in Oceanography* **53**(3), 250-269.

15. Whitney F.A., Crawford W.R., Harrison P.J. 2005 Physical processes that enhance nutrient transport and primary productivity in the coastal and open ocean of the subarctic NE Pacific. *Deep Sea Research Part II: Topical Studies in Oceanography* **52**(5–6), 681-706. (doi:http://dx.doi.org/10.1016/j.dsr2.2004.12.023).

16. Whitney F.A. 2015 Anomalous winter winds decrease 2014 transition zone productivity in the NE Pacific. *Geophysical Research Letters* **42**(2), 428-431. (doi:10.1002/2014GL062634).

17. Peterson W.T., Fisher J.L., Strub P.T., Du X., Risien C., Peterson J., Shaw C.T. 2017 The pelagic ecosystem in the Northern California Current off Oregon during the 2014-2016 warm anomalies within the context of the past 20 years. *Journal of Geophysical Research: Oceans* **122**(9), 7267-7290. (doi:10.1002/2017jc012952).

18. von Biela V.R., Arimitsu M.L., Piatt J.F., Heflin B., Schoen Sk Trowbridge J.L., Clawson C.M. 2019 Extreme reduction in nutritional value of a key forage fish during the Pacific marine heatwave of 2014-2016. *Marine Ecology Progress Series* **613**, 171-182. (doi:10.3354/meps12891).

19. Thalmann H.L., Daly E.A., Brodeur R.D. 2020 Two anomalously warm years in the northern California Current: impacts on early marine Steelhead diet composition, morphology, and potential survival. *Transactions of the American Fisheries Society*. (doi:10.1002/tafs.10244).

20. Gálvez C., Pardo M.A., Elorriaga-Verplancken F.R. 2020 Impacts of extreme ocean warming on the early development of a marine top predator: The Guadalupe fur seal. *Progress in Oceanography* **180**. (doi:10.1016/j.pocean.2019.102220).

21. Piatt J.F., Parrish J.K., Renner H.M., Schoen S.K., Jones T.T., Arimitsu M.L., Kuletz K.J., Bodenstein B., Garcia-Reyes M., Duerr R.S., et al. 2020 Extreme mortality and reproductive failure of common murres resulting from the northeast Pacific marine heatwave of 2014-2016. *PLoS One* **15**(1), e0226087. (doi:10.1371/journal.pone.0226087).

22. Jones T., Parrish J.K., Peterson W.T., Bjorkstedt E.P., Bond N.A., Ballance L.T., Bowes V., Hipfner J.M., Burgess H.K., Dolliver J.E., et al. 2018 Massive Mortality of a

Planktivorous Seabird in Response to a Marine Heatwave. *Geophysical Research Letters* **45**(7), 3193-3202. (doi:10.1002/2017gl076164).

23. McCabe R.M., Hickey B.M., Kudela R.M., Lefebvre K.A., Adams N.G., Bill B.D., Gulland F.M.D., Thomson R.E., Cochlan W.P., Trainer V.L. 2016 An unprecedented coastwide toxic algal bloom linked to anomalous ocean conditions. *Geophysical Research Letters* **43**(19), 10,366-310,376. (doi:10.1002/2016gl070023).

24. Zhu Z., Qu P., Fu F., Tennenbaum N., Tatters A.O., Hutchins D.A. 2017 Understanding the blob bloom: Warming increases toxicity and abundance of the harmful bloom diatom Pseudo-nitzschia in California coastal waters. *Harmful algae* **67**, 36-43. (doi:10.1016/j.hal.2017.06.004).

25. Cavole L., Demko A., Diner R., Giddings A., Koester I., Pagniello C., Paulsen M.-L., Ramirez-Valdez A., Schwenck S., Yen N., et al. 2016 Biological Impacts of the 2013–2015 Warm-Water Anomaly in the Northeast Pacific: Winners, Losers, and the Future. *Oceanography* **29**(2). (doi:10.5670/oceanog.2016.32).

26. Moffitt S.E., Moffitt R.A., Sauthoff W., Davis C.V., Hewett K., Hill T.M. 2015 Paleoceanographic insights on recent oxygen minimum zone expansion: lessons for modern oceanography. *PLoS One* **10**(1), e0115246. (doi:10.1371/journal.pone.0115246).

27. Whitney F.A., Freeland H.J., Robert M. 2007 Persistently declining oxygen levels in the interior waters of the eastern subarctic Pacific. *Progress in Oceanography* **75**(2), 179-199. (doi:10.1016/j.pocean.2007.08.007).

28. Hofmann A.F., Peltzer E.T., Walz P.M., Brewer P.G. 2011 Hypoxia by degrees: Establishing definitions for a changing ocean. *Deep Sea Research Part I: Oceanographic Research Papers* **58**(12), 1212-1226. (doi:10.1016/j.dsr.2011.09.004).

29. Seibel B.A. 2011 Critical oxygen levels and metabolic suppression in oceanic oxygen minimum zones. *The Journal of experimental biology* **214**(Pt 2), 326-336. (doi:10.1242/jeb.049171).

30. Breitburg D., Levin L.A., Oschlies A., Gregoire M., Chavez F.P., Conley D.J., Garcon V., Gilbert D., Gutierrez D., Isensee K., et al. 2018 Declining oxygen in the global ocean and coastal waters. *Science* **359**(6371). (doi:10.1126/science.aam7240).

31. Evans M.R., Moustakas A. 2018 Plasticity in foraging behaviour as a possible response to climate change. *Ecological Informatics* **47**, 61-66. (doi:10.1016/j.ecoinf.2017.08.001).

32. Kuhn C. 2011 The influence of subsurface thermal structure on the diving behavior of northern fur seals (<i>Callorhinus ursinus</i>) during the breeding season. *Marine Biology* **158**(3), 649-663. (doi:10.1007/s00227-010-1589-z).

33. Green D.B., Bestley S., Trebilco R., Corney S.P., Lehodey P., McMahon C.R., Guinet C., Hindell M.A. 2020 Modelled mid-trophic pelagic prey fields improve understanding of marine predator foraging behaviour. *Ecography*. (doi:10.1111/ecog.04939).

34. Abrahms B., Scales K.L., Hazen E.L., Bograd S.J., Schick R.S., Robinson P.W., Costa D.P. 2018 Mesoscale activity facilitates energy gain in a top predator. *Proceedings Biological sciences / The Royal Society* **285**(1885). (doi:10.1098/rspb.2018.1101).

35. Naito Y., Costa D.P., Adachi T., Robinson P.W., Peterson S.H., Mitani Y., Takahashi A. 2017 Oxygen minimum zone: An important oceanographic habitat for deep-diving northern elephant seals, Mirounga angustirostris. *Ecol Evol* **7**(16), 6259-6270. (doi:10.1002/ece3.3202).

36. Dewitt T.J., Sih A., Wilson D.S. 1998 Costs and limits of phenotypic plasticity. *Trends in ecology & evolution* **13**(2), 77-81.

37. Biuw M., Boehme L., Guinet C., Hindell M., Costa D., Charrassin J.B., Roquet F., Bailleul F., Meredith M., Thorpe S., et al. 2007 Variations in behavior and condition of a Southern Ocean top predator in relation to in situ oceanographic conditions. *Proceedings of the National Academy of Sciences of the United States of America* **104**(34), 13705-13710. (doi:10.1073/pnas.0701121104).

38. Robinson P.W., Costa D.P., Crocker D.E., Gallo-Reynoso J.P., Champagne C.D., Fowler M.A., Goetsch C., Goetz K.T., Hassrick J.L., Hückstädt L.A. 2012 Foraging behavior and success of a mesopelagic predator in the northeast Pacific Ocean: insights from a data-rich species, the northern elephant seal. *PLoS One* **7**(5), e36728.

39. Saijo D., Mitani Y., Abe T., Sasaki H., Goetsch C., Costa D.P., Miyashita K. 2016 Linking mesopelagic prey abundance and distribution to the foraging behavior of a deep-diving predator, the northern elephant seal. *Deep Sea Research Part II: Topical Studies in Oceanography*. (doi:10.1016/j.dsr2.2016.11.007).

40. Crocker D.E., Costa D.P., Le Boeuf B.J., Webb P.M., Houser D.S. 2006 Impact of El Niño on the foraging behavior of female northern elephant seals. *Marine Ecology-Progress Series* **309**.

41. Costa D.P., Robinson P.W., Arnould J.P., Harrison A.L., Simmons S.E., Hassrick J.L., Hoskins A.J., Kirkman S.P., Oosthuizen H., Villegas-Amtmann S., et al. 2010 Accuracy of ARGOS locations of Pinnipeds at-sea estimated using Fastloc GPS. *PLoS One* **5**(1), e8677. (doi:10.1371/journal.pone.0008677).

42. Gales N.J., Burton H.R. 1987 Ultrasonic Measurement of Blubber Thickness of the Southern Elephant Seal, Mirounga-Leonina (Linn). *Aust J Zool* **35**(3), 207-217. (doi:Doi 10.1071/Zo9870207).

43. R Core Team. 2019 R: A language and environment for statistical computing. (Vienna, Austria, R Foundation for Statistical Computing.

44. Johnson D.S., London J.M., Lea M.A., Durban J.W. 2008 Continuous-time correlated random walk model for animal telemetry data. *Ecology* **89**(5), 1208-1215.

45. Crocker D.E., Le Boeuf B.J., Costa D.P. 1997 Drift diving in female northern elephant seals: Implications for food processing. *Canadian Journal of Zoology* **75**(1), 27-39. (doi:DOI 10.1139/z97-004).

46. Robinson P.W., Simmons S.E., Crocker D.E., Costa D.P. 2010 Measurements of foraging success in a highly pelagic marine predator, the northern elephant seal. *Journal of Animal Ecology* **79**(6), 1146-1156.

47. Bates D., Mächler M., Bolker B., Walker S. 2014 Fitting linear mixed-effects models using lme4. *arXiv preprint arXiv:14065823*.

48. Wood S.N. 2017 *Generalized Additive Models: An Introduction with R*. Second ed, CRC Press.

49. Barton K. 2019 MuMIn: Multi-Model Interence. (R package version 1.43.6. ed.

50. Osborne O.E., O'Hara P.D., Whelan S., Zandbergen P., Hatch S.A., Elliott K.H. 2020 Breeding seabirds increase foraging range in response to an extreme marine heatwave. *Marine Ecology Progress Series* **646**, 161-173. (doi:10.3354/meps13392).

51. Wernberg T., Smale D.A., Tuya F., Thomsen M.S., Langlois T.J., de Bettignies T., Bennett S., Rousseaux C.S. 2013 An extreme climatic event alters marine ecosystem structure in a global biodiversity hotspot. *Nature Climate Change* **3**(1), 78-82. (doi:10.1038/Nclimate1627).

52. Goetsch C. 2018 lluminating the Twilight Zone: Diet and Foraging Strategies of a Deep-Sea Predator, the Northern Elephant Seal, University of California, Santa Cruz.

53. Leising A.W., Schroeder I.D., Bograd S.J., Abell J., Durazo R., Gaxiola-Castro G., Bjorkstedt E.P., Field J., Sakuma K., Robertson R.R., et al. 2015 State of the California Current 2014-15: Impacts of the Warm-Water "Blob". *Cal Coop Ocean Fish* **56**, 31-68.

54. Jiménez-Quiroz M.d.C., Cervantes-Duarte R., Funes-Rodríguez R., Barón-Campis S.A., García-Romero F.d.J., Hernández-Trujillo S., Hernández-Becerril D.U., González-Armas R., Martell-Dubois R., Cerdeira-Estrada S., et al. 2019 Impact of "The Blob" and "El Niño" in the SW Baja California Peninsula: Plankton and Environmental Variability of Bahia Magdalena. *Frontiers in Marine Science* **6**. (doi:10.3389/fmars.2019.00025).

55. Hristova H.G., Ladd C., Stabeno P.J. 2019 Variability and Trends of the Alaska Gyre From Argo and Satellite Altimetry. *Journal of Geophysical Research: Oceans* **124**(8), 5870-5887. (doi:10.1029/2019jc015231).

56. Robinson P.W., Tremblay Y., Crocker D.E., Kappes M.A., Kuhn C.E., Shaffer S.A., Simmons S.E., Costa D.P. 2007 A comparison of indirect measures of feeding

behaviour based on ARGOS tracking data. *Deep Sea Research Part II: Topical Studies in Oceanography* **54**(3-4), 356-368. (doi:10.1016/j.dsr2.2006.11.020).

57. Naito Y., Costa D.P., Adachi T., Robinson P.W., Fowler M., Takahashi A., Franklin C. 2013 Unravelling the mysteries of a mesopelagic diet: a large apex predator specializes on small prey. *Functional Ecology* **27**(3), 710-717. (doi:10.1111/1365-2435.12083).

58. Irigoien X., Klevjer T.A., Rostad A., Martinez U., Boyra G., Acuna J.L., Bode A., Echevarria F., Gonzalez-Gordillo J.I., Hernandez-Leon S., et al. 2014 Large mesopelagic fishes biomass and trophic efficiency in the open ocean. *Nature communications* **5**, 3271. (doi:10.1038/ncomms4271).

59. Costa D.P., Kuhn C.E., Weise M.J., Shaffer S.A., Arnould J.P.Y. 2004 When does physiology limit the foraging behaviour of freely diving mammals? *International Congress Series* **1275**(0), 359-366. (doi:http://dx.doi.org/10.1016/j.ics.2004.08.058).

60. Crocker D.E., Costa D.P. 2009 Pinniped Physiology. 873-878. (doi:10.1016/b978-0-12-373553-9.00201-7).

61. Crocker D.E., Williams J.D., Costa D.P., Le Boeuf B.J. 2001 Maternal traits and reproductive effort in northern elephant seals. *Ecology* **82**(12), 3541-3555. (doi:10.1890/0012-9658(2001)082[3541:Mtarei]2.0.Co;2).

62. Goetsch C., Conners M.G., Budge S.M., Mitani Y., Walker W.A., Bromaghin J.F., Simmons S.E., Reichmuth C., Costa D.P. 2018 Energy-Rich Mesopelagic Fishes Revealed as a Critical Prey Resource for a Deep-Diving Predator Using Quantitative Fatty Acid Signature Analysis. *Frontiers in Marine Science* **5**. (doi:10.3389/fmars.2018.00430).

63. Sutton T.T., Clark M.R., Dunn D.C., Halpin P.N., Rogers A.D., Guinotte J., Bograd S.J., Angel M.V., Perez J.A.A., Wishner K., et al. 2017 A global biogeographic classification of the mesopelagic zone. *Deep Sea Research Part I: Oceanographic Research Papers* **126**, 85-102. (doi:10.1016/j.dsr.2017.05.006).

64. Maresh J.L., Adachi T., Takahashi A., Naito Y., Crocker D.E., Horning M., Williams T.M., Costa D.P. 2015 Summing the strokes: energy economy in northern elephant seals during large-scale foraging migrations. *Mov Ecol* **3**(1), 22. (doi:10.1186/s40462-015-0049-2).

65. Yoshino K., Takahashi A., Adachi T., Costa D.P., Robinson P.W., Peterson S.H., Huckstadt L.A., Holser R.R., Naito Y. 2020 Acceleration-triggered animal-borne videos show a dominance of fish in the diet of female northern elephant seals. *The Journal of experimental biology* **223**(Pt 5). (doi:10.1242/jeb.212936).

66. Costa D.P., Schwarz L., Robinson P., Schick R.S., Morris P.A., Condit R., Crocker D.E., Kilpatrick A.M. 2016 A Bioenergetics Approach to Understanding the Population

Consequences of Disturbance: Elephant Seals as a Model System. *Adv Exp Med Biol* **875**, 161-169. (doi:10.1007/978-1-4939-2981-8_19).

67. Peterson S.H., Peterson M.G., Debier C., Covaci A., Dirtu A.C., Malarvannan G., Crocker D.E., Schwarz L.K., Costa D.P. 2015 Deep-ocean foraging northern elephant seals bioaccumulate persistent organic pollutants. *The Science of the total environment* **533**, 144-155. (doi:10.1016/j.scitotenv.2015.06.097).

Table 2.1 - Sample sizes for each year and season by data type.

Year	Post-Breeding				Post-Molting			
	Deployed	Body Comp	Track	Dive	Deployed	Body Comp	Track	Dive
2004	7	4	5	5	25	23	17	21
2005	19	18	16	18	25	22	18	20
2006	20	17	16	17	22	20	16	17
2007	20	15	17	16	21	18	20	20
2008	23	22	22	22	20	14	14	12
2009	24	19	17	18	8	7	6	7
2010	24	23	23	21	21	15	18	18
2011	22	20	22	18	20	15	14	15
2012	20	19	19	19	22	16	16	16
2013	22	15	14	14	22	16	17	17
2014	20	19	18	17	20	15	15	13
2015	20	18	18	18	20	15	15	15
2016	20	16	17	16	20	13	15	12
2017	9	7	7	6	10	8	8	6
2018	9	9	8	8	14	11	11	11
2019	10	8	8	7	--	--	--	--
Total	289	249	247	240	290	228	220	220
Blob	40	37	36	35	40	30	30	28
Non-Blob	249	212	211	205	250	198	190	192

Table 2.2 – Post-breeding trip and foraging success statistics. Values in bold are significantly different ($p<0.05$).

Year	Post-Breeding						
	Trip Length (Days)	Total Distance (km)	Max Distance (km)	Mass Gain (kg)	Arrival Adipose (%)	Lean Gain (kg)	Energy Gain Rate (MJ d^{-1})
2004	83.7 ± 9.5	5732 ± 1889	2513 ± 1033	51.9 ± 21.6	31.4 ± 3.2	27.2 ± 13.0	12.8 ± 7.2
2005	77.3 ± 7.9	4983 ± 1070	2239 ± 534	72.3 ± 23.7	31.3 ± 1.4	50.0 ± 17.0	14.1 ± 7.0
2006	76.7 ± 11.1	4952 ± 1067	2178 ± 565	69.0 ± 24.7	30.7 ± 2.7	44.2 ± 14.7	14.5 ± 7.5
2007	71.2 ± 8.9	4662 ± 1220	2086 ± 631	82.4 ± 19.1	31.2 ± 1.1	51.7 ± 10.1	19.6 ± 7.5
2008	74.0 ± 8.9	4893 ± 859	2047 ± 384	74.4 ± 25.0	30.3 ± 2.4	47.8 ± 16.8	16.7 ± 7.3
2009	73.8 ± 10.5	4691 ± 1141	1990 ± 591	77.3 ± 25.8	31.7 ± 2.6	42.1 ± 15.1	20.5 ± 10.5
2010	73.8 ± 5.8	5270 ± 746	2251 ± 457	80.8 ± 18.9	**33.0 ± 1.7**	42.6 ± 10.7	22.0 ± 8.1
2011	74.8 ± 17.3	4918 ± 1241	2073 ± 548	63.8 ± 23.8	31.6 ± 1.8	32.0 ± 16.8	17.8 ± 6.8
2012	72.7 ± 10.8	4828 ± 1027	2013 ± 446	80.7 ± 18.7	31.2 ± 2.4	46.4 ± 16.0	20.2 ± 6.9
2013	73.1 ± 11.4	4689 ± 946	1954 ± 455	76.1 ± 19.4	31.5 ± 2.2	44.2 ± 16.5	19.5 ± 6.6
2014	76.1 ± 9.5	5237 ± 1926	1922 ± 705	**95.5 ± 31.2**	**33.3 ± 2.8**	47.5 ± 22.4	**26.4 ± 9.5**
2015	75.5 ± 17.2	5591 ± 1571	2051 ± 549	70.5 ± 23.6	31.9 ± 2.7	42.5 ± 18.4	17.1 ± 6.0
2016	73.9 ± 14.2	5354 ± 1154	2255 ± 459	69.2 ± 22.8	**33.3 ± 2.1**	36.5 ± 19.3	19.3 ± 5.7
2017	77.6 ± 8.1	5579 ± 661	2041 ± 703	76.9 ± 18.7	29.6 ± 1.6	53.2 ± 16.6	15.3 ± 6.0
2018	76.9 ± 13.2	5804 ± 2133	2216 ± 729	88.0 ± 14.1	28.8 ± 2.2	57.3 ± 14.0	18.8 ± 2.3
2019	73.4 ± 10.0	5872 ± 2255	2271 ± 806	65.6 ± 13.7	28.8 ± 2.4	41.3 ± 17.8	15.2 ± 4.8
Blob	75.8 ± 13.6	5414 ± 1742	1986 ± 626	83.3 ± 30.2	32.6 ± 2.8	45.1 ± 20.4	**21.9 ± 9.2**
Non-Blob	74.6 ± 11.0	4977 ± 1316	2107 ± 583	74.5 ± 22.2	31.3 ± 2.4	44.1 ± 16.4	**18.1 ± 7.5**
All	74.8 ± 11.4	5099 ± 1293	2108 ± 562	75.8 ± 23.7	31.5 ± 2.5	44.3 ± 17.0	18.7 ± 7.9

Table 2.3 – Post-molt trip and foraging success statistics. Values in bold are significantly different ($p<0.05$).

	Post-Molting						
Year	Trip Length (Days)	Total Distance (km)	Max Distance (km)	Mass Gain (kg)	Arrival Adipose (%)	Lean Gain (kg)	Energy Gain Rate (MJ d^{-1})
2004	223.3 ± 13.3	9522 ± 1633	3310 ± 813	270.0 ± 41.7	36.6 ± 2.0	177.0 ± 32.7	19.7 ± 3.0
2005	213.2 ± 30.3	8879 ± 1691	3049 ± 1015	266.9 ± 65.4	35.1 ± 2.9	182.4 ± 53.4	19.2 ± 3.3
2006	214.0 ± 25.8	9653 ± 1340	3327 ± 1032	241.7 ± 82.8	33.8 ± 2.2	174.9 ± 64.2	15.8 ± 4.4
2007	219.2 ± 38.5	10905 ± 2963	3295 ± 968	249.7 ± 55.1	32.6 ± 2.7	184.3 ± 46.8	**15.2 ± 3.5**
2008	221.8 ± 38.5	9649 ± 2198	3170 ± 840	260.8 ± 77.6	34.5 ± 3.2	183.0 ± 56.6	17.5 ± 5.5
2009	210.0 ± 30.9	10468 ± 2690	2834 ± 1092	271.4 ± 58.0	**38.0 ± 2.4**	174.0 ± 48.6	21.8 ± 3.5
2010	218.8 ± 35.4	9429 ± 2249	2943 ± 1013	273.3 ± 51.9	32.3 ± 2.5	208.5 ± 44.0	16.3 ± 2.1
2011	222.3 ± 4.0	9754 ± 2071	3248 ± 1294	282.9 ± 42.0	33.1 ± 4.4	207.2 ± 44.0	17.9 ± 2.2
2012	220.7 ± 16.5	10373 ± 1228	3364 ± 670	273.7 ± 38.9	34.7 ± 3.0	189.1 ± 29.0	18.9 ± 3.3
2013	210.3 ± 35.7	**11109 ± 2618**	3027 ± 1009	277.7 ± 82.6	**31.4 ± 1.3**	199.7 ± 60.0	19.0 ± 5.9
2014	223.2 ± 36.7	**11666 ± 2743**	3806 ± 1093	267.7 ± 51.9	**37.8 ± 2.5**	173.0 ± 50.5	20.3 ± 4.3
2015	225.8 ± 5.0	**12133 ± 3601**	3261 ± 1072	273.1 ± 38.9	**37.7 ± 2.2**	173.7 ± 30.5	20.4 ± 3.8
2016	232.8 ± 24.7	**11921 ± 2584**	3568 ± 1222	266.6 ± 66.5	35.3 ± 3.0	189.6 ± 46.5	17.0 ± 5.1
2017	202.7 ± 36.2	**12601 ± 2493**	3787 ± 813	224.8 ± 57.0	34.9 ± 3.7	151.9 ± 57.3	17.8 ± 3.8
2018	219.3 ± 11.9	**11884 ± 1103**	3824 ± 979	268.1 ± 73.1	33.7 ± 2.4	190.9 ± 57.9	17.9 ± 4.4
2019							
Blob	224.5 ± 25.8	**11900 ± 3154**	3533 ± 1099	270.3 ± 45.1	**37.8 ± 2.3**	173.3 ± 41.0	**20.4 ± 4.0**
Non-Blob	218.2 ± 28.2	**9958 ± 2710**	3224 ± 1053	264.3 ± 62.1	**34.2 ± 3.2**	186.4 ± 49.9	**17.9 ± 4.2**
All	220.8 ± 26.7	10543 ± 2496	3303 ± 1010	265.1 ± 60.1	34.7 ± 3.3	184.7 ± 49.0	18.2 ± 4.2

Table 2.4 – Summary of model results, models with lower AICc are shown in bold.

Candidate Model	AICc	Intercept	Adjusted R^2	Model Type	Figure
(a)					
PMTripDist ~ fYear	**4087.7**	**9522**	**0.144**	**LM**	**Fig. S4**
PMTripDist ~ 1	4106.2	10540			
(b)					
NDeepDives ~ s(DriftRate) + TOPPID(re)	**246770**	**2.201**	**0.276**	**GAMM**	**Fig. 2.3**
NDeepDives ~ 1	260797	2.170			

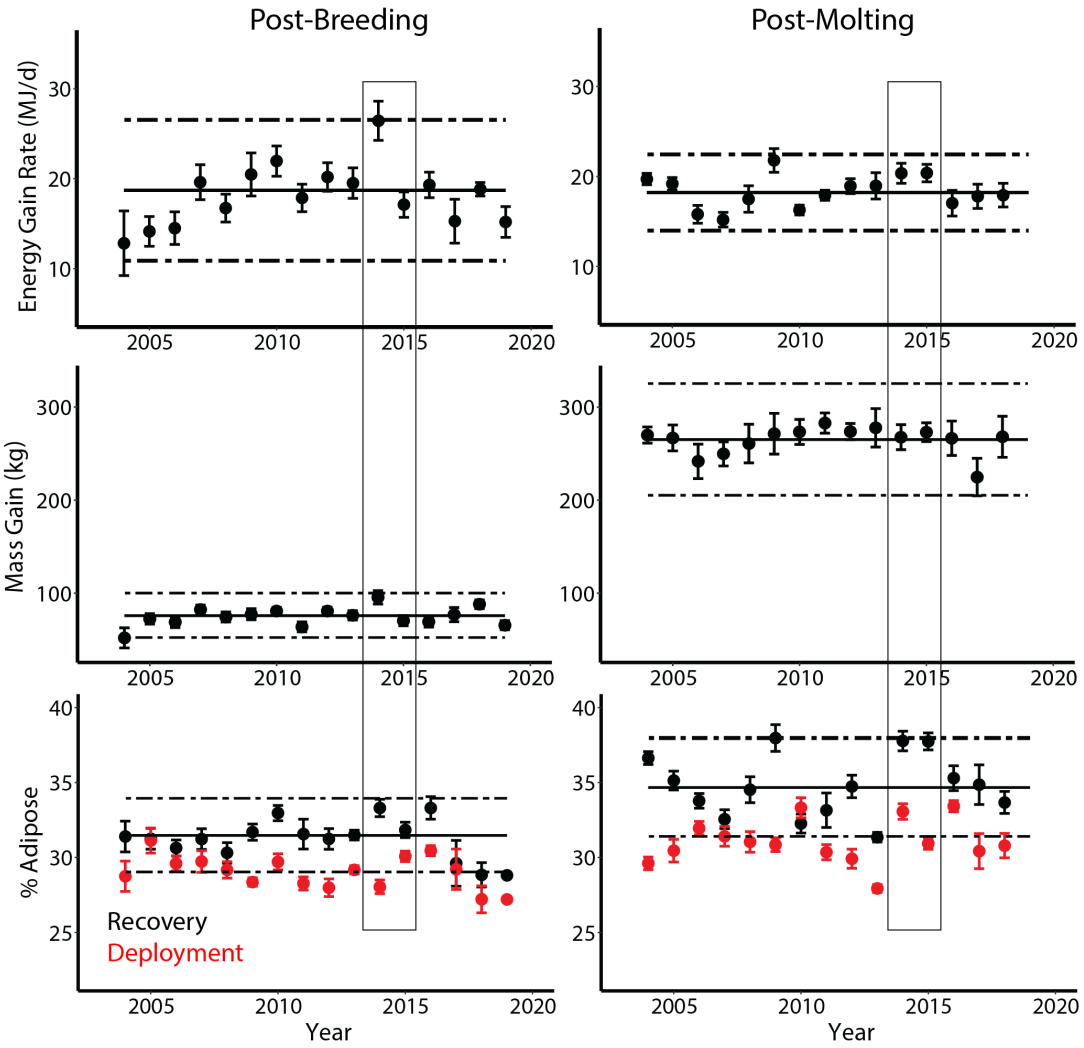

Fig. 2.1 - Variation in foraging success from 2004-2018; left panels show data from the post-breeding foraging trip (~11 weeks) and right panels from the post-molt trip (~32 weeks). **A** and **B** show mean rate of energy gain (MJ/day) and standard error. **C** and **D** show mean mass gain (kg) and standard error. **E** and **F** show mean percent adipose and standard error at deployment (red) and recovery (black). Black horizontal lines show the grand mean (solid) and standard deviation (dashed) for each set of recovery measurements. Boxes highlight data from the years of the Blob.

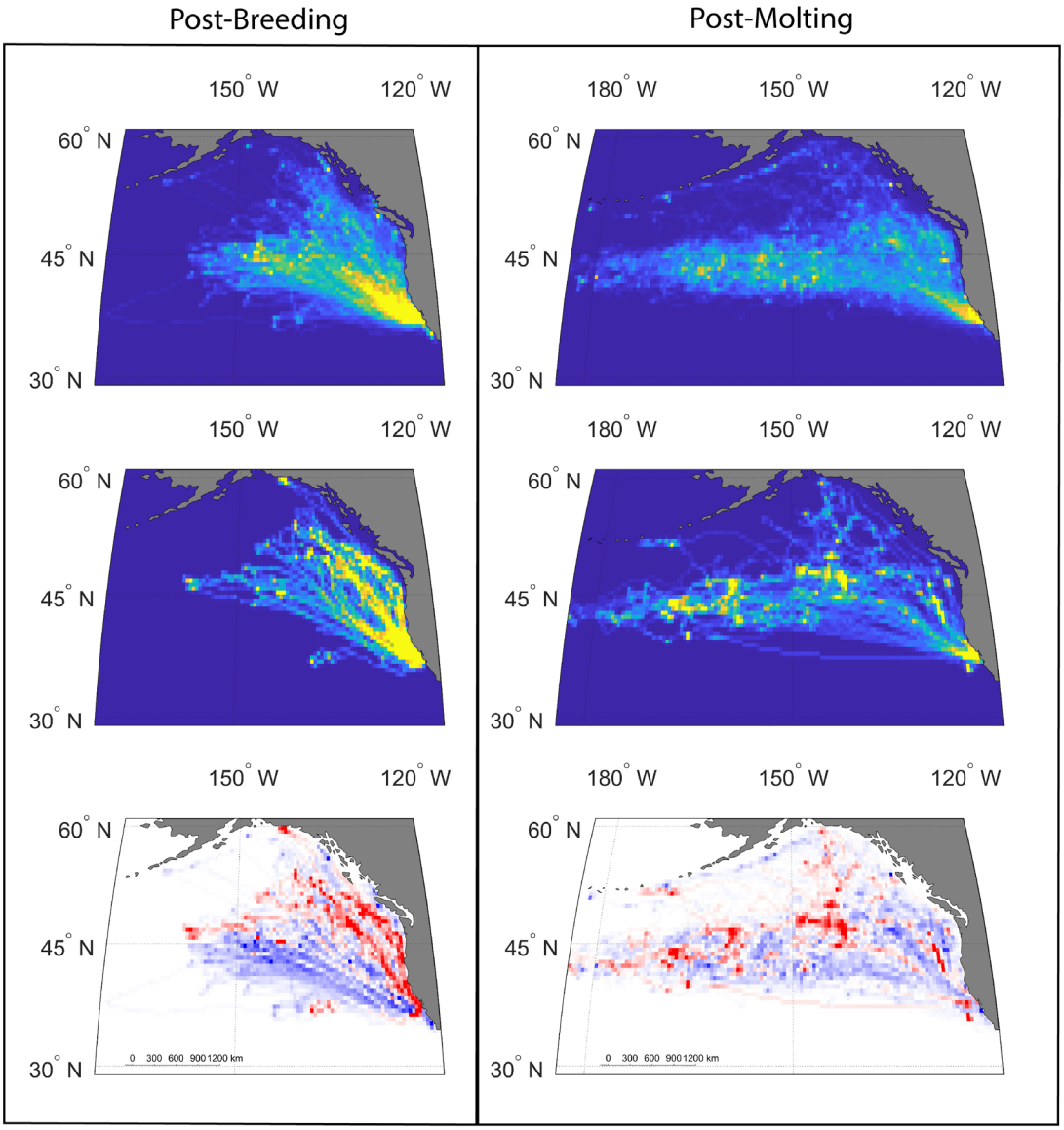

Fig. 2.2 – Spatial use of adult female elephant seals and extent of the marine heatwave during post-breeding (**left panels**) and post-molt (**right panels**) foraging trips. **Top panels** show the kernel density distributions of all tracks collected from 2004-2013 and 2016-2018. **Middle panels** show the kernel density distributions of all tracks collected during the Blob (2014-2015). **Bottom panels** show changes in spatial use, calculated from the difference in kernel density between 2014-2015 and sets of 40 random tracks pulled from all other years, repeated 1000 times, red indicates increased use of an area and blue decreased use.

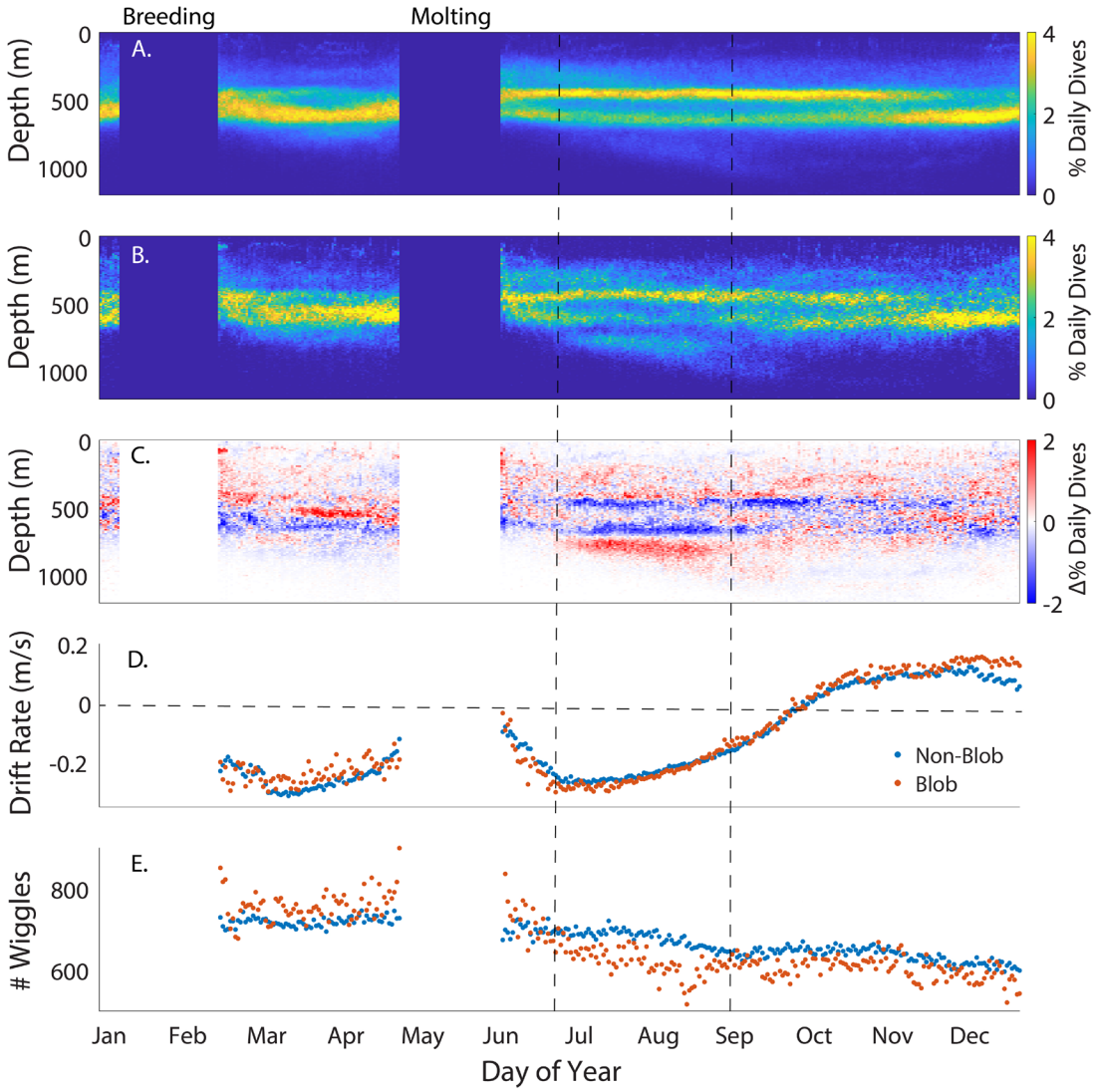

Fig. 2.3 - Patterns in depth use and foraging effort across seasons. For **A-C**, depth was divided into 10 m bins from 0-1200 m for each day of the year. The percent of total dives per day (excluding drift dives) that fell within a depth bin was calculated for each depth, each day of the year. **A**. Daily depth use calculated from all records collected from 2004-2013 and 2016-2018. **B**. Daily depth use during the Blob, calculated from all 2014-2015 records. **C** shows the change in depth use during the Blob (**B** minus **A**) where red denotes an increase in use and blue a decrease. **D** shows mean daily drift rate calculated from all drift dives collected during non-Blob (blue) and Blob (red) years. Negative drift rates correspond to negatively buoyant body composition and positive drift rates indicate positive buoyancy. **E** shows number of dive bottom wiggles normalized to sample size for each day in non-Blob (blue) and Blob (red) years.

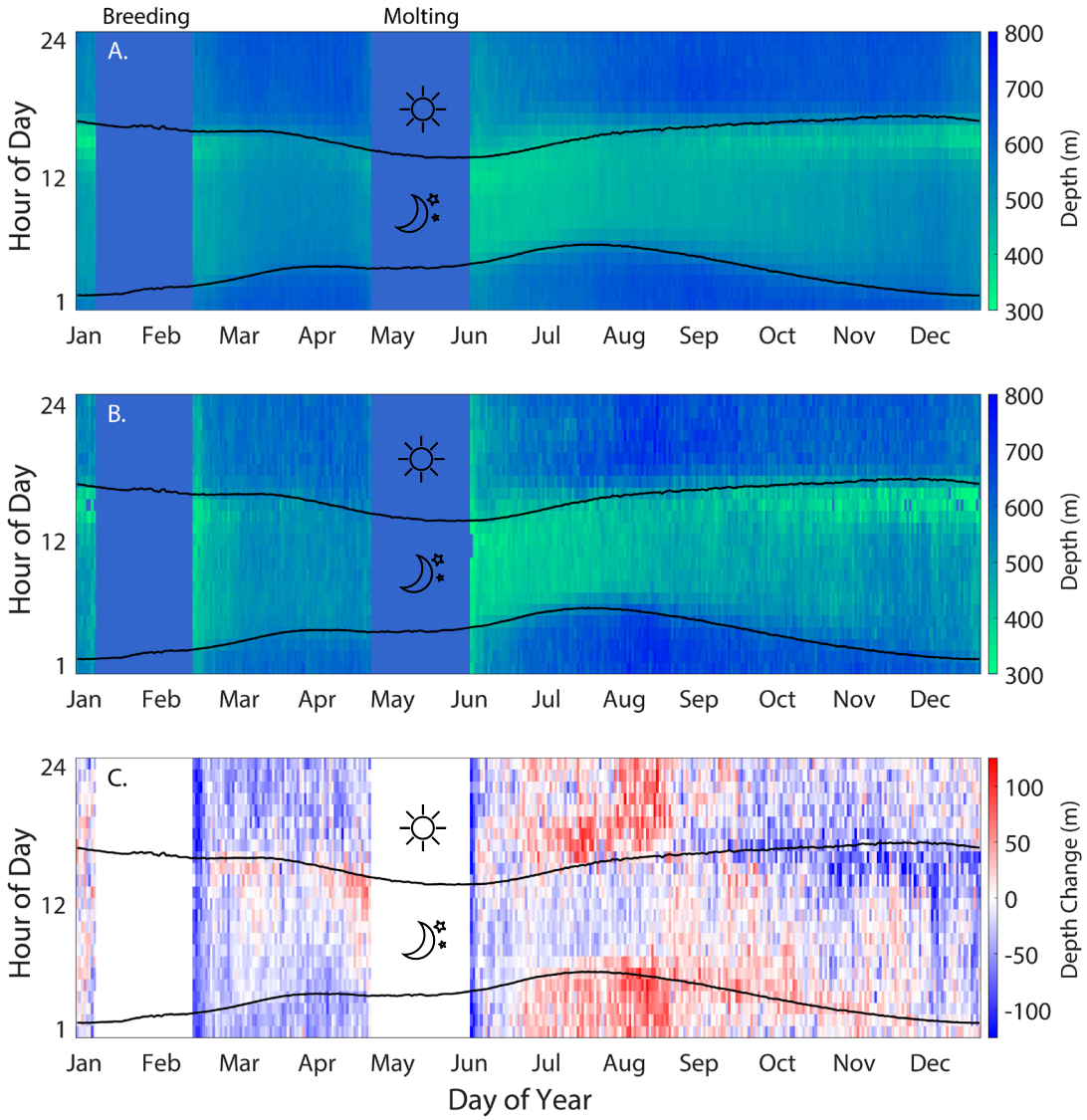

Fig. 2.4 - Diel and seasonal patterns in dive depth (meters), excluding drift dives. Contour lines indicate transition from day to night calculated from the date and the location of the animals. **A.** Mean dive depth calculated for each hour of the day, each day of the year, from all dive records collected in 2004-2013 and 2016-2018. **B.** Mean dive depth during the Blob, calculated as in A. from 2014-2015 records. **C.** Difference in dive depth during the Blob compared to all other years (B minus A); red indicates deeper diving during the Blob and blue shallower diving. The breeding and molting haul-outs and were excluded.

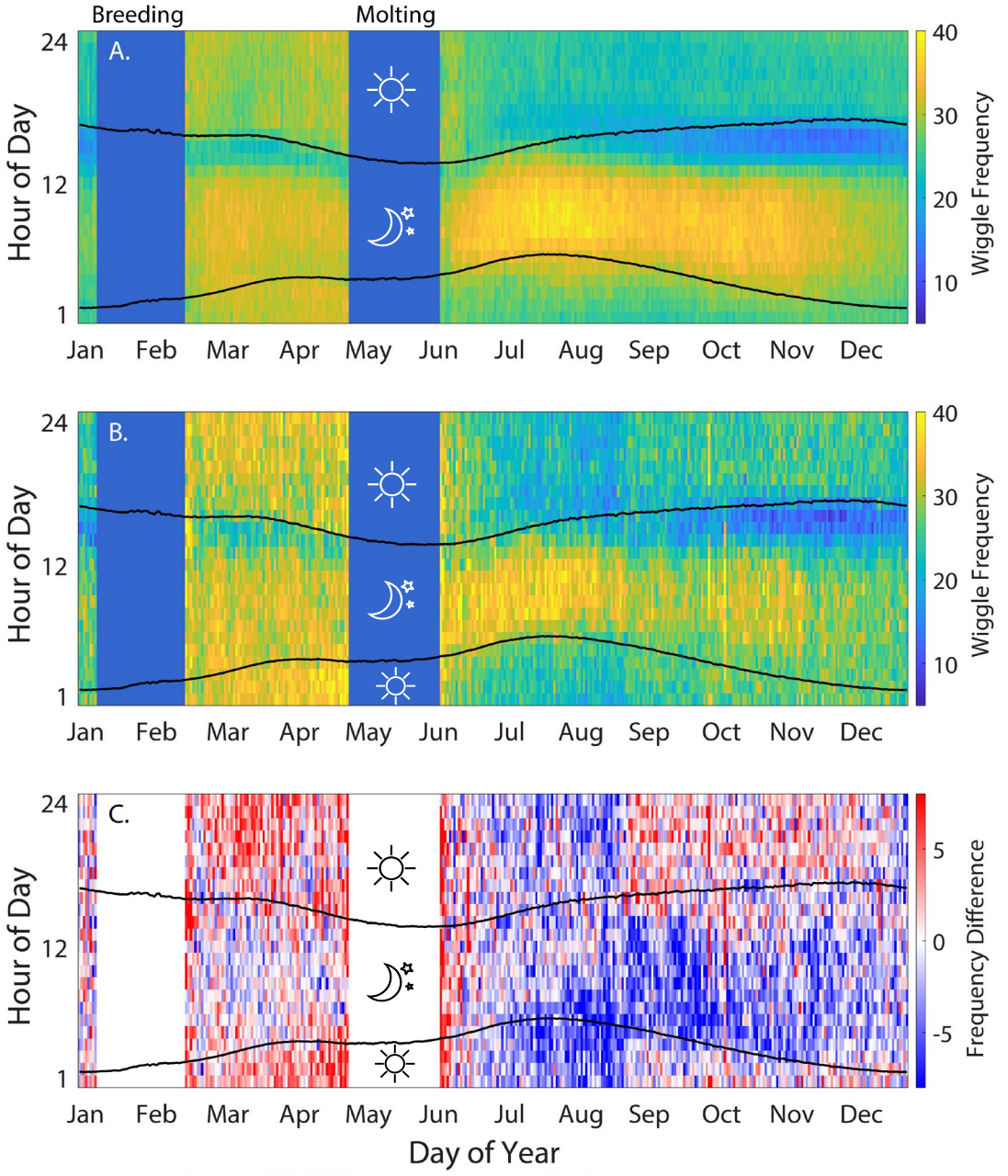

Fig. 2.5 - Diel and seasonal patterns in dive bottom wiggles, a proxy for foraging effort. All values are normalized to the number of animals contributing to the dive record on each day so that frequency values are comparable between seasons and periods. Contour lines indicate transitions between day and night. **A.** Dive bottom wiggles by hour of the day, each day of the year, from all dive records collected in 2004-2013 and 2016-2018. **B.** Dive bottom wiggles during the Blob (2014-2015 records). **C.** Difference in wiggle frequency between Blob and Non-Blob years, red indicates an increase in wiggle frequency during the Blob and blue a decrease.

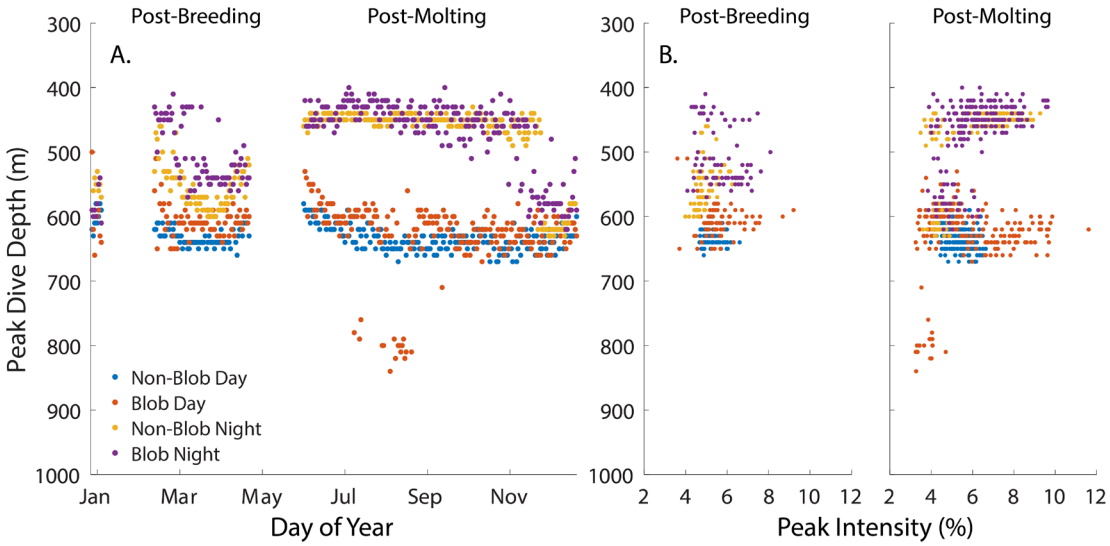

Fig. 2.6 - Peak dive depth (A) and corresponding peak intensity (B) during day and night in Blob and non-Blob years. Peak depth is defined as the depth of maximum use calculated for day (S4) and night (S5) separately. Peak intensity is the percentage of that day's dives that occurred at peak depth. Day and night were separated by solar elevation > 0° and < 0° respectively.

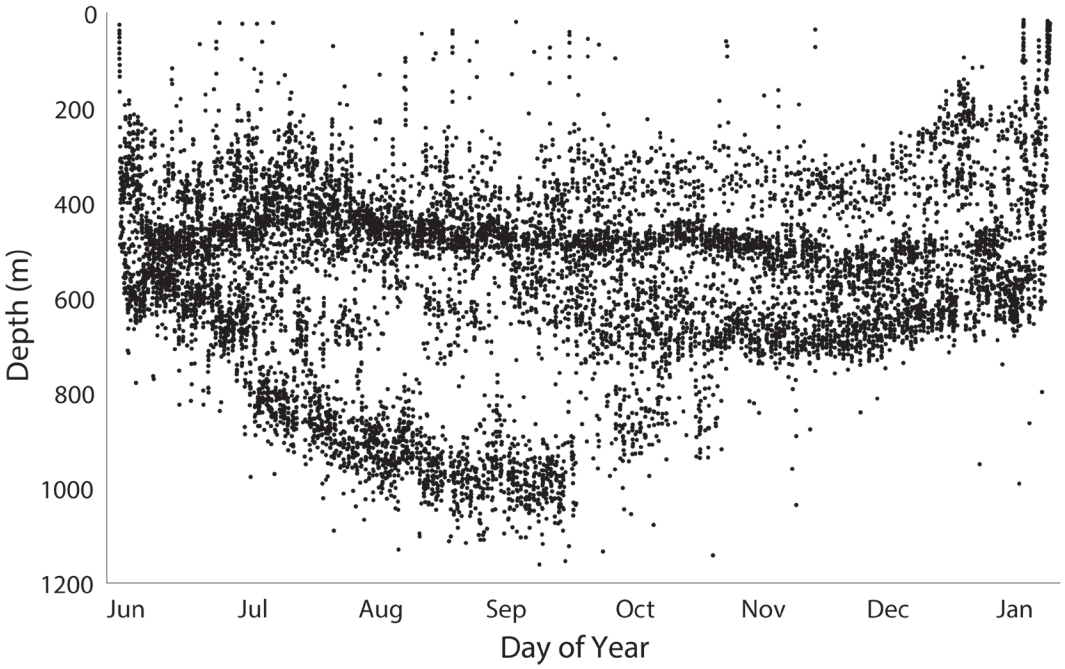

Fig. 2.7 - Example dive record of an individual exhibiting deep diving strategy during post-molt foraging trip. Points indicate max depth of each dive.

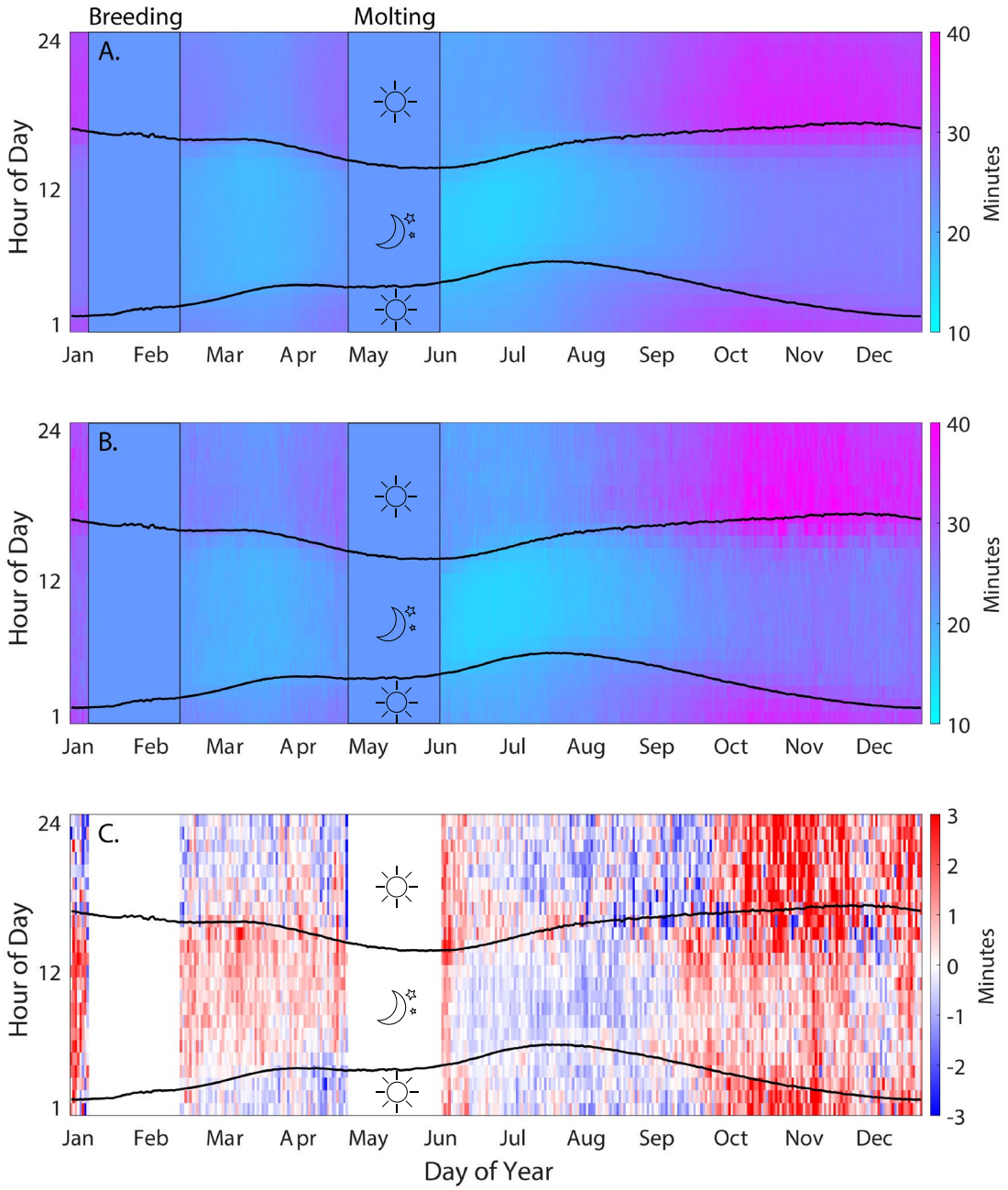

Fig. 2.8 - Diel and seasonal patterns in dive duration (minutes), excluding drift dives. Contour lines indicate transition from day to night calculated from the date and the location of the animals. **A.** Mean dive duration calculated for each hour of the day, each day of the year, from all dive records collected in 2004-2013 and 2016-2018. **B.** Mean dive duration during the Blob, calculated as in A. from 2014-2015 records. **C.** Difference in dive duration during the Blob compared to all other years (B minus A); red indicates an increase in duration during the Blob and blue a decrease. As in Fig. 2.2, the breeding and molting haul-outs and were excluded from C.

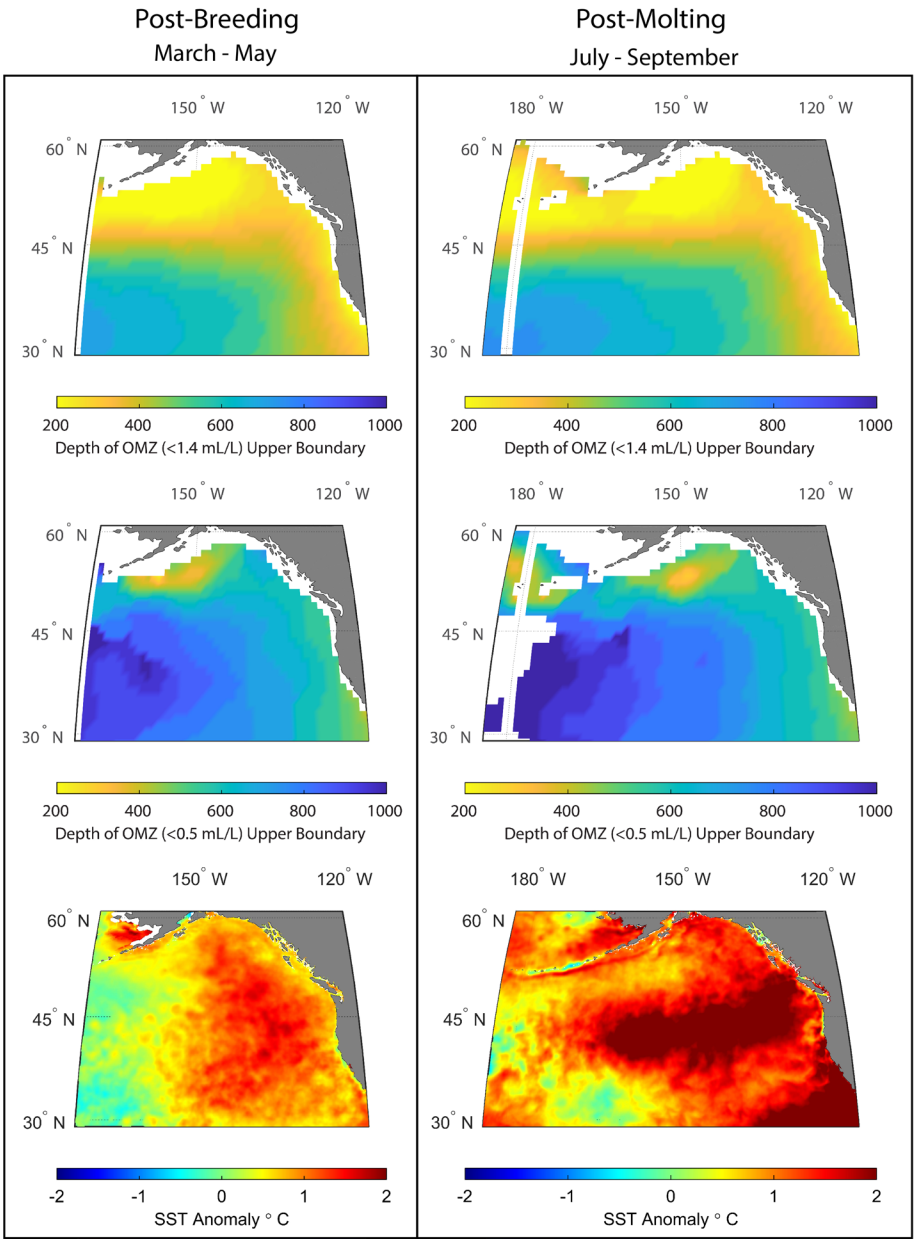

Fig. 2.9 – Representative ocean conditions experienced during post-breeding (left panels) and post-molt (right panels) foraging trips using 3-month mean values. Top panels show depth of the upper boundary of hypoxic water ($[O_2]$ < 1.4 mL/L) from climatology. Mid panels show upper boundary depth of severely hypoxic water ($[O_2]$ <0.5 mL/L) from climatology. Bottom panels show average extent and magnitude of sea surface temperature anomalies from 2014-2015 for March-May and July-September. Oxygen climatology data are from World Ocean Atlas 2018 [45] and sea surface temperature anomaly from POES AVHRR, 0.1° monthly composite, NOAA NESDIS CoastWatch [44].

Chapter 3: Density dependent effects on reproductive success in a capital breeding carnivore, the northern elephant seal (*Mirounga angustirostris*)

Rachel R. Holser, Daniel E. Crocker, Patrick W. Robinson, Richard Condit, Daniel P. Costa

3.1 Abstract

All organisms face resource limitations that will ultimately restrict population growth, but the controlling mechanisms vary across ecosystems, taxa, and reproductive strategies. Our understanding of density-dependent effects on large mammal populations is primarily to ungulates, while comparatively little is known about carnivores. Here we examine reproductive outcomes under varying environmental and population density conditions in a capital-breeding carnivore, the northern elephant seal (*Mirounga angustirostris*), using a four-decade data set of individual reproductive effort. This species provides a unique opportunity to examine the relative importance of resource acquisition and density-dependence on breeding success. Capital breeding strategies, where individuals accrue resources over large temporal and spatial scales for use during an abbreviated reproductive period, may have evolved, in part, to confer resilience to short-term environmental variability. We observed density-dependent effects on both weaning mass and male offspring-biased allocation of resources. Furthermore, maternal age (experience) was more important than oceanographic conditions or maternal mass in determining offspring weaning mass, and this effect was density dependent. Together these findings show that the mechanisms controlling reproductive output are conserved across terrestrial and marine systems and vary with population dynamics, an important

consideration when assessing the effect of extrinsic changes, such as climate change, on a population.

3.2 Introduction

Density-dependent feedback on population growth is one of the most critical ecological controls on a species [1]. While all organisms face some form of resource limitation that ultimately restricts population growth, the controlling mechanisms vary among ecosystems, taxa, and reproductive strategies [1-3]. Our understanding of density-dependent effects on wild populations of large mammals is limited primarily to ungulates [4-10], while comparatively little is known about carnivores [11, 12]. Furthermore, the interaction between population density and environmental stochasticity is understudied [7, 13]. This study shows that reproductive parameters (weaning weight, pup sex, natality) change as density increases across years with varying environmental conditions in a large, capital-breeding carnivore.

Traits that exhibit density-dependent responses are those associated with survival and reproduction, including age at reproductive maturity, body size, parasite load, foraging success, and adult and offspring survival [11]. Generally, non-harvested large-bodied animals exhibit mean population levels close to carrying capacity (K') and are not expected to experience density-dependent changes in survival and reproduction until the population approaches K' [2, 3]. In these species, as a population approaches K', factors such as competition, social organization, spatial distribution, etc. act synergistically to produce an exaggerated response that further limits population growth [2, 10]. Both population size and resource availability affect the success of resource allocation in reproduction, thereby affecting reproductive success and, ultimately, offspring survival.

Animals support reproductive processes by relying on either stored resources (capital breeding) or resources gained from active foraging during reproduction (income breeding) [14, 15]. As the temporal and spatial constraints on foraging are reduced in capital breeders, they are expected to be less sensitive to environmental change than income breeders [15-17]. Within the context of lactation, a capital breeding mammal relies on energy acquired prior to parturition to sustain lactation, consequently maternal body stores at parturition are an upper limit to the nutrition her offspring may receive prior to weaning [16]. This strategy favors females with larger body size due to the corresponding increase in metabolic efficiency and greater total resources available to allocate to offspring [14, 15, 18]. Many iteroparous species exhibit indeterminant growth, which, coupled with low rates of population growth and low adult mortality, can favor increased reproductive effort with age [19-22]. This increase may be a function of either increased body size, experience, other physiological traits, or a combination thereof, and the mechanism likely varies between taxa [6, 19, 23]. High rates of population growth, however, can favor increased investment in early reproduction, reducing the importance of age in reproductive success [24, 25]. Offspring traits can also influence patterns of individual reproductive effort. Many vertebrate species exhibit a sex-biased allocation of resources to offspring [7, 13, 26-28]. Trivers and Willard proposed that if the reproductive potential is higher in one sex and is influenced by parental investment, then females should invest more in that sex when resources are abundant. When resources are scarce due to either environmental stochasticity or population density, they should invest in both sexes equally.

Elephant seals (*Mirounga sp.*) are excellent systems for investigating the dynamics of population growth and reproduction. They are highly polygynous, sexually dimorphic, capital breeding phocids that fast entirely throughout lactation and are the largest pinniped [29]. The northern species has colonies from Baja California, Mexico to northern California, USA. This species was hunted to the brink of extinction; by the early 1900s they had been extirpated from the US, with a remnant population estimated at fewer than 100 individuals surviving on Isla Guadalupe, Mexico [30]. During the 20th century, the species rebounded and recolonized much of its historic range. Prior to parturition, female elephant seals spend eight months foraging in the mesopelagic Northeast Pacific Ocean, accumulating body stores to sustain lactation and gestating their pup [31]. They produce high energy content milk while fasting over a 27-day lactation period [32], allowing pups to rapidly put on mass until they are abruptly weaned. The demography of the colony at Año Nuevo State Park, CA, has been studied continuously for nearly 60 years. Body condition data have been collected since the 1990s, which allows linkage between female foraging success, reproductive success, and varying oceanographic conditions [31, 33, 34]. This time series includes multiple El Niño Southern Oscillation (ENSO) events and the marine heatwave of 2014-2015. This marine heatwave was characterized by anomalously warm sea surface temperatures (SST) that developed in the Northeast Pacific Ocean in late 2013 and persisted through 2015, causing ecosystem-level disturbances [35, 36].

In this study, we examine reproductive outcomes under varying environmental conditions and population densities in the northern elephant seal. We use weaning mass data from 1984-2019 to explore the effects of environmental variability and population

density on reproductive traits, including offspring quality and sex-biased allocation of resources, in a highly polygynous, sexually dimorphic species. We hypothesize that: (1) offspring quality (e.g., weaning mass) will exhibit density dependence: as population size increases, quality will decrease; (2) older females will cope better with a high density population; and (3) sex allocation of resources will be male-biased in years with lower population density and/or more abundant resources, per Trivers-Willard. Long-term data sets in large mammal species are rare, but they can provide powerful insight into the fundamental principles of population dynamics that enhance our understanding of how species will respond to changing conditions.

3.3 Methods

3.3.1 Study Site and Ethics

This study was conducted at the northern elephant seal colony at Año Nuevo State Park, San Mateo County, California, U.S.A. The colony includes approximately two miles of mainland beaches in addition to the small nearby island. The population increased until 2002 [37] then plateaued, suggesting that it has reached carrying capacity.

3.3.2 Adult Female Mass and Pup Mass

Elephant seals come to shore for extended fasting periods during both breeding (Jan-Feb) and moulting (Apr-Jun), allowing us to access them for monitoring and sampling. Between these haulout periods, the animals are at sea continuously for ~3 months (post-breeding) and ~8 months (post-moult). Adult female mass gain during the gestational (post-moult) foraging trip was measured in approximately 20 individuals per year from 2004 – 2018. Females were sedated a few days prior to departure at the end of the moulting fast, and again upon return to shore during the breeding season, following

standard protocols [31]. These individuals were equipped with time-depth recorders (TDRs) and satellite transmitters (Wildlife Computers, Redmond, WA, USA or Sea Mammal Research Unit, St. Andrews, Scotland) that provided location information through the Argos network. At each handling, the animal was weighed in a canvas sling suspended from a hanging scale with a precision of ± 1 kg. During the breeding season instruments were recovered on the fifth day following birth. During these procedures, the female's pup was also weighed and flipper tagged. Adult females were also sedated for physiological studies in 1991, 1992, 1995-1997, 2001-2006, and 2009. These procedures provided additional data on female arrival mass, pup birth mass, and pup weaning mass, but not mass gain during foraging.

All measured masses were corrected to account for changes in mass due to fasting and lactation and to account for variation in the time spent onshore before and after measurements were taken. The equations used can be found in S1. The measured mass of the pup was corrected to birth mass based on an average mass gain of 2.2 kg day^{-1} during the first few days of lactation [38]. In adult females, days spent fasting without lactating (prior to parturition) (df) were assumed to cost 3.0 kg day^{-1} [39], while lactation days (dl) were assumed to cost the female 7.5 kg day^{-1} [18]. Departure from and arrival at the colony was determined from either TDR or satellite records. Animals were resighted daily after arrival to assess whether they had given birth.

3.3.3 Female Skip Breeding and Mortality

Satellite tracked adult females who returned to Año Nuevo at non-breeding times of year and did not give birth to a pup were categorized as skip breeders. Instrumented females that never returned to the colony and were not seen in subsequent seasons were

presumed dead. These two groups combined constitute the non-reproductive females for each breeding season. Logit-linked binomial GAMs were used to test whether adult female skip breeding or mortality were functions of departure mass, age, or current oceanographic conditions (ENSOPM, PDOPM, DepartMass, age).

3.3.4 Weanling Mass and Sex Ratio

A sample of weanling pups at Año Nuevo mainland have been weighed every year since 1978 (except 1979, 1981, and 1983) following the methods outlined in Le Boeuf and Crocker [33]. Briefly, pups were marked with a unique identifier using hair bleach prior to weaning and were designated as pup (with adult female) or weanling (independent) during subsequent daily resight efforts. Weaned pups quickly move away from harems, making it possible to distinguish weanlings easily. Once weaned, animals were captured in a nylon restraint bag, flipper tagged, and weighed from a hanging scale with a precision of +/- 1 kg. As with pup and adult masses, weaning mass was corrected for days spent fasting between weaning and weighing (determined from the resight effort described above) using the equation shown in Table 1 from Le Boeuf and Crocker [33].

Sex ratios (# Male: # Pups Total) were calculated from all flipper tagged young of the year that were born to flipper tagged females. This subset of individuals was selected to mitigate known sampling biases during weighing and tagging efforts due to differing study objectives between years and differences in behavior between male and female pups. Values for each year were tested against unity using a two-tailed binomial test.

3.3.5 Population Data

We used the annual number of pup births as a proxy for population size. Values prior to 2011 are from Le Boeuf et al. [37], and subsequent data were collected using the same

methods. Briefly, colony censuses were completed weekly by an experienced observer on foot. The total number of adult females was estimated using the count of adult females at peak breeding plus the count of adult females 32 or 33 days prior to and following that date [40]. The number of births is assumed to be 97.5% of the total number of adult females based on previous studies [40]. Pre-weaning pup survival (%) was calculated from the total number of pups born and the total number of weanlings counted during the censuses mentioned above. Pups were first observed on the island in 1961, and on the mainland in 1974. The population increased until 2002 when peak pup production reached 2108 [37].

Most of the weanling and adult female data were derived from the mainland portion of the colony, therefore we only used data from the mainland for these analyses. The time period included in this study was characterized by a rapid increase in the mainland population up through 2002, at which point the trend in the annual rate of change of births reaches zero [37]. Hereafter, we will refer to 1984-2002 as the growth or increasing density period, and from 2003 onward as the high-density period (Fig. 1).

3.3.6 Quantitative Analysis

Statistical analyses were completed in R 3.6.1 [41]. Differences between years were tested using ANOVA and Tukey's post hoc test. We only included years with a sample size greater than 50 for this analysis, which excluded 1978, 1980, 1982, and 1986. Differences between the sexes were tested using student t-tests. Values are reported as mean ± standard deviation (sd) or standard error (se), and will be specified. Generalized Additive Models (GAMs) were used to assess the effect of various environmental and biological covariates on weaning mass using the R package *mgcv* [42]. For all models,

Pearson's correlation coefficients were calculated for covariates to ensure that correlated covariates were not included together. Model selection was completed based on the Akaike Information Criterion (AICc) using the package MuMIn [43].

Three different indices of ocean conditions were evaluated, the Multivariate El Niño Southern Oscillation (ENSO) Index (Wolter 1993) , the Pacific Decadal Oscillation (PDO) index [44], and the Northern Oscillation Index (NOI) [45]. These indices are based on surface ocean conditions that can significantly influence primary productivity, but the temporal sensitivity of the mesopelagic food web to surface conditions is not well understood [46]. To account for a potential lag time between anomalous surface conditions and alteration in elephant seal foraging resources, we included average oceanographic indices from two and three years prior to each breeding season in addition to average indices from the gestational foraging trip prior to the breeding season (see S2 for a complete list of covariates).

Any data that violated the assumption that a single mother nursed a single pup throughout the average lactation period were removed from the analysis. This included weanlings above 170 kg of mass ("super-weaners" who nursed from multiple females) and those below 80 kg (pups abandoned or separated from their mother). Ideally, pups weaned early would be included in this analysis. However, the nature of the elephant seal colony makes it extremely difficult to distinguish between pups that were separated from their mother due to storms or conspecifics as opposed to pups whose mother left early. These values represent the mean ±2 standard deviations. Similarly, if multiple weanlings were assigned to a single female in the same year, they were all removed. The resulting data set spanned all years of the study except 2000 (N=1413). For a few weanlings

(n=109 between 1991-2018), we also had values for pup mass at birth and maternal arrival mass, and these additional covariates were included in an analysis of that subset of animals.

3.4 Results and Discussion

We found that weaning mass exhibited density-dependence, with relatively little sensitivity to oceanographic conditions. Maternal age was the strongest predictor of weaning mass, and the importance of maternal age was greater as population density increased. There was a male bias in maternal resource allocation, which declined as density-dependence increased. The reduction in male offspring investment under high-density conditions supports the Trivers and Willard model of sex-biased resource allocation.

3.4.1 Weanling Mass and Ocean Conditions

During years of population growth (1984-2002), weanling masses were significantly higher than the years of high density (2003-2019) (127.5 ± 0.52 versus 125.1 ± 0.42 (se), respectively; p=0.0024). Weaning mass was predicted by a combination of maternal age, population size, pup sex, and various ocean indices, and the controlling mechanisms differed notably between the period of increasing population density and the period of high density (Table 1). At high density, the relative importance of maternal age increased (33.5% vs. 30.7% of deviance explained), while neither pup sex nor population size was significant and different ocean indices were significant. The best-fitting generalized additive model (GAM) for the entire time series (N=1413) included Sex, MomAge, Population, Pacific Decadal Oscillation (PDO) during gestation, El Niño Southern Oscillation (ENSO) during gestation, and El Niño Southern Oscillation three years prior to

birth (see S2 for all tested covariates). This model explained 37.8% of the deviance in weaning mass, while maternal age alone explained 31.2% of the deviance. Weaning mass increased with both birth mass (S3, $F_{1,143} = 40.0$, $p=3.1x10^{-9}$, $R^2 = 0.213$) and maternal arrival mass (S4, $F_{1,272} = 42.33$, $p=3.7x10^{-10}$, $R^2 =0.132$). Still, neither of those traits were as important as maternal age and population size in predicting weaning mass within the subset of weanlings for whom those additional measurements were available (n=109).

Life-history theory suggests that offspring condition in large-bodied animals may be affected by population density when carrying capacity is reached [2, 9]. The colony at Año Nuevo transitioned from a low density, high growth rate population to a high-density population with no growth and shows clear density-dependence in offspring quality (Fig. 1). At high-density, weaning masses were significantly lower, the importance of maternal age as a driver of weaning mass increased, and the influence of ocean conditions decreased relative to low-density conditions (Table 1). This is consistent with work on bighorn sheep (*Ovis canadensis*), a large, capital breeding, terrestrial mammal that exhibits density dependence in the relationship between maternal mass and reproductive success. At high density, larger mass was advantageous for natality, whereas at low density reproductive success was independent of mass [5, 13].

Elephant seal weaning mass integrates maternal effects (energy stores available, milk quality, age, behavior), on-shore conditions (colony density, alpha male quality, beach quality, tides, and storms), and characteristics intrinsic to the pup (behavior, individual metabolic rate) [18, 23, 47]. An essential resource for reproductive success in elephant seals is the female's location on the beach. A high-quality location has enough space for females to maximize nursing time by minimizing disturbance and energy expended on

interactions with conspecifics. It also allows them to adjust to high tide and swell conditions. All of these features will increase the pup's weaning mass and improve its chance of survival. Harem density affects female reproductive success, with young females showing particularly reduced success in a high-density harem compared to either more experienced individuals in the same harem or young females in a low-density harem [20].

Older females produced heavier pups than younger females of the same mass (Fig. 2). While we found that larger females gave birth to larger pups (S5, $F_{1,253}$=33.73, p=1.9x10^{-8}, R^2 = 0.114) and weaned larger pups (S4; also as in [34, 38]), our models indicate that maternal age was a better predictor of pup mass at weaning than either maternal mass or pup mass at birth (Table 1). While age and size covary in this species, size is often assumed to be the variable of import when it comes to maternal reproductive success [34]. Our findings, however, demonstrate that age is more important and should not simply be considered a proxy for size. Maternal mass captures the energetic component of reproduction, with larger females delivering more milk energy over lactation [18]. However, this effect decreases with female age, as females grow more rapidly in their early reproductive years (S6). Maternal age represents an integration of both body condition and experience; older females have both physiological and behavioral advantages in rearing their pups [18, 23, 48]. Previous work shows that maternal age is 2.5 times more important to offspring growth efficiency than the amount of energy delivered [23]. Experienced females are better able to modify pup behavior to minimize the energy wasted through activity [23]. They are more likely to secure optimum positions within harems, thereby reducing their energy expenditure on activities other

than lactation and increasing their overall efficiency [18, 20]. Furthermore, the fat content of milk produced at the start of lactation is significantly lower in young females than that provided by prime-age females [48].

Elephant seal weaning mass varied as a function of both PDO and ENSO ocean condition indices, but both maternal age and population size were more robust explanatory variables (Table 1). Weaning mass in some years following unusual ocean events was significantly lower (e.g., 1999 and 2015, following 1998 El Niño and 2014 marine heatwave; Table 2), while other years it was not (e.g., 1984, 2016, and 2017 following 2015 marine heatwave and 1983 and 2016 El Niño). Previous studies reported that weaning mass declined during the warm, sardine-dominated phase of the PDO [33]. Furthermore, during the 1998 El Niño the rate of mass gain was lower and foraging trips were longer in adult female elephant seals during their pre-gestation foraging trip [49]. While successful reproduction is fundamentally linked to successful foraging, weaning mass is not as direct a reflection of foraging success or ocean conditions as previously thought [33, 34], which is consistent with capital breeding species being less sensitive to environmental disturbance than income breeders [15-17]. In contrast, southern elephant seals exhibit a stronger relationship between reproductive investment and ocean conditions [50-53]. Further comparisons between the species would provide insight into the interaction between population dynamics and the environment. Population-level indicators of poor foraging conditions may be found in other metrics, like adult female survival and frequency of skip breeding (S7 and supplemental results). For long-lived species, sacrificing one reproductive opportunity to ensure future reproduction may be a

higher fitness strategy than attempting to reproduce at marginal body condition, which may compromise their ability to survive, risking future reproduction [13, 54].

Northern elephant seals exhibited sex-bias resource allocation that is consistent with Trivers-Willard [27]. Male weanlings were, on average, heavier than female weanlings by 4.2 kg (p=1.6x10^{-10}). However, the magnitude of the difference varied highly between years, and in most years, there was no significant difference between the sexes (Table 2, S8, and S9). The mass of male weanlings declined significantly (p=0.00028) from the growth phase (130.3 ± 24.0) to the high-density phase (126.7 ± 22.1). In contrast, the average weaning mass of female pups did not change, indicating that male-biased resource allocation is density-dependent.

Furthermore, young (3-5-year-old) female elephant seals reduced resource allocation for both sexes, whereas older females (7+ years) appeared to increase investment in female pups and decrease investment in male pups at high density (Fig. 3, S10). Northern elephant seals are a highly polygynous species, and successful males have much higher reproductive potential (up to 121 pups [21]) than the most successful female (16 pups [34]). Under the model by Trivers and Willard, females should invest more heavily in sons than in daughters when food resources are abundant, as greater weaning mass increases the chances of survival to reproductive age [55, 56]. Studies in southern elephant seals (*Mirounga leonida*) [51, 57] and Antarctic fur seals (*Arctocephalus gazella*) [58, 59] also found sex-biased allocation following Trivers and Willard, although a study on variation in northern elephant seal sex ratio concluded that the Resource Competition model explained the variation seen [26, 60] (see also SI for sex ratio results). In bighorn sheep, sex bias was predicted by maternal age and reproductive history in addition to

environmental conditions, with older females exhibiting greater control over resource allocation to minimize the cost of reproduction [13]. While Trivers-Willard would predict the resulting sex-bias, the added interaction of age and reproductive history supports the Cost of Reproduction hypothesis (Cockburn 2002). We cannot rule out this mechanism in the elephant seal system given the different trends seen with age and population density between the sexes (Fig. 3c) but were unable to assess the additional effect of reproductive history.

3.4.2 Adult Female Mass Gain, Pregnancy, and Survival

There were no significant differences between years in departure mass, arrival mass, mass gain, or percent mass gain during post-molt foraging trips (S7, S11). There was an increase in the frequency of failed breeding across the study period, driven by a significant increase in mortality (S7). On average, 13% of instrumented adult females skip breeding each year, and the probability of skipping was independent of year or age. Both year and age influenced the probability that a female did not survive at sea, with higher mortality in recent years and higher mortality among young (4 to 6-year-old) females. Mass at departure did not predict either mortality or skip breeding.

The influence of varying ocean conditions on the population may be seen in adult female survival and natality rates. Although adult females have been shown to compensate for poor foraging conditions by lengthening their time at sea during the post-breeding foraging trip [49], during this time period their embryo is in diapause and their trip length is not constrained by fetal development. During their longer post-molt trip they are actively gestating and cannot extend their trip unless they are not pregnant. A female encountering relatively poor foraging conditions during gestation and unable to acquire

the stores needed to adequately provision a pup may abort her pregnancy and use the year to rebuild her body condition; periodic skipping is a component of the optimal reproductive strategy in the southern elephant seal [54, 61], which shares many life history traits with the northern species. In 2014 and 2015, 41% and 50% of deployment females failed to reproduce (S7), and in both years lower mass animals were missing from the reproductive group, with minimum arrival mass at 542 kg and 558 kg respectively compared to a 489 kg minimum averaged across all other years (S7, S11). Females that survive and successfully reproduce in years with poor foraging conditions are likely to be larger, more experienced animals as larger body size provides a greater buffer against marginal foraging conditions.

3.4.3 Pup Mass and Sex Differences

Pup mass at birth was 35.0 ± 5.39 kg (n=247) and did not differ significantly between the sexes. Overall, male and female pups had different masses at weaning (p=1.6x10^{-10}): female mean mass was 124.1 ± 22.0 kg while mean mass of males was 128.3 ± 23.1 kg. Although the difference between the sexes was not significant in all years (Table 2, S8, S9, S10), male weanlings were heavier than females (by 5.7-18.3 kg) in all instances when the difference was significant. During the growth phase, male weanlings had an average mass of 130.3 ± 24.0 and female weanlings had an average mass of 124.7 ± 22.6. In the period since 2003, the average male mass was significantly lower than the growth phase (126.7 ± 22.1, p=0.00028) and the female mass did not change significantly (123.6 ± 21.2). The sex difference in weanling mass is significant in both time periods (p=7.7x10^{-8} and p=0.00022) , although less pronounced after 2002; fewer years show significant

differences between the sexes and the overall difference decreased between the sexes decreased (S8, S9, S10).

The weanlings in the 5% tails of the distribution represent animals that were most likely abandoned or separated from their mother prematurely (<80 kg, "orphans"), or were very successful at nursing off of females in addition to their mother (>170 kg, "super-weaners"). The orphan group included 129 individuals over the length of the study with a sex ratio of 0.47 male and average maternal age of 5 years (33 mothers of known age). There were 94 super-weaners weighed during the study, with a significantly male biased sex ratio (0.64, $p < 0.05$) and mean maternal age of 7.6 years (23 known-age mothers).

While there is a significant relationship between mass at birth and at weaning (S3), the lack of sex difference at birth indicates that the sex difference in weaning mass is a result of lactation, not gestation. This finding differs from results found at the southern colonies at Islas San Benito (Mexico) where male pups were larger at birth but no significant difference was found between the sexes at weaning [62]. Prior studies at Año Nuevo indicate that milk stealing may also be an important driver in the difference between male and female weanling mass; male pups were documented successfully stealing milk more often than females [20, 32]. This mechanism for generating heavier male weanlings is supported by a study that found no difference in costs to the mother for producing male versus female offspring in terms of future reproduction [63]. The male-skewed sex ratio of super-weaners further supports the importance of milk stealing in producing heavier males. It is possible that differences in female behavior, on shore environment, and colony structure explain the lack of difference between the sexes at weaning found at Islas San Benito.

The sex ratio across all years was 0.51 male. Only in 1987 (0.39) and 2012 (0.31) were sex ratios statistically different from unity given the sample size. Variation in the sex ratio of pups at weaning at Año Nuevo does not appear to be linked with ocean conditions, and we find no direct evidence that supports either the Trivers and Willard [27] or Resource Competition [26] models for deviation from unity. In both years with skewed sex ratios (1987 and 2012, Table 2), the bias was toward female pups, the average weaning mass was not different from the long-term average, nor were there unusual ocean conditions. This differs from a study conducted at the Farallon Islands (California, USA) which found a relationship between sex ratio and the NOI, where El Niño conditions correlated with an increase in sex ratio (more male pups), particularly during the 1998 El Niño event [60]. There is evidence that young females produce more female than male pups in both southern [64, 65] and northern [34] elephant seals, although the difference seen in northern elephant seals is minor compared to that reported for the southern species. It is possible that variations in the age structure of the breeding population contributed to the anomalous sex ratios seen at both Año Nuevo and the Farrallones.

3.5 Conclusion

Our results have important implications for understanding the mechanisms controlling reproduction in capital-breeding mammals. Life-history theory is at the core of ecological and population dynamics, but understanding the varying patterns observed in nature and their underlying mechanisms requires long-term studies of populations, which makes testing hypotheses challenging, especially in large-bodied animals with slow reproductive rates and long lifespans. Time series data that have recorded changes in reproductive output as a population rapidly grows after extirpation are rare, particularly

for a carnivore. Our findings regarding density dependence and resource allocation support previous work in the field [4-9, 13] and show that these mechanisms are conserved across terrestrial and marine systems. These results also reveal points of contradiction with previous studies (e.g. offspring sex ratio and sex bias in northern elephant seals [60, 62]; importance of ocean conditions on weaning mass in northern and southern elephant seals [33, 51, 52]), which illustrates the complexity of these questions and invites further investigation. The mechanisms controlling reproductive output may vary with population dynamics, as seen here, which is an essential consideration in analyses striving to assess the effect of extrinsic changes on a population.

Understanding population dynamics depends on a knowledge of vital rates and how those rates may change under varying environmental conditions. Capital breeding strategies may have evolved, in part, to confer resilience to short-term environmental variability. As a result, some species (e.g., many phocid seals) appear to avoid years of population-wide reproductive failure resulting from environmental variability that are seen in income breeding species within the same environment (e.g., otariids, sea birds). Individuals that attempt to breed are generally successful, even in years with poor foraging conditions, while individuals with compromised states may skip breeding and restore body condition for subsequent breeding attempts. In northern elephant seals, these traits contributed to rapid population recovery from near extinction and dramatic changes in colony density over a short period. Our findings show density-dependent changes in the mechanisms controlling reproductive success and that maternal experience and behaviour during breeding, not just body condition, is a critical determinant of parental investment in capital breeders.

3.6 References

1. Hairston N.G.S., Frederick E.; Slobodkin, Lawrence B. 1960 Community Structure, Population Control, and Competition. *The American Naturalist* **94**(879), 421-425.

2. Fowler C. 1981 Density Dependence as Related to Life History Strategy. *Ecology* **62**.

3. Stubs M. 1977 Density Dependence in the Life-Cycles of Animals and its Importance in K- and RStrategies. *J Anim Ecol* **46**.

4. Coulson T., Albon S., Guinness F., Pemberton J., CluttonBrock T. 1997 Population substructure, local density, and calf winter survival in red deer (Cervus elaphus). *Ecology* **78**(3), 852-863.

5. Festa-Bianchet M., Gaillard J.M., Jorgenson J.T. 1998 Mass- and density-dependent reproductive success and reproductive costs in a capital breeder. *Am Nat* **152**(3), 367-379. (doi:10.1086/286175).

6. Côté S.D., Festa-Bianchet M. 2001 Reproductive success in female mountain goats: the influence of age and social rank. *Animal Behaviour* **62**(1), 173-181. (doi:10.1006/anbe.2001.1719).

7. Kruuk L.E., Clutton-Brock T.H., Albon S.D., Pemberton J.M., Guinness F.E. 1999 Population density affects sex ratio variation in red deer. *Nature* **399**(6735), 459-461. (doi:10.1038/20917).

8. Stopher K.V., Pemberton J.M., Clutton-Brock T.H., Coulson T. 2008 Individual differences, density dependence and offspring birth traits in a population of red deer. *Proc Roy Soc B* **275**(1647), 2137-2145. (doi:10.1098/rspb.2008.0502).

9. Clutton-Brock T.H., Albon S.D., Guinness F.E. 1987 Interactions Between Population Density and Maternal Characteristics Affecting Fecundity and Juvenile Survival in Red Deer. *The Journal of Animal Ecology* **56**(3), 857-871. (doi:10.2307/4953).

10. McCullough D.R. 1979 *The George Reserve deer herd: population ecology of a K-selected species [Michigan]*.

11. Fowler C.W. 1990 Density Dependence in Northern Fur Seals (Callorhinus-Ursinus). *Marine Mammal Science* **6**(3), 171-195. (doi:10.1111/j.1748-7692.1990.tb00242.x).

12. Levi T., Wilmers C.C. 2012 Wolves-coyotes-foxes: a cascade among carnivores. *Ecology* **93**(4), 921-929. (doi:10.1890/11-0165.1).

13. Martin J., Festa-Bianchet M. 2011 Sex ratio bias and reproductive strategies: What sex to produce when? *Ecology* **92**(2), 441-449.

14. Drent R.H., Daan S. 1980 The Prudent Parent - Energetic Adjustments in Avian Breeding. *Ardea* **68**(1-4), 225-252.

15. Stephens P.A., Boyd I.L., McNamara J.M., Houston A.I. 2009 Capital breeding and income breeding: their meaning, measurement, and worth. *Ecology* **90**(8), 2057-2067. (doi:10.1890/08-1369.1).

16. Boyd I.L. 2000 State-dependent fertility in pinnipeds: contrasting capital and income breeders. *Functional Ecology* **14**(5), 623-630. (doi:10.1046/j.1365-2435.2000.t01-1-00463.x).

17. McHuron E.A., Costa D.P., Schwarz L., Mangel M., Matthiopoulos J. 2017 State-dependent behavioural theory for assessing the fitness consequences of anthropogenic disturbance on capital and income breeders. *Methods in Ecology and Evolution* **8**(5), 552-560. (doi:10.1111/2041-210x.12701).

18. Crocker D.E., Williams J.D., Costa D.P., Le Boeuf B.J. 2001 Maternal traits and reproductive effort in northern elephant seals. *Ecology* **82**(12), 3541-3555. (doi:10.1890/0012-9658(2001)082[3541:Mtarei]2.0.Co;2).

19. Clutton-Brock T.H. 1984 Reproductive Effort and Terminal Investment in Iteroparous Animals. *The American Naturalist* **123**(2), 212-229. (doi:10.1086/284198).

20. Reiter J., Panken K.J., Le Boeuf B.J. 1981 Female Competition and Reproductive Success in Northern Elephant Seals. *Animal Behaviour* **29**(Aug), 670-687. (doi:10.1016/S0003-3472(81)80002-4).

21. Le Boeuf B., Reiter J. 1988 Lifetime reproductive success in northern elephant seals. *Reproductive success University of Chicago Press, Chicago*, 344-362.

22. Charlesworth B., Leon J.A. 1976 The relation of reproductive effort to age. *The American Naturalist* **110**(973), 449-459.

23. Hooper A.W., Berger R.W., Rubin L.S., McDonald B.I., Crocker D.E. 2019 Maternal age influences offspring behaviour and growth efficiency during provisioning in northern elephant seals. *Animal Behaviour* **151**, 121-130. (doi:10.1016/j.anbehav.2019.03.007).

24. Cole L.C. 1954 The population consequences of life history phenomena. *Q Rev Biol* **29**(2), 103-137. (doi:10.1086/400074).

25. Stearns S.C. 1976 Life-history tactics: a review of the ideas. *Q Rev Biol* **51**(1), 3-47. (doi:10.1086/409052).

26. Clark A.B. 1978 Sex ratio and local resource competition in a prosimian primate. *Science* **201**(4351), 163-165. (doi:10.1126/science.201.4351.163).

27. Trivers R.L., Willard D.E. 1973 Natural selection of parental ability to vary the sex ratio of offspring. *Science* **179**(4068), 90-92. (doi:10.1126/science.179.4068.90).

28. Hardy I.C.W. 1997 Possible factors influencing vertebrate sex ratios: An introductory overview. *Appl Anim Behav Sci* **51**(3-4), 217-241. (doi:10.1016/S0168-1591(96)01106-9).

29. Le Boeuf B.J. 1972 Sexual behavior of the northern elephant seal Mirounga angustirostris. *Behaviour* **41**, 1-26.

30. Lowry M.S., Condit R., Hatfield B., Allen S.G., Berger R., Morris P.A., Le Boeuf B.J., Reiter J. 2014 Abundance, Distribution, and Population Growth of the Northern Elephant Seal (Mirounga angustirostris) in the United States from 1991 to 2010. *Aquatic Mammals* **40**(1), 20-31. (doi:10.1578/Am.40.1.2014.20).

31. Robinson P.W., Costa D.P., Crocker D.E., Gallo-Reynoso J.P., Champagne C.D., Fowler M.A., Goetsch C., Goetz K.T., Hassrick J.L., Hückstädt L.A. 2012 Foraging behavior and success of a mesopelagic predator in the northeast Pacific Ocean: insights from a data-rich species, the northern elephant seal. *PLoS One* **7**(5), e36728.

32. Reiter J., Stinson N.L., Le Boeuf B.J. 1978 Northern Elephant Seal Development: The Transition from Weaning to Nutritional Independence. *Behavioral Ecology and Sociobiology* **3**(4), 337-367.

33. Le Boeuf B.J., Crocker D.E. 2005 Ocean climate and seal condition. *BMC biology* **3**, 9. (doi:10.1186/1741-7007-3-9).

34. Le Boeuf B.J., Condit R., Reiter J. 2019 Lifetime reproductive success of northern elephant seals, Mirounga angustirostris . *Canadian Journal of Zoology*. (doi:10.1139/cjz-2019-0104).

35. Bond N.A., Cronin M.F., Freeland H., Mantua N. 2015 Causes and impacts of the 2014 warm anomaly in the NE Pacific. *Geophysical Research Letters* **42**(9), 3414-3420. (doi:10.1002/2015gl063306).

36. Di Lorenzo E., Mantua N. 2016 Multi-year persistence of the 2014/15 North Pacific marine heatwave. *Nature Climate Change*. (doi:10.1038/nclimate3082).

37. Le Boeuf B.J., Condit R., Morris P.A., Reiter J. 2011 The Northern Elephant Seal (Mirounga angustirostris) Rookery at Año Nuevo: A Case Study in Colonization. *Aquatic Mammals* **37**(4), 486-501. (doi:10.1578/AM.37.4.2011.486).

38. Deutsch C.J., Crocker D.E., Costa D.P., Le Boeuf B.J. 1994 Sex-and age-related variation in reproductive effort of northern elephant seals. In *Elephant seals: Population ecology, behavior, and physiology* (pp. 169-210.

39. Worthy G.A.J., Morris P.A., Costa D.P., Le Boeuf B.J. 1992 Molt Energetics of the Northern Elephant Seal (Mirounga-Angustirostris). *Journal of Zoology* **227**, 257-265.

40. Condit R., Le Boeuf B.J., Morris P.A., Sylvan M. 2007 Estimating Population Size in Asynchronous Aggregations: A Bayesian Approach and Test with Elephant Seal Censuses. *Marine Mammal Science* **23**(4), 834-855. (doi:10.1111/j.1748-7692.2007.00141.x).

41. R Core Team. 2019 R: A language and environment for statistical computing. (Vienna, Austria, R Foundation for Statistical Computing.

42. Wood S.N. 2017 *Generalized Additive Models: An Introduction with R*. Second ed, CRC Press.

43. Barton K. 2019 MuMIn: Multi-Model Interence. (R package version 1.43.6. ed.

44. Mantua N.J., Hare S.R. 2002 The Pacific decadal oscillation. *Journal of Oceanography* **58**(1), 35-44.

45. Schwing F.B., Murphree T., Green P.M. 2002 The Northern Oscillation Index (NOI): a new climate index for the northeast Pacific. *Progress in Oceanography* **53**(2-4), 115-139. (doi:10.1016/S0079-6611(02)00027-7).

46. St. John M.A., Borja A., Chust G., Heath M., Grigorov I., Mariani P., Martin A.P., Santos R.S. 2016 A Dark Hole in Our Understanding of Marine Ecosystems and Their Services: Perspectives from the Mesopelagic Community. *Frontiers in Marine Science* **3**. (doi:10.3389/fmars.2016.00031).

47. Costa D.P., Le Boeuf B.J., Huntley A.C., Ortiz C.L. 1986 The Energetics of Lactation in the Northern Elephant Seal, Mirounga-Angustirostris. *Journal of Zoology* **209**, 21-33.

48. McDonald B.I., Crocker D.E. 2006 Physiology and behavior influence lactation efficiency in northern elephant seals (Mirounga angustirostris). *Physiological and biochemical zoology : PBZ* **79**(3), 484-496. (doi:10.1086/501056).

49. Crocker D.E., Costa D.P., Le Boeuf B.J., Webb P.M., Houser D.S. 2006 Impact of El Niño on the foraging behavior of female northern elephant seals. *Marine Ecology-Progress Series* **309**.

50. Hindell M.A., Sumner M., Bestley S., Wotherspoon S., Harcourt R.G., Lea M.A., Alderman R., McMahon C.R. 2017 Decadal changes in habitat characteristics influence population trajectories of southern elephant seals. *Global change biology*. (doi:10.1111/gcb.13776).

51. McMahon C.R., Harcourt R.G., Burton H.R., Daniel O., Hindell M.A. 2017 Seal mothers expend more on offspring under favourable conditions and less when resources are limited. *J Anim Ecol* **86**(2), 359-370. (doi:10.1111/1365-2656.12611).

52. Clausius E., McMahon C.R., Hindell M.A. 2017 Five decades on: Use of historical weaning size data reveals that a decrease in maternal foraging success underpins the long-term decline in population of southern elephant seals (Mirounga leonina). *PLoS One* **12**(3), e0173427. (doi:10.1371/journal.pone.0173427).

53. Clausius E., McMahon C.R., Harcourt R., Hindell M.A. 2017 Effect of climate variability on weaning mass in a declining population of southern elephant seals Mirounga leonina. *Marine Ecology Progress Series* **568**, 249-260. (doi:10.3354/meps12085).

54. Desprez M., Gimenez O., McMahon C.R., Hindell M.A., Harcourt R.G. 2018 Optimizing lifetime reproductive output: Intermittent breeding as a tactic for females in a long-lived, multiparous mammal. *J Anim Ecol* **87**(1), 199-211. (doi:10.1111/1365-2656.12775).

55. McMahon C.R., Burton H.R., Bester M.N. 2000 Weaning mass and the future survival of juvenile southern elephant seals, Mirounga leonina, at Macquarie Island. *Antarctic Science* **12**(2), 149-153. (doi:10.1017/S0954102000000195).

56. Costa D.P., Schwarz L., Robinson P., Schick R.S., Morris P.A., Condit R., Crocker D.E., Kilpatrick A.M. 2016 A Bioenergetics Approach to Understanding the Population Consequences of Disturbance: Elephant Seals as a Model System. *Adv Exp Med Biol* **875**, 161-169. (doi:10.1007/978-1-4939-2981-8_19).

57. Arnbom T., Fedak M.A., Boyd I.L., Mcconnell B.J. 1993 Variation in Weaning Mass of Pups in Relation to Maternal Mass, Postweaning Fast Duration, and Weaned Pup Behavior in Southern Elephant Seals (Mirounga-Leonina) at South-Georgia. *Can J Zool* **71**(9), 1772-1781. (doi:10.1139/z93-252).

58. Costa D.P., Trillmich F., Croxall J.P. 1988 Intraspecific Allometry of Neonatal Size in the Antarctic Fur-Seal (Arctocephalus-Galapagoensis). *Behavioral Ecology and Sociobiology* **22**(5), 361-364.

59. Boyd I.L., Mccann T.S. 1989 Pre-Natal Investment in Reproduction by Female Antarctic Fur Seals. *Behavioral Ecology and Sociobiology* **24**(6), 377-385. (doi:10.1007/Bf00293265).

60. Lee D.E., Sydeman W.J. 2009 North Pacific Climate Mediates Offspring Sex Ratio in Northern Elephant Seals. *Journal of Mammalogy* **90**(1), 1-8. (doi:10.1644/08-Mamm-a-130.1).

61. Griffen B.D. 2018 Reproductive skipping as an optimal life history strategy in the southern elephant seal, Mirounga leonina. *Ecology and Evolution*. (doi:10.1002/ece3.4408).

62. Salogni E., Galimberti F., Sanvito S., Miller E.H. 2019 Male and female pups of the highly sexually dimorphic northern elephant seal (Mirounga angustirostris) differ slightly in body size. *Canadian Journal of Zoology* **97**(3), 241-250. (doi:10.1139/cjz-2018-0220).

63. Le Boeuf B.J., Condit R., Reiter J. 1989 Parental investment and the secondary sex ratio in northern elephant seals. *Behavioral Ecology and Sociobiology* **25**(2), 109-117. (doi:10.1007/bf00302927).

64. Arnbom T., Fedak M.A., Rothery P. 1994 Offspring Sex-Ratio in Relation to Female Size in Southern Elephant Seals, Mirounga-Leonina. *Behavioral Ecology and Sociobiology* **35**(6), 373-378. (doi:Doi 10.1007/Bf00165838).

65. Wilkinson I.S., van Aarde R.J. 2001 Investment in sons and daughters by southern elephant seals, Mirounga leonina, at Marion Island. *Marine Mammal Science* **17**(4), 873-887. (doi:DOI 10.1111/j.1748-7692.2001.tb01303.x).

Table 3.1 - Best fitting models to explain variation in weaning mass for the entire data set, the growth period, the stable period, and the subset of animals for whom birth mass and maternal arrival mass were also available

Dataset	Model	N	AICc	Deviance Explained	GCV
All (1984 – 2019)	WeanMass ~ Sex + MomAge + Population + PDOPM + ENSOPM + ENSO3	1413	11676.4	37.8%	226.8
	WeanMass ~ Sex + MomAge + Year (RE)	1413	11690.2	38.2%	228.4
	WeanMass ~ Sex + MomAge + Population	1413	11700.1	36.1%	230.6
	WeanMass ~ MomAge + Population	1413	11710.8	35.6%	232.4
	WeanMass ~ MomAge	1413	11789.6	31.2%	244.7
Increasing Density (1984 – 2002)	WeanMass ~ Sex + MomAge + Population + PDOPM + ENSOPM	824	6801.9	39.2%	224.5
	WeanMass ~ Sex + MomAge + Year (RE)	824	6808.7	39.2%	226.3
	WeanMass ~ Sex + MomAge + Population	824	6818.3	37.6%	229.0
	WeanMass ~ MomAge + Population	824	6825.9	36.9%	231.2
	WeanMass ~ MomAge	824	6886.9	30.7%	249.0
High Density (2003 – 2019)	WeanMass ~ MomAge + PDO2	589	4881.4	36.1%	231.8
	WeanMass ~ MomAge + Year (RE)	589	4886.6	36.2%	233.8
	WeanMass ~ MomAge	589	4897.1	33.5%	238.1
Pup Mass (1991 - 2019)	WeanMass ~ MomAge + Year (RE)	109	864.1	54.1%	156.1
	WeanMass ~ MomAge + Population	109	863.2	51.2%	156.1
	WeanMass ~ MomAge	109	873.8	47.0%	171.8

Table 3.2 - Summary of interannual differences in weaning mass, sex bias, and pup production for the mainland Año Nuevo northern elephant seal colony. Values in bold are significant ($p < 0.05$). Years highlighted in yellow indicate breeding seasons following significant ENSO events and the 2014-2015 marine heatwave.

Year	N	Mean Weaning mass	Male - Female Mass	Sex Ratio (N)	Births	Pup Survival
All	4691	126.1 ± 22.5	**4.2**	0.51 (3376)	--	92.8%
Increasing	2000	**127.5 ± 23.5**	**5.6**	0.51 (2047)	27902	92.2%
High	2691	**125.1 ± 21.7**	**3.0**	0.51 (1326)	29426	92.9%
1984	80	***134.0 ± 19.8***	7.8	0.56 (89)	741	92.0%
1985	85	***136.7 ± 23.5***	3.4	0.59 (113)	700	90.6%
1987	81	127.1 ± 25.3	9.1	***0.39 (108)***	797	88.7%
1988	207	***133.1 ± 27.8***	***7.8***	0.49 (153)	960	89.7%
1989	206	***131.3 ± 25.0***	2.2	0.48 (172)	1087	**86.7%**
1990	88	124.8 ± 25.4	1.7	0.49 (122)	1177	93.0%
1991	55	130.0 ± 22.1	5.5	0.51 (83)	1432	92.9%
1992	102	125.0 ± 21.3	3.9	0.51 (110)	1633	95.2%
1993	54	***117.4 ± 20.8***	3.3	0.49 (63)	1623	91.4%
1994	83	128.7 ± 22.2	-2.6	0.49 (108)	1624	92.7%
1995	105	***118.5 ± 20.2***	***10.4***	0.53 (172)	2041	98.1%
1996	187	124.7 ± 21.0	5.7	0.56 (277)	1776	96.5%
1997	97	123.3 ± 23.3	***17.6***	0.56 (78)	2011	**83.7%**
1998	175	127.6 ± 19.1	4.6	0.64 (33)	1958	99.2%
1999	86	***120.4 ± 22.9***	5.0	--	1818	90.4%
2000	82	123.7 ± 25.4	***18.3***	0.44 (18)	1837	94.3%
2001	92	130.1 ± 21.1	5.8	0.52 (123)	1932	91.2%
2002	113	130.0 ± 22.3	-1.1	0.53 (139)	1926	93.9%
2003	148	127.4 ± 29.6	3.5	0.48 (97)	2108	95.8%
2004	166	125.7 ± 22.5	-2.6	0.48 (104)	1962	92.2%
2005	135	124.0 ± 22.7	3.9	0.53 (150)	1981	98.9%
2006	101	122.4 ± 18.6	3.4	0.53 (110)	2063	96.4%
2007	68	124.8 ± 17.3	4.7	0.48 (80)	1935	96.0%
2008	72	122.4 ± 18.8	6.8	0.58 (67)	1877	96.1%
2009	99	124.7 ± 18.9	***8.0***	0.58 (66)	1670	92.5%
2010	119	***121.0 ± 20.8***	-0.2	0.62 (52)	1735	88.6%
2011	183	128.5 ± 21.3	4.3	0.46 (57)	1549	92.8%
2012	202	128.5 ± 21.9	3.2	***0.31 (75)***	1527	93.4%
2013	239	***132.2 ± 22.6***	1.1	0.52 (103)	1463	92.6%
2014	86	127.9 ± 20.8	2.6	0.43 (28)	1549	94.6%
2015	95	***120.9 ± 21.5***	7.9	0.58 (40)	1533	**80.0%**
2016	184	121.8 ± 21.4	4.1	0.42 (71)	1617	92.4%
2017	269	123.3 ± 20.9	***5.7***	0.60 (68)	1597	94.6%
2018	274	121.9 ± 20.0	2.5	0.52 (58)	1647	94.4%
2019	250	124.7 ± 20.3	3.4	0.53 (96)	1613	**87.2%**

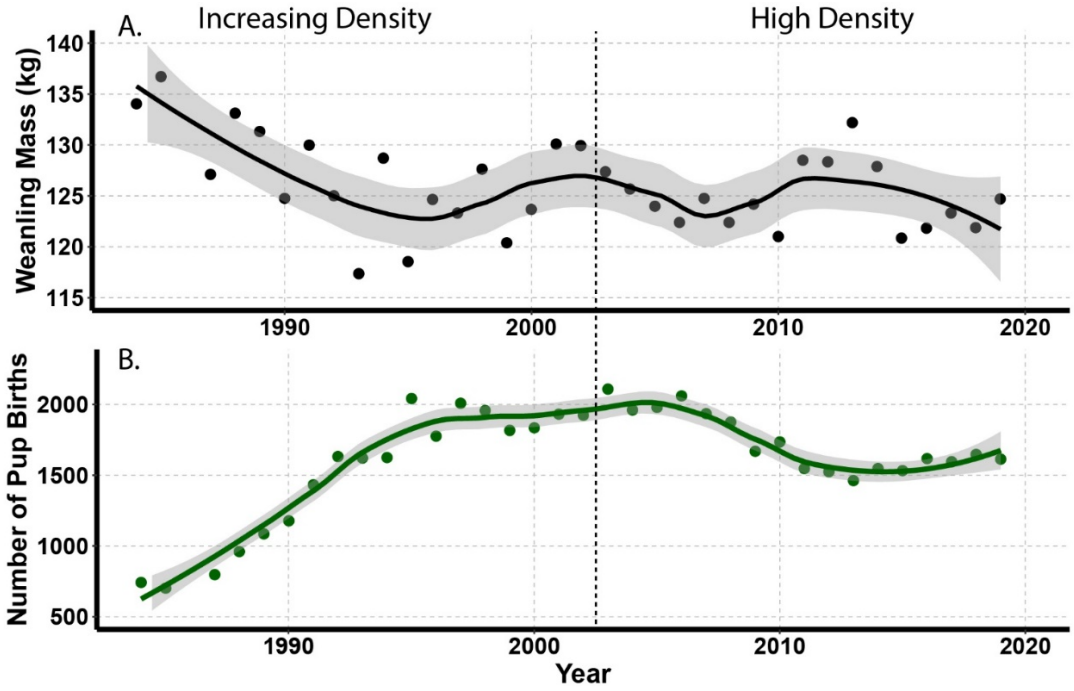

Fig. 3.1 – Annual mean weaning mass (**A**) and number of pup births (**B**) at the mainland portion of the Año Nuevo colony with Loess regression smoothers. The vertical dotted line indicates the transition from increasing population density to high density conditions.

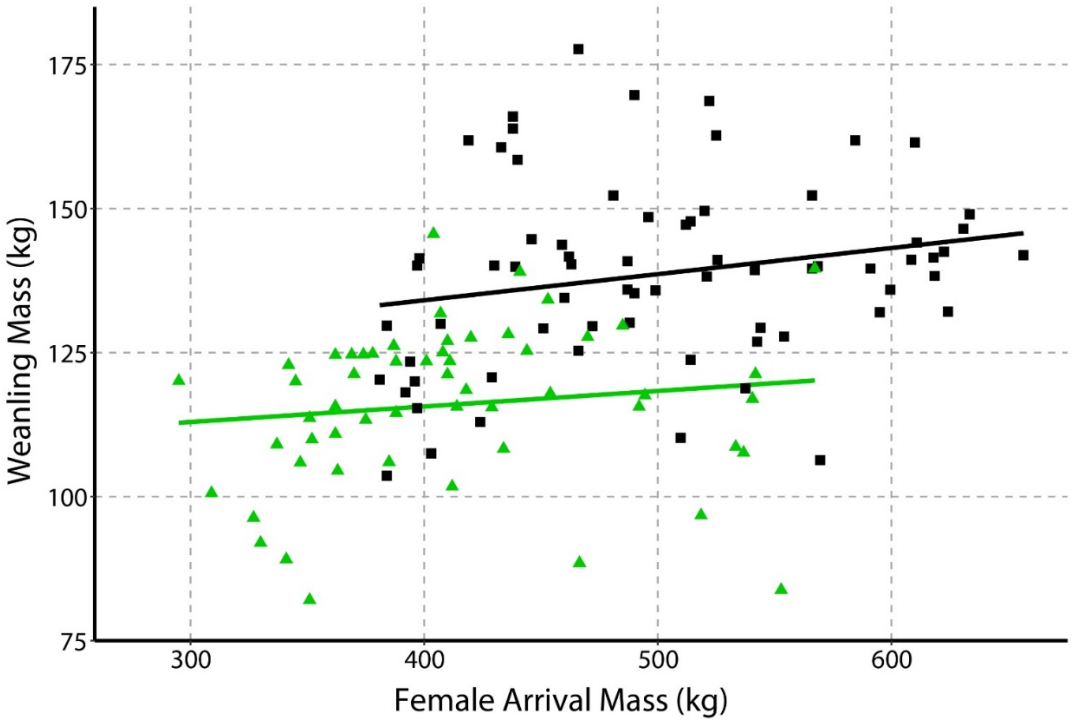

Fig. 3.2 - Pup wean mass as a function of female arrival mass of young (3 to 5-year-olds; green diamonds) and old (9+ years of age; black squares) mothers with linear regression trendlines.

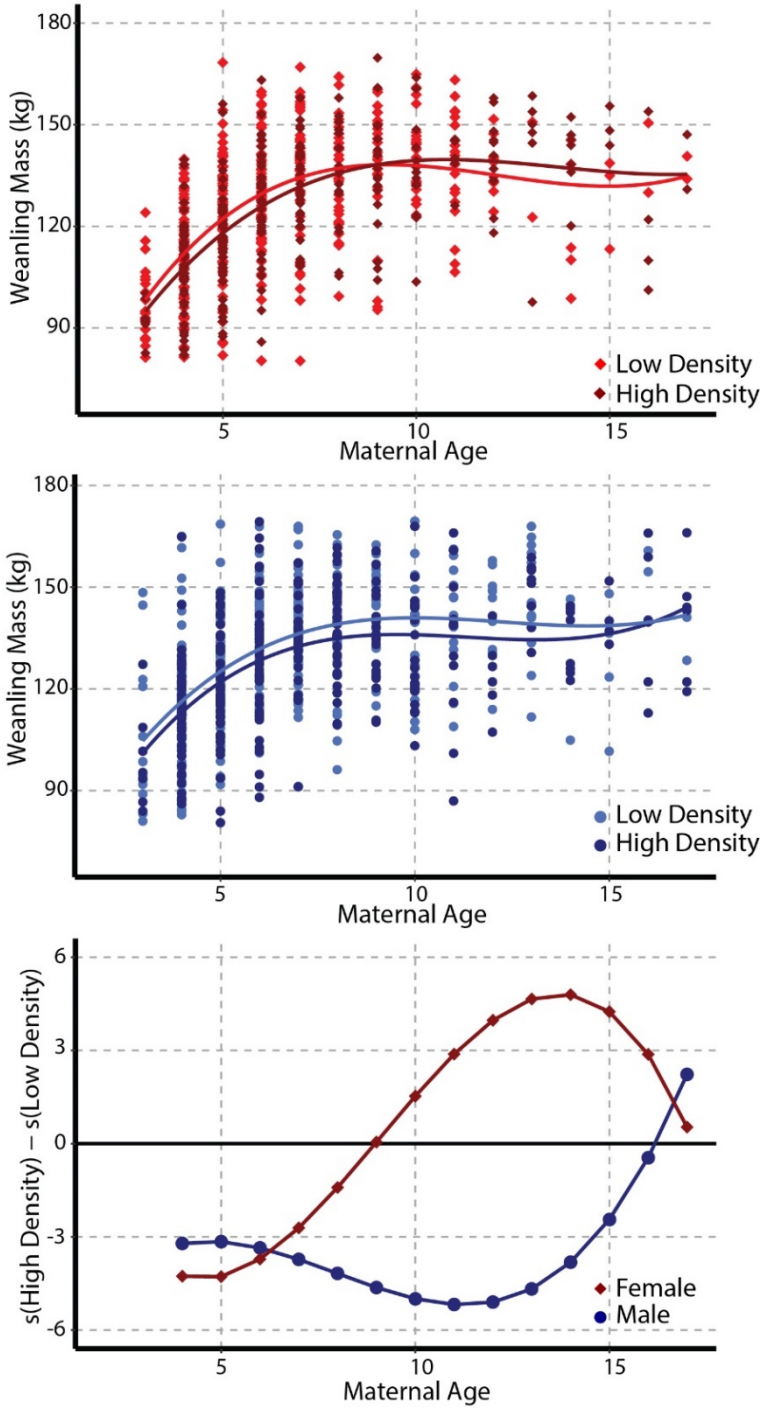

Fig 3.3 - Weanling mass as a function of maternal age, with spline regression curves for **A.** female pups during high (dark red) and low (bright red) density time periods; and **B.** male pups during high (dark blue) and low (bright blue) density time periods. **C.** Difference between high- and low-density smoothing curves at each age for males (blue circles) and females (red diamonds).

Synthesis

Northern elephant seals are expected to be less sensitive to environmental variation than other top predators that have more restrictive life history and foraging strategies. As wide-ranging, capital breeding, generalist carnivores, elephant seals benefit from reduced temporal and spatial restrictions on their foraging and the translation of energy into reproduction. This thesis examined the physical extent of a marine heatwave (Chapter 1), then assessed the foraging (Chapter 2) and reproductive (Chapter 3) consequences of that event on the northern elephant seal. The findings in Chapters 2 and 3 aligned with the general expectation of northern elephant seal resilience, highlighting the importance of behavioral traits in assessing a species' vulnerability to both extreme climate events and climate change.

The Northeast Pacific Blob 2015 was a severe marine heatwave that first appeared in 2014, had sustained sea surface temperature anomalies through 2015, and caused substantial ecosystem disturbance. Analyses of this event have focused primarily on the surface anomaly and top 200 m of the water column, and marine heatwave meta-analyses have categorized the Blob as a phenomenon affecting 10's of meters of the water column [1-3]. The high-resolution *in situ* data collected by northern elephant seals analyzed here (Chapter 1) shows significant anomalies much deeper than previously reported, with standardized temperature anomalies up to 4.2 sd at 800 m depth relative to climatology. Further analysis of temperature and salinity anomalies at the base of the pycnocline indicate that lateral advection may have contributed to the buildup and maintenance of subsurface anomalies that were still apparent at the end of 2017. These findings are important to assessing how the Blob changed ecosystem dynamics in the Northeast

Pacific Ocean, as water column structure and thermal content will affect mixing, alter concentrations of dissolved nutrients, and can create physiological barriers to organisms.

Northern elephant seals exhibited plasticity in their foraging behavior during the peak of the marine heatwave at the population level (Chapter 2). During both post-breeding and post-molting foraging trips, there was an increased use of the Alaska Gyre and a broader distribution of diving within the water column during 2014 and 2015 when compared to all other years. As a result, their foraging success was similar or better than what was observed in normal years. The altered movement patterns and high body compositions indicate that they may have relied on different prey species through those years. While they were able to acquire sufficient energy, the reduced lean tissue gain seen in 2015 could have fitness consequences if that dietary composition becomes "typical" in the future. Reduced lean tissue gain could result in reduced lactation time, as lean tissue stores are what likely limits milk production, lowering weaning mass and the probability of offspring survival [4, 5]. Furthermore, different foraging behaviors influence the accumulation of persistent organic pollutants (POPs) and heavy metals in elephant seal tissue, with higher burdens of some POPs seen in individuals using more coastal and northerly foraging areas [6].

These findings support our expectation regarding elephant seal resilience, but it is important to note that the observed behavioral plasticity was measured in animals that survived their foraging trips in 2014 and 2015. During the post-breeding trips we did not observe unusual mortality among our deployment animals, but the post-molt trip in 2014 included high rates of both at-sea mortality (25%) and skip breeding (25%) among the female seals that were tracked (Chapter 3). Looking at patterns in movement and diving

behavior that results in mortality or reproductive failure is an important step in evaluating the population's response to this climate event.

Weaning mass (or size) is often used as a proxy for maternal foraging success in pinnipeds, and variation in weaning mass may be indicative of changes in the foraging environment. The link between foraging and offspring energy gain is direct and immediate in income breeding species: these animals are dependent on consistently finding food throughout lactation to fuel milk production. Capital breeding species, however, take a different strategy and accumulate tissue stores before giving birth that they can then mobilize for milk production. This creates a temporal and spatial separation between foraging and reproduction, attenuating the link between foraging success and weaning mass. Chapter 3 evaluated multiple factors that could contribute to variations in weaning mass in northern elephant seals, including several ocean indices. Those analyses demonstrated that maternal age was the single most important factor governing weaning mass, while ocean indices were only minor contributors. The average weaning mass of northern elephant seals at Año Nuevo showed a clear decline over the first 15 years of the mainland time series. Previous work on the colony suggested that this decline was due to the dominance of the warm-phase of the Pacific Decadal Oscillation from 1975-1998 [7]. Since that work was completed, the Pacific Ocean has experienced primarily cool-phase PDO but weaning mass has remained lower than at the start of the time series. Furthermore, recent analysis found that, starting in the late 1980s, the relationship between the PDO index and ecological processes in the NEP has weakened, decreasing its usefulness as an environmental indicator over multiple decades [8].

The increase in colony density over time was an important driver of decreasing weaning mass. Increasing density had a negative effect on the weaning weight of pups of younger mothers, but there was no detectable difference in older (>7) mothers under different density conditions. This finding is supported by observations of the difference in behavior between young and experienced females in high- and low-density harems [9]. The influence of maternal age over size in predicting pup weaning mass highlights the importance of experience and behavior over sheer resource availability for producing high-quality offspring. While weaning mass can be an important indicator of foraging conditions in some species, in the northern elephant seal other vital rates (e.g. fecundity, adult survival) are more likely to reflect changing foraging conditions.

Northern elephant seals coped with the disruption to their environment, but they serve as an indicator of changes to a system that supports other, more cryptic predator species, such as beaked whales. While this species did not experience a mass mortality event or reproductive failure, as was seen in surface-foraging predators in the region [10-12], they were affected by the marine heatwave of 2014-2015. The changes in their foraging behavior, survival rate, and skip breeding rate indicate that this extreme climate event caused ecosystem disruption down into the mesopelagic, not just the surface ocean. Although the deep temperature anomalies were much smaller in absolute magnitude (~0.2-0.5°C), they still represent significant deviations from normal temperatures at depths over 300 m, influencing the distribution and abundance of biota in that region.

References

1. Holbrook N.J., Sen Gupta A., Oliver E.C.J., Hobday A.J., Benthuysen J.A., Scannell H.A., Smale D.A., Wernberg T. 2020 Keeping pace with marine heatwaves. *Nature Reviews Earth & Environment*. (doi:10.1038/s43017-020-0068-4).

2. Hobday A., Oliver E., Sen Gupta A., Benthuysen J., Burrows M., Donat M., Holbrook N., Moore P., Thomsen M., Wernberg T., et al. 2018 Categorizing and Naming Marine Heatwaves. *Oceanography* **31**(2). (doi:10.5670/oceanog.2018.205).

3. Holbrook N.J., Scannell H.A., Sen Gupta A., Benthuysen J.A., Feng M., Oliver E.C.J., Alexander L.V., Burrows M.T., Donat M.G., Hobday A.J., et al. 2019 A global assessment of marine heatwaves and their drivers. *Nature communications* **10**(1), 2624. (doi:10.1038/s41467-019-10206-z).

4. Crocker D.E., Williams J.D., Costa D.P., Le Boeuf B.J. 2001 Maternal traits and reproductive effort in northern elephant seals. *Ecology* **82**(12), 3541-3555. (doi:10.1890/0012-9658(2001)082[3541:Mtarei]2.0.Co;2).

5. Costa D.P., Schwarz L., Robinson P., Schick R.S., Morris P.A., Condit R., Crocker D.E., Kilpatrick A.M. 2016 A Bioenergetics Approach to Understanding the Population Consequences of Disturbance: Elephant Seals as a Model System. *Adv Exp Med Biol* **875**, 161-169. (doi:10.1007/978-1-4939-2981-8_19).

6. Peterson S.H., Peterson M.G., Debier C., Covaci A., Dirtu A.C., Malarvannan G., Crocker D.E., Schwarz L.K., Costa D.P. 2015 Deep-ocean foraging northern elephant seals bioaccumulate persistent organic pollutants. *The Science of the total environment* **533**, 144-155. (doi:10.1016/j.scitotenv.2015.06.097).

7. Le Boeuf B.J., Crocker D.E. 2005 Ocean climate and seal condition. *BMC biology* **3**, 9. (doi:10.1186/1741-7007-3-9).

8. Litzow M.A., Hunsicker M.E., Bond N.A., Burke B.J., Cunningham C.J., Gosselin J.L., Norton E.L., Ward E.J., Zador S.G. 2020 The changing physical and ecological meanings of North Pacific Ocean climate indices. *Proceedings of the National Academy of Sciences of the United States of America* **117**(14), 7665-7671. (doi:10.1073/pnas.1921266117).

9. Reiter J., Panken K.J., Le Boeuf B.J. 1981 Female Competition and Reproductive Success in Northern Elephant Seals. *Animal Behaviour* **29**(Aug), 670-687. (doi:10.1016/S0003-3472(81)80002-4).

10. Piatt J.F., Parrish J.K., Renner H.M., Schoen S.K., Jones T.T., Arimitsu M.L., Kuletz K.J., Bodenstein B., Garcia-Reyes M., Duerr R.S., et al. 2020 Extreme mortality and reproductive failure of common murres resulting from the northeast Pacific marine heatwave of 2014-2016. *PLoS One* **15**(1), e0226087. (doi:10.1371/journal.pone.0226087).

11. Gálvez C., Pardo M.A., Elorriaga-Verplancken F.R. 2020 Impacts of extreme ocean warming on the early development of a marine top predator: The Guadalupe fur seal. *Progress in Oceanography* **180**. (doi:10.1016/j.pocean.2019.102220).

12. Osborne O.E., O'Hara P.D., Whelan S., Zandbergen P., Hatch S.A., Elliott K.H. 2020 Breeding seabirds increase foraging range in response to an extreme marine heatwave. *Marine Ecology Progress Series* **646**, 161-173. (doi:10.3354/meps13392).

Table S2.1 – Mean departure and arrival day of year and date for post-breeding and post-molt trips, calculated from all movement observed by biologging. Post-molt arrival dates were only calculated from females who were reproductive.

	Post-Breeding				Post-Molt			
	N	Day	Date	Date Range	N	Day	Date	Date Range
Departure	290	47 ± 9	Feb 16	Feb 7 – Feb 25	293	159 ± 13	Jun 8	May 17 – June 22
Arrival	285	120 ± 15	Apr 30	Apr 15 – May 15	258	9 ± 33	Jan 9	Dec 7 – Feb 11

Table S2.2 – Trip length and foraging success statistics for post-molt deployments split by females who were reproductive (left) versus females who skipped breeding (right). Values that are significantly different based on ANOVA and Tukey's HSD are shown in bold

	Breeding Females						Skip Females					
Year	N	Trip Length (Days)	Mass Gain (kg)	Recover % Adipose	Lean Gain (kg)	Energy Gain Rate (MJ d^{-1})	N	Trip Length (Days)	Mass Gain (kg)	Recover % Adipose	Lean Gain (kg)	Energy Gain Rate (MJ d^{-1})
2004	22	226.8 ± 5.8	275.8 ± 31.8	36.5 ± 2.0	182.4 ± 20.8	19.7 ± 3.1	1	168	142.2	39.7	59.6	19.5
2005	18	222.9 ± 5.5	292.5 ± 60.5	35.3 ± 2.6	204.6 ± 22.6	19.6 ± 3.0	4	176.2 ± 62.7	151.4 ± 54.2	35.9 ± 5.2	82.9 ± 29.9	16.8 ± 3.8
2006	17	224.3 ± 5.1	272.8 ± 33.8	33.8 ± 2.1	199.3 ± 25.3	17.2 ± 2.6	3	155.1 ± 2.8	65.3 ± 33.2	33.5 ± 3.4	36.3 ± 13.6	8.0 ± 5.0
2007	15	224.5 ± 7.1	266.4 ± 33.3	32.5 ± 2.4	198.7 ± 34.5	16.2 ± 2.2	3	243.3 ± 82.4	166.4 ± 74.4	33.0 ± 4.4	112.5 ± 31.3	10.0 ± 4.3
2008	12	223.9 ± 5.5	284.7 ± 45.2	34.9 ± 3.4	201.2 ± 30.1	18.8 ± 4.7	2	209.3 ± 136.3	117.2 ± 88.1	32.5 ± 0.2	73.8 ± 62.2	9.5 ± 0.1
2009	6	221.7 ± 3.4	287.5 ± 43.2	**38.2 ± 2.5**	188.1 ± 34.2	**21.2 ± 3.4**	1	140	175.0	36.7	89.5	25.3
2010	13	220.8 ± 7.1	284.8 ± 38.2	33.2 ± 4.4	218.9 ± 33.9	16.8 ± 1.7	4	202.3 ± 77.3	198.7 ± 86.1	30.5 ± 5.0	140.6 ± 50.7	12.9 ± 1.1
2011	15	222.3 ± 4.0	282.9 ± 42.0	33.1 ± 4.4	207.2 ± 44.0	17.9 ± 2.2	0	--	--	--	--	--
2012	15	224.8 ± 3.2	279.6 ± 26.5	34.8 ± 3.1	194.0 ± 22.1	18.9 ± 3.4	1	160	185.2	34.5	115.8	19.7
2013	13	221.3 ± 5.2	308.9 ± 27.4	31.8 ± 0.8	223.1 ± 20.7	20.1 ± 1.8	3	152.3 ± 67.5	142.5 ± 113.4	29.5 ± 1.5	98.1 ± 73.3	14.2 ± 14.0
2014	10	219.4 ± 5.0	300.2 ± 20.2	**37.4 ± 2.1**	204.8 ± 16.4	21.2 ± 2.8	5	231.3 ± 67.4	202.6 ± 23.7	38.6 ± 3.3	109.4 ± 27.4	18.6 ± 6.5
2015	13	224.9 ± 4.2	271.9 ± 31.7	**37.7 ± 2.3**	**177.3 ± 27.5**	19.8 ± 3.2	2	231.5 ± 7.7	280.9 ± 94.7	38.3 ± 4.3	150.1 ± 52.0	23.9 ± 7.1
2016	13	223.9 ± 6.7	277.4 ± 61.2	35.7 ± 2.7	198.9 ± 42.8	18.1 ± 4.5	2	291 ± 12.7	206.9 ± 84.1	33.0 ± 4.3	138.0 ± 35.8	11.2 ± 6.1
2017	5	221.9 ± 5.1	258.7 ± 27.1	33.4 ± 2.8	188.2 ± 14.2	16.5 ± 3.4	3	170.8 ± 45.6	168.3 ± 47.0	37.3 ± 4.4	91.4 ± 47.9	19.9 ± 4.2
2018	9	221.0 ± 5.8	298.6 ± 27.1	33.5 ± 1.8	215.0 ± 24.5	19.5 ± 1.8	2	211.8 ± 31.7	130.7 ± 37.7	34.4 ± 5.6	82.6 ± 7.3	11.0 ± 6.9
Total	196	223.2 ± 5.5	282.6 ± 36.3	34.7 ± 3.1	199.9 ± 30.5	18.7 ± 3.2	36	199.7 ± 65.0	165.2 ± 71.1	34.6 ± 4.3	97.9 ± 43.8	15.2 ± 7.1

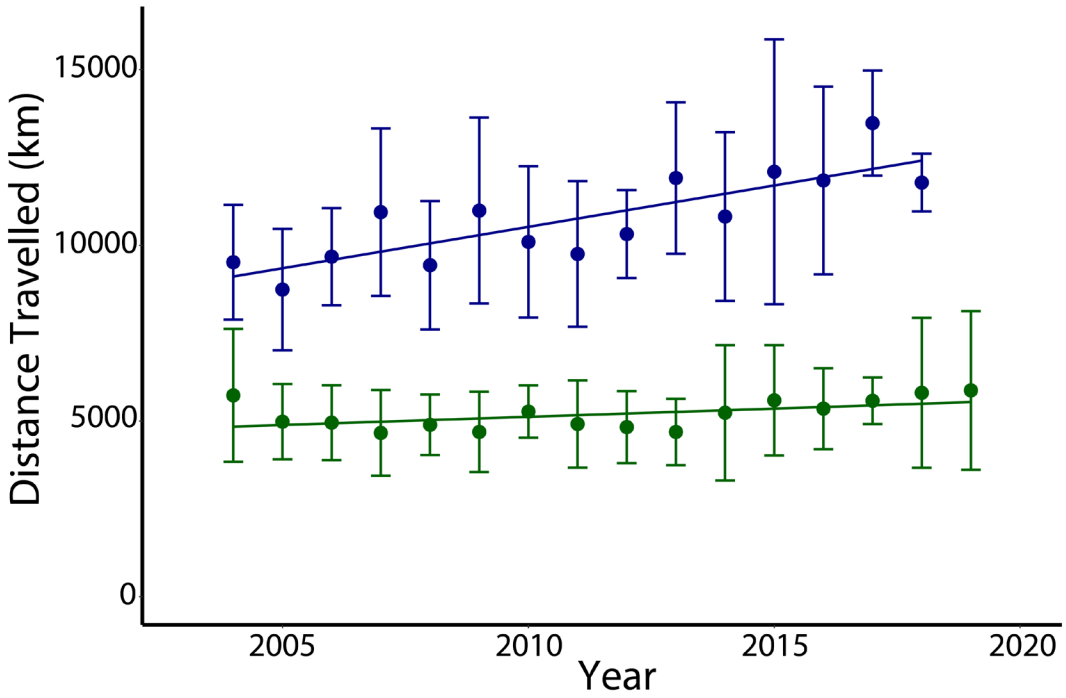

S2.3 - Distance travelled over post-breeding (green) and post-molt (blue) foraging trips with linear regression lines. Error bars indicate standard deviations.

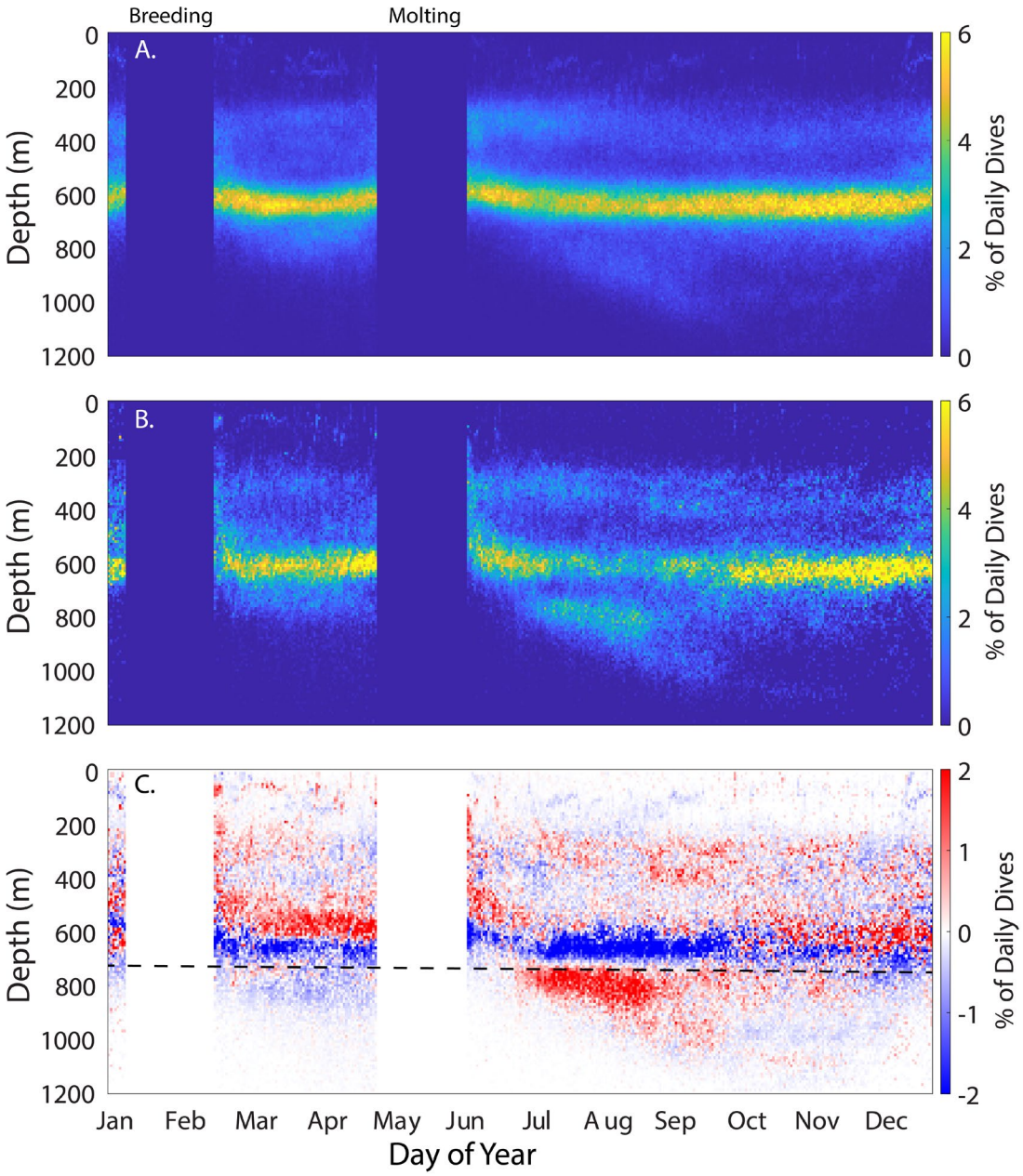

S2.4 - Patterns in day (solar elevation > 0°) depth use across seasons. Depth was divided into 10 m bins from 0-1200 m for each day of the year. The percent of total dives per day (excluding drift dives) that fell within a depth bin was calculated for each depth, each day of the year. **A**. Daily depth use calculated from all records collected from 2004-2013 and 2016-2018. **B**. Daily depth use during the Blob, calculated from all 2014-2015 records. **C** shows the change in depth use during the Blob (**B** minus **A**) where red denotes an increase in use and blue a decrease.

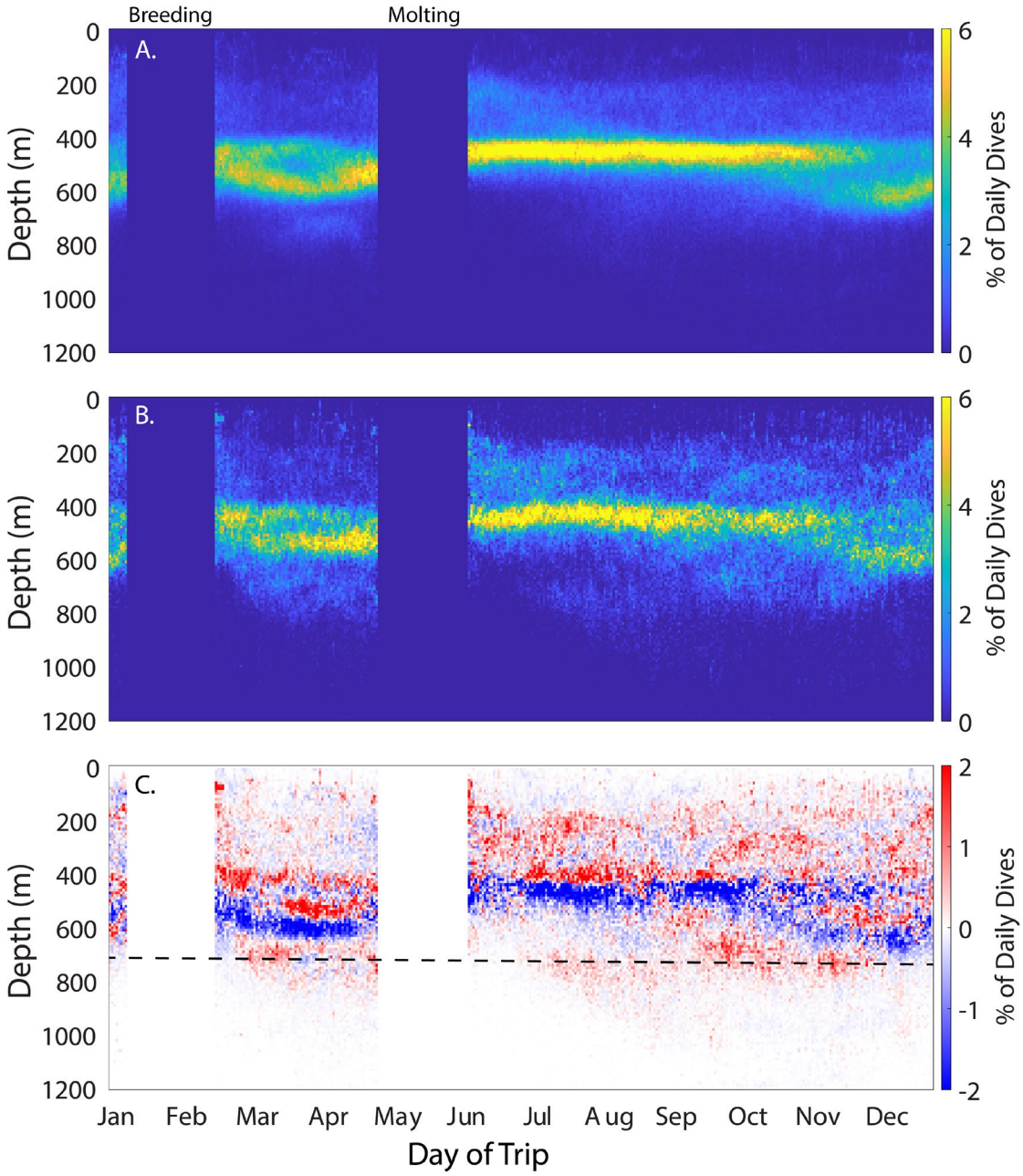

S2.5 - Patterns in night (solar elevation < 0°) depth use across seasons. Depth was divided into 10 m bins from 0-1200 m for each day of the year. The percent of total dives per day (excluding drift dives) that fell within a depth bin was calculated for each depth, each day of the year. **A**. Daily depth use calculated from all records collected from 2004-2013 and 2016-2018. **B**. Daily depth use during the Blob, calculated from all 2014-2015 records. **C** shows the change in depth use during the Blob (**B** minus **A**) where red denotes an increase in use and blue a decrease.

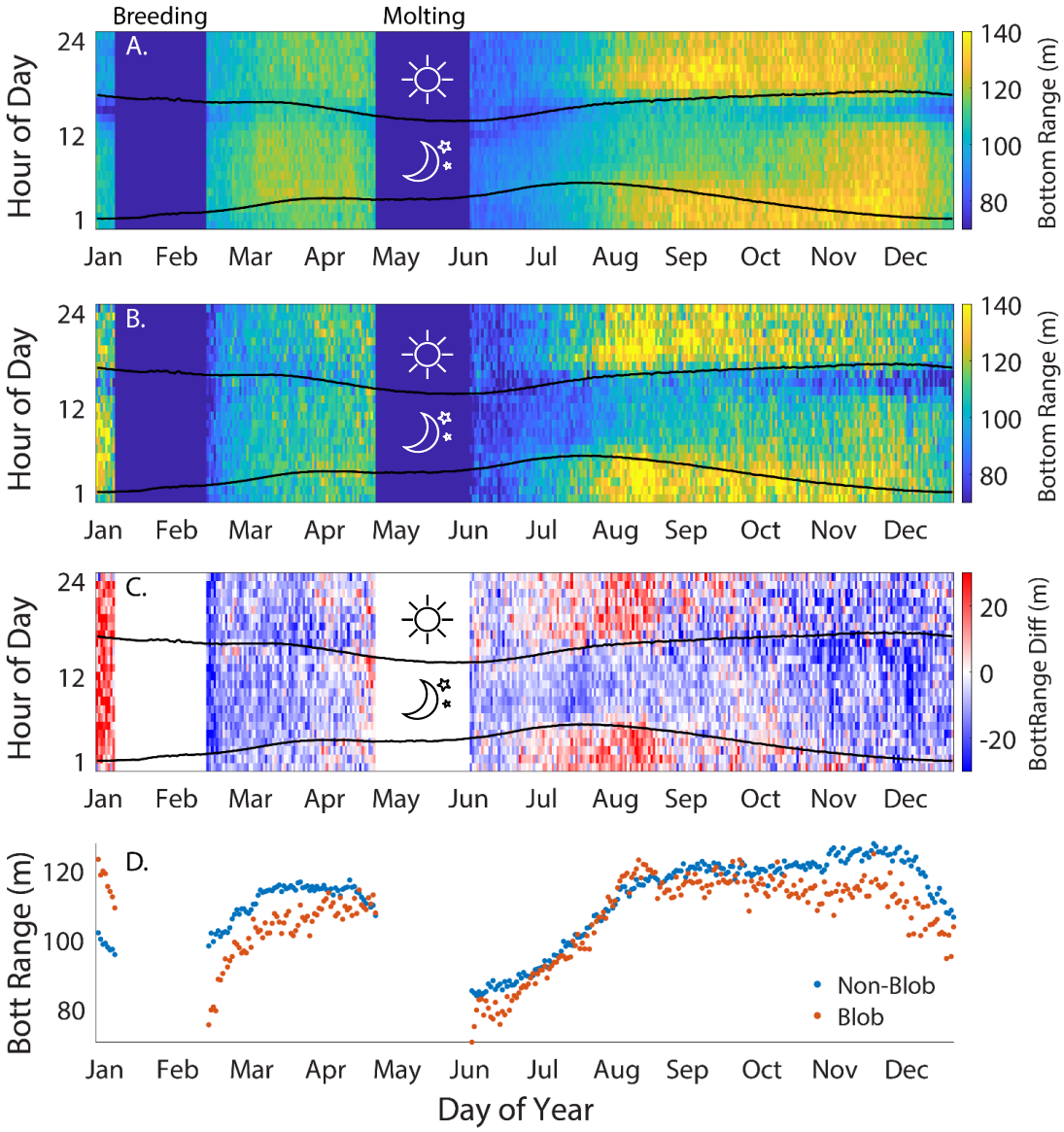

S2.6 – Diel and seasonal patterns in bottom range. Contour lines indicate transitions between day and night calculated from the date and the location of the animals. **A.** Mean bottom range (m) by hour of the day for each day of the year, from all dive records collected in 2004-2013 and 2016-2018. **B.** Mean bottom range (m) during the Blob, calculated as in A. from 2014-2015 records. **C.** Difference in bottom range during the Blob compared to all other years (B minus A); red indicates increased bottom range during the Blob and blue decreased range. **D.** Daily mean bottom range (m) each day of the year during Blob (red) and Non-Blob years (blue).

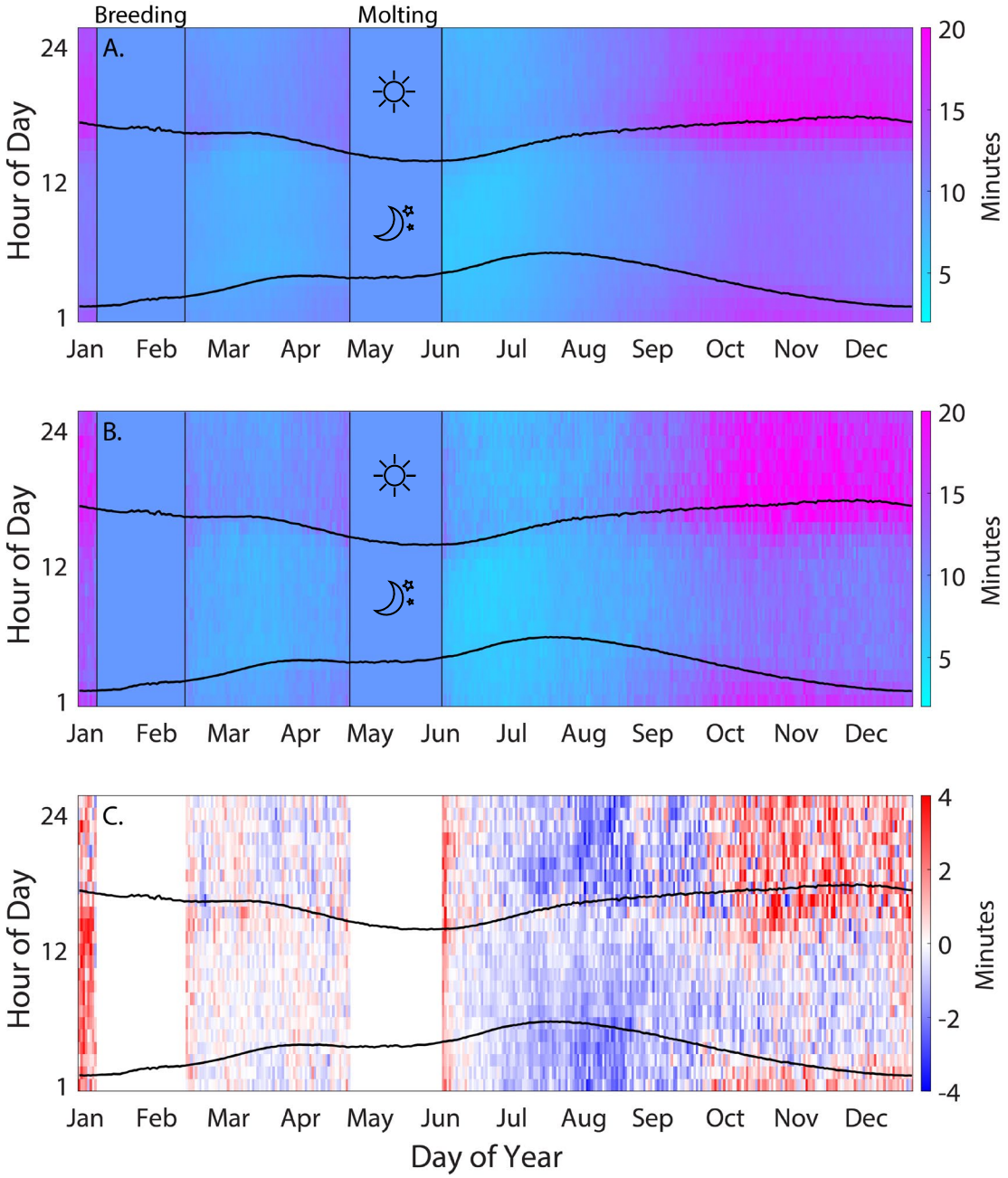

S2.7 - Diel and seasonal patterns in dive bottom time (minutes), excluding drift dives. Contour lines indicate transition from day to night calculated from the date and the location of the animals. **A.** Mean dive efficiency calculated for each hour of the day, each day of the year, from all dive records collected in 2004-2013 and 2016-2018. **B.** Mean dive bottom time during the Blob, calculated as in A from 2014-2015 records. **C.** Difference in dive bottom time during the Blob compared to all other years (B minus A); red indicates increased bottom time during the Blob and blue decreased bottom time. As in previous figure, the breeding and molting haul-outs and were excluded from C.

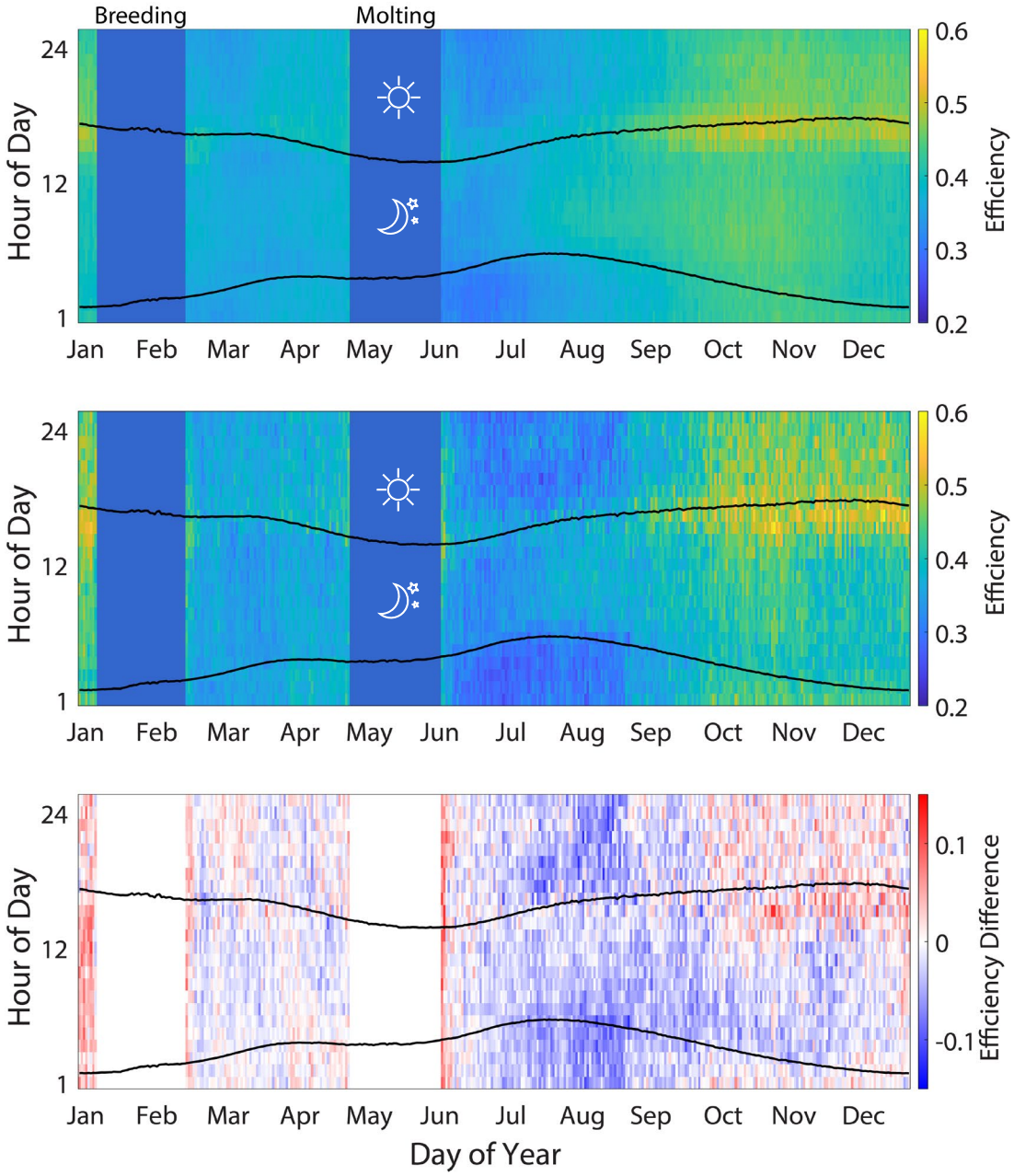

S2.8 - Diel and seasonal patterns in dive efficiency (bottom time:(total duration + post-dive surface Interval)), excluding drift dives. Contour lines indicate transition from day to night calculated from the date and the location of the animals. **A.** Mean dive efficiency calculated for each hour of the day, each day of the year, from all dive records collected in 2004-2013 and 2016-2018. **B.** Mean dive efficiency during the Blob, calculated as in A. from 2014-2015 records. **C.** Difference in dive efficiency during the Blob compared to all other years (B minus A); red indicates increased efficiency during the Blob and blue decreased efficiency (less bottom time relative to dive duration). As in previous figure, the breeding and molting haul-outs and were excluded from C.

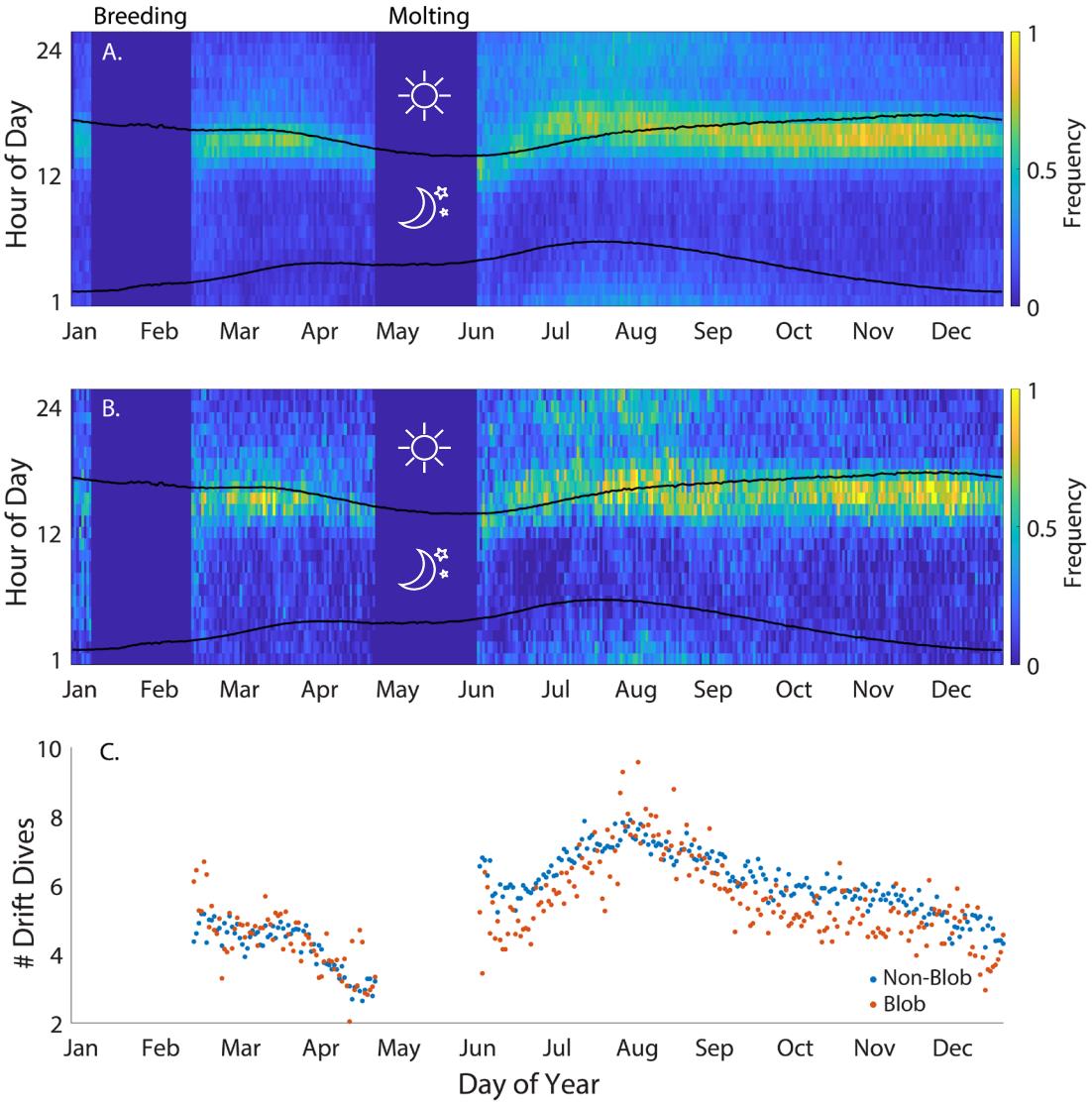

S2.9 - Diel and seasonal patterns in drift dive frequency. All values are normalized to dive record sample size for each period (see Table 2.1) so that frequency values are comparable between seasons and years. Contour lines indicate transitions between day and night calculated from the date and the location of the animals. **A.** Drift dive frequency (normalized to number of animals sampled) by hour of the day, each day of the year, from all dive records collected in 2004-2013 and 2016-2018. **B.** Drift dive frequency during the Blob, calculated as in A. from 2014-2015 records. **C.** Number of drift dives performed, on average, by each animal each day of the year during Blob (red) and Non-Blob years (blue).

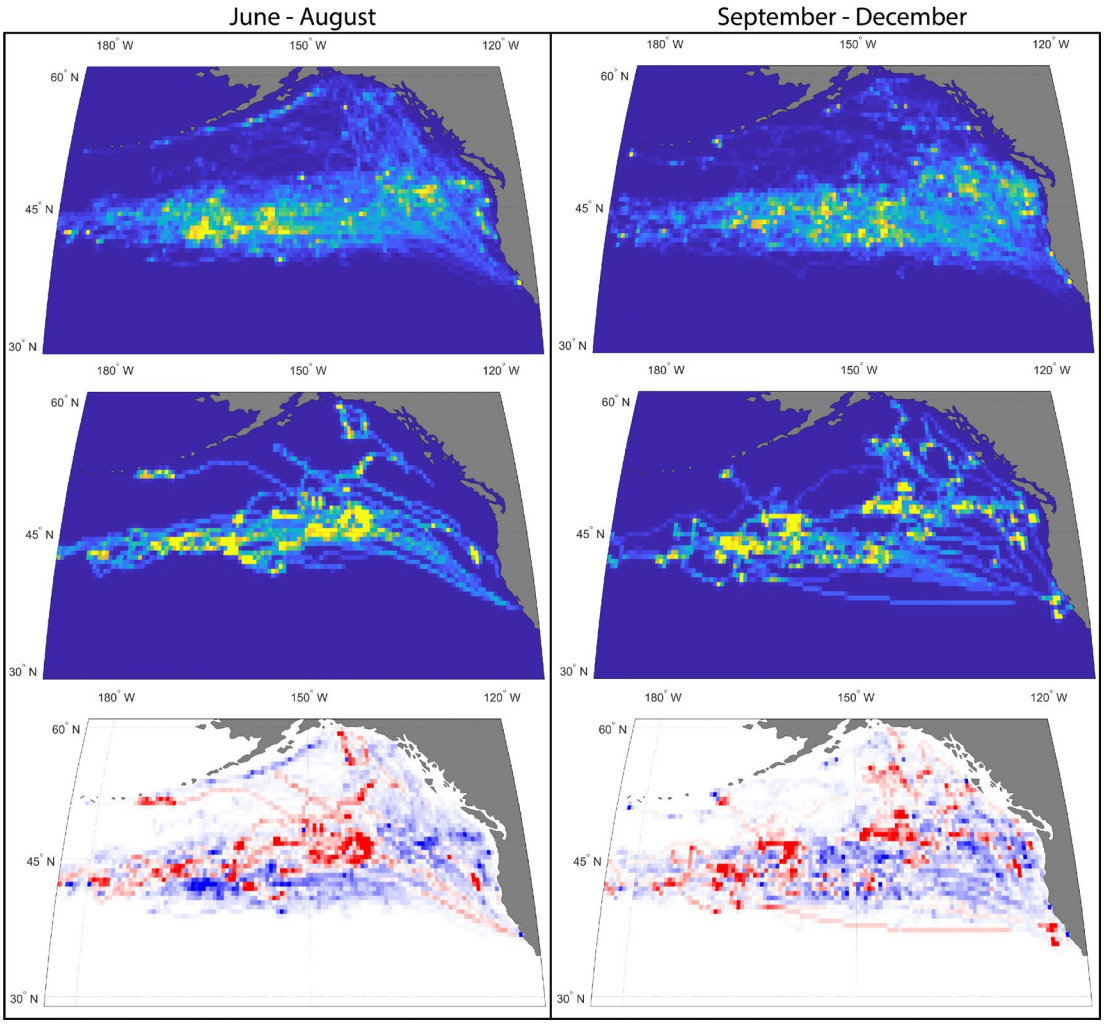

S2.10 - Post-molt foraging distribution during non-Blob years (top panels), Blob years (middle panels), and the difference in distribution (bottom panels). Difference in distributions were calculated as in Fig. 2.2, but with the trip split between early (Jun-Aug, left panels) and late (Sep-Dec) months to highlight areas used when deep-diving behavior was observed in the early trip, as in Fig. 2.3.

Table S2.11 – Changes in body composition and duration of time onshore during the molt in all animals tracked during both PB and PM the same year. Fat free mass (FFM) calculated assuming 10% water content in adipose tissue.

SealID	Days On Shore	Early Molt %Adip	Early Molt Mass (kg)	Late Molt %Adip	Late Molt Mass (kg)	Early Molt FFM (kg)	Late Molt FFM (kg)	FFM Lost (kg)	%FFM Lost
1113	44.7	0.298	345	0.294	250	252.5	183.9	68.6	0.272
1317	43.2								
1914	44.9	0.32	340	0.312	252	242.1	181.2	60.8	0.251
4534	42.5	0.291	364	0.284	267	268.7	198.8	69.9	0.260
5572	41.4	0.362	324	0.335	231	218.4	161.4	57.1	0.261
5842	40.8								
9678	40.6	0.348	447	0.346	331	307.0	227.9	79.1	0.258
N410	43.0	0.313	386	0.274	288	277.3	217.0	60.3	0.217
O858	42.0	0.324	391	0.283	301	277.0	224.3	52.6	0.190
R999	39.8	0.327	413	0.306	319	291.5	231.1	60.3	0.207
T 35	43.7	0.332	423	0.317	327	296.6	233.7	62.9	0.212
U256	47.2								
U448	43.6	0.311	412	0.299	298	296.7	217.8	78.9	0.266
U481	41.3								
U848	44.8	0.321	433	0.274	325	307.9	244.9	63.1	0.205
X349	35.6								
X387	43.7	0.337	388	0.282	259	270.3	193.3	77.1	0.285
Mean	42.5	0.324	388.8	0.301	287.3	275.5	209.6	65.9	0.240
StDev	2.50	0.019	37.4	0.022	33.2	26.1	24.4	8.4	0.030

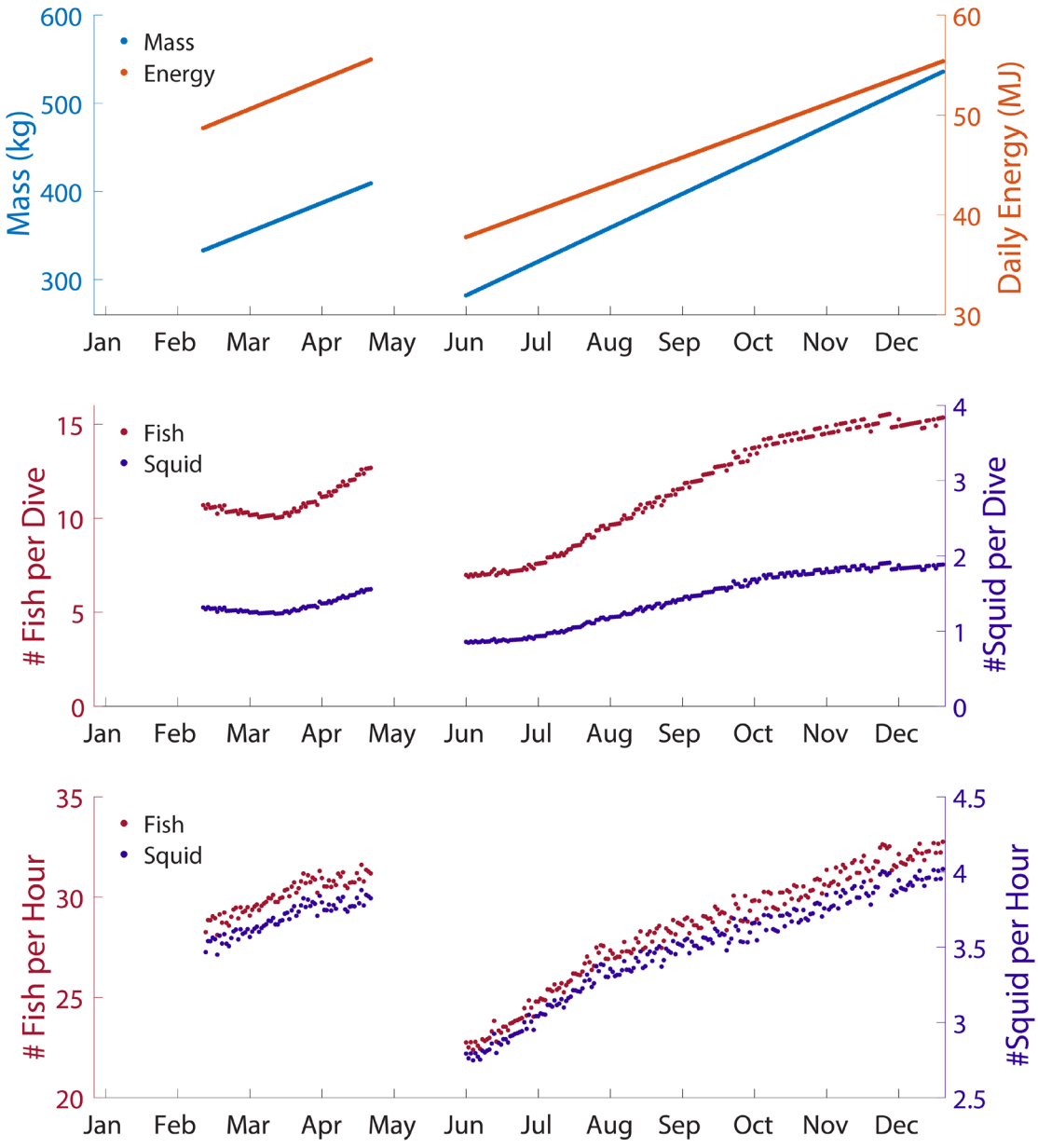

S2.12 - Changes in mass, energy, and required prey consumption rates across foraging trips, assuming a linear increase in body mass across foraging trips.

Table S3.1 - Equations used to calculate corrected masses for pups and adult females as described in methods. Mass loss values from [14-17].

Mass Correction Equations

$\boldsymbol{PupBirthMass = PupMass - dl * 2.2}$	dl = days of early season lactation
$\boldsymbol{ArriveMass = RecoverMass + df * 3.0 + dl * 7.5 + PupBirthMass}$	df = days of non-lactation fasting
$\boldsymbol{DepartMass = DeployMass - dL * 7.5}$	dL = days of late season lactation
$\boldsymbol{WeaningMass = WeighedMass * \left(e^{k*d}\right)}$	d = days since weaning k = 0.00596

Table S3.2 - Covariates included in GAMs to evaluate drivers of weaning mass; *indicates covariates included only for a subset of weanlings where female arrival mass was available. Covariates in bold were included in final model selections.

COVARIATE	DESCRIPTION
MomAge	**Age of mother at time of birth**
MomID	Identity of mother
Sex	**Sex of weanling**
MomArriveMass*	Mass of mother at arrival prior to birth
PupBirthMass*	Mass of pup at birth
Population	**Number of mainland births**
ENSOW	Mean ENSO during Jan-Mar of the breeding season
PDOW	Mean PDO during Jan-Mar of the breeding season
ENSOPM	Mean ENSO during Jul-Dec of the prior year (during gestation)
ENSO2	Mean ENSO during Jan-Dec two years prior to the breeding season
ENSO3	**Mean ENSO during Jan-Dec three years prior to the breeding season**
PDOPM	**Mean PDO during Jul-Dec of the prior year (during gestation)**
PDO2	**Mean PDO during Jan-Dec two years prior to the breeding season**
PDO3	Mean PDO during Jan-Dec three years prior to the breeding season
NOIPM	Mean NOI during Jul-Dec of the prior year (during gestation)
NOI2	Mean NOI during Jan-Dec two years prior to the breeding season
NOI3	Mean NOI during Jan-Dec three years prior to the breeding season

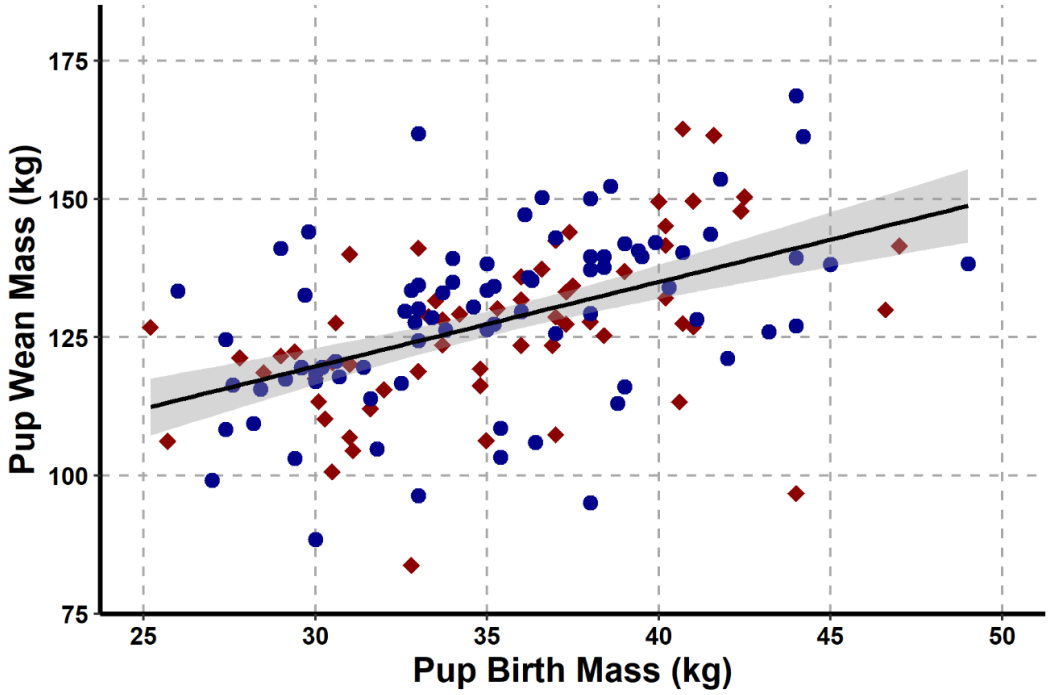

S3.3 - Pup weaning mass as a function of pup birth mass with a linear regression line (R^2 = 0.219), the shaded area indicates 95% confidence intervals. Blue circles indicate male, red diamonds female pups. There is no significant differences between the sexes.

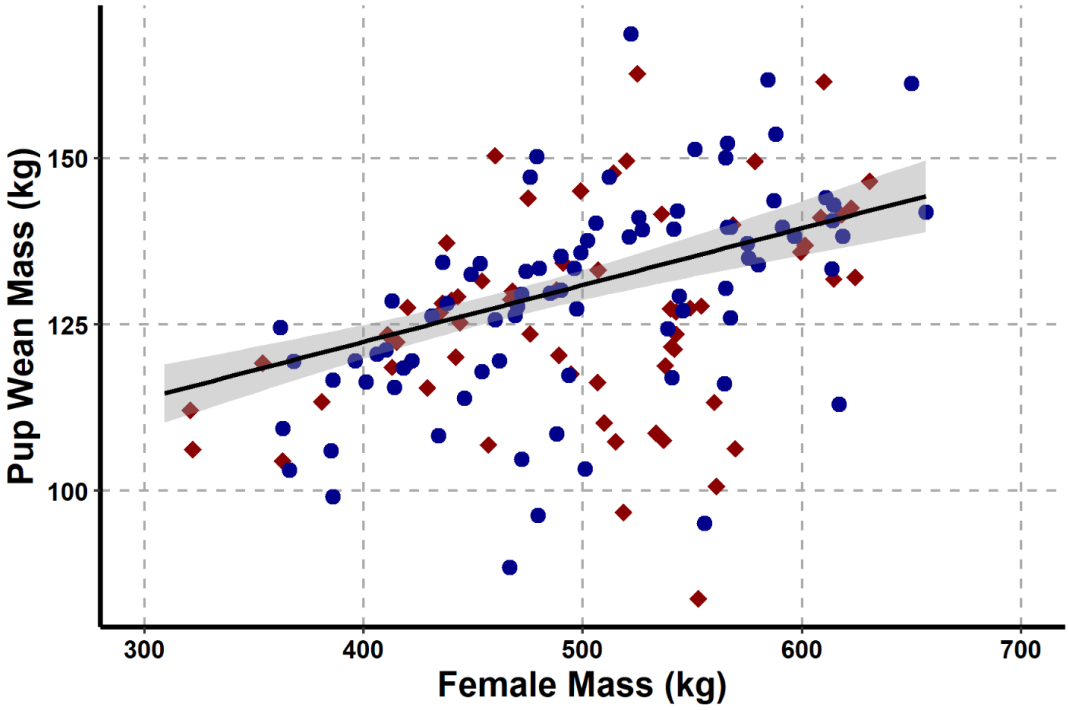

S3.4 - Pup weaning mass as a function of maternal mass with linear regression line (R^2 = 0.132). Shaded areas indicate 95% confidence intervals, red diamonds are female pups, blue circles males.

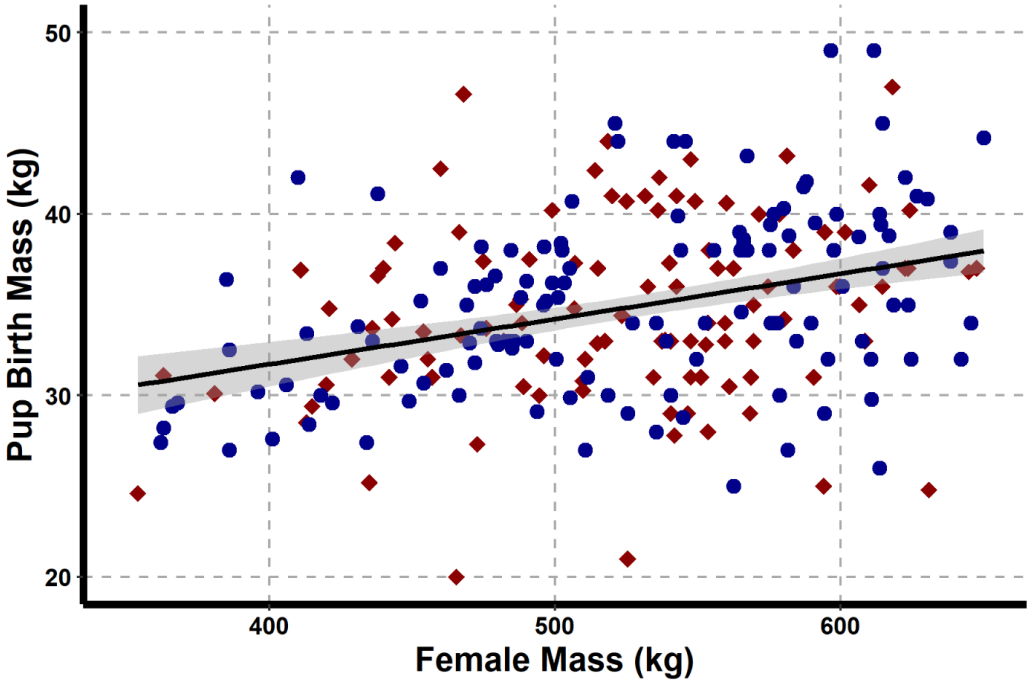

S5 - Pup birth mass as a function of female arrival mass, red diamonds indicate female pups and blue circles indicate males, with a linear regression line ($R^2 = 0.117$) and shaded area indicates 95% confidence intervals.

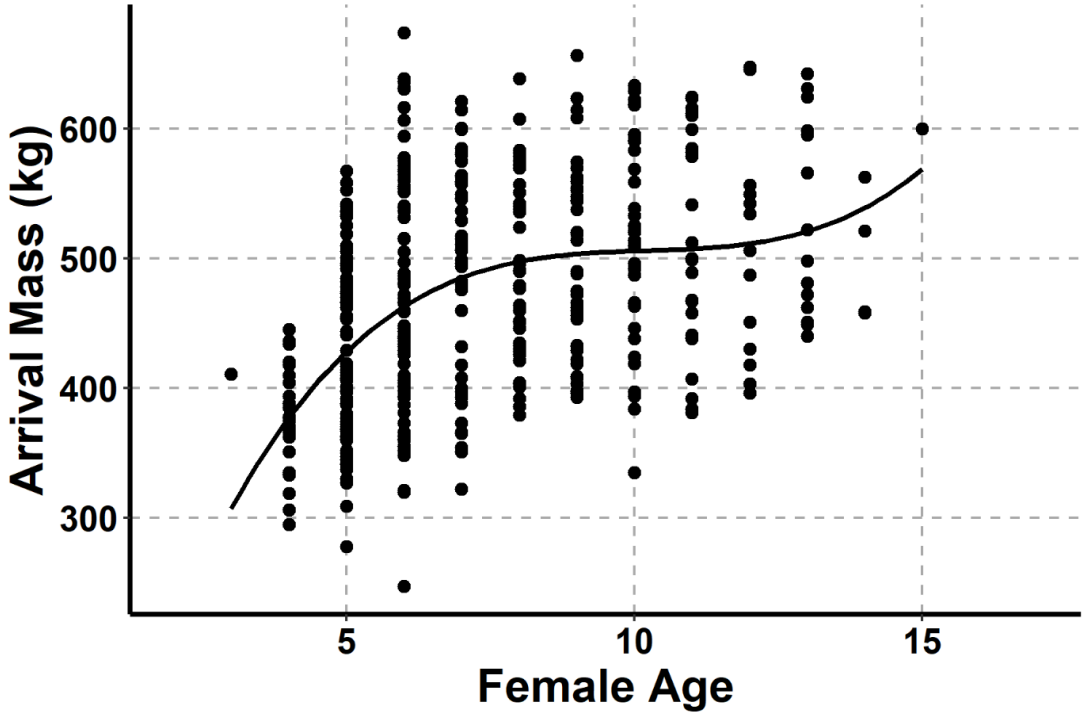

S3.6 – Adult female mass as a function of age. Mass increases with age until age 10, although the range of masses at each age is similar from age 7 onward.

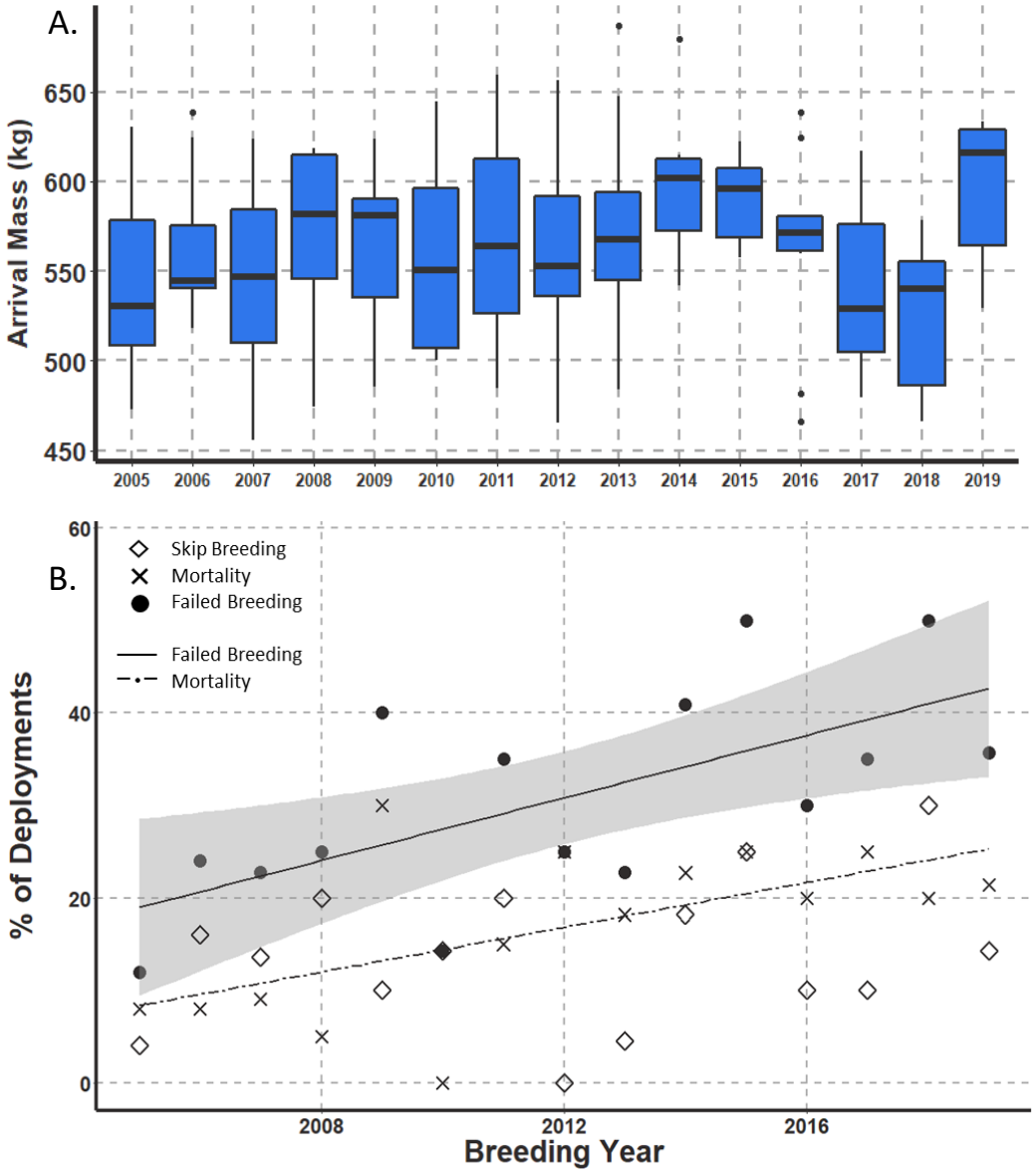

S3.7 – Foraging and reproductive success of satellite tagged adult females from 2004 – 2019. A) Arrival mass of females who gave birth to a pup. B) Percent breeding failure with trendlines showing the increase in overall reproductive failures (solid line), driven by an increase in at-sea mortality (dashed line).

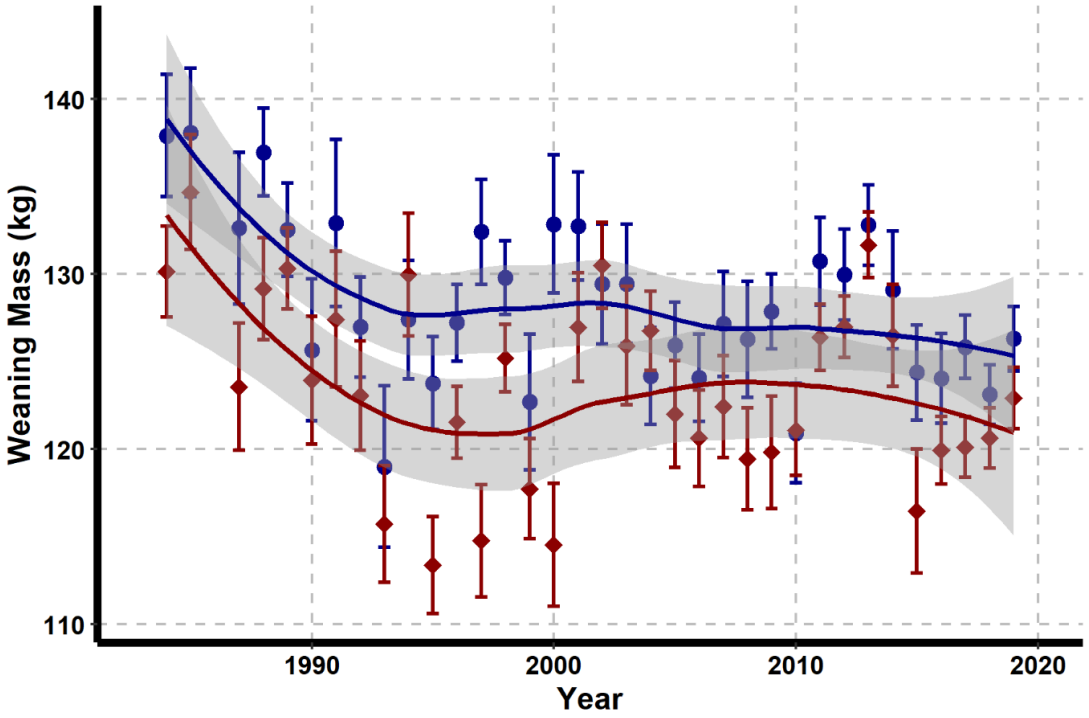

S3.8 - Weanling masses of male (blue circle) and female (red diamond) pups across years, with Loess regression curves and shaded 95% confidence intervals.

Table S3.9 – Annual average (± standard deviation) measurements of weanlings on the mainland breeding colony at Año Nuevo State Park during population growth (1984 – 2002). SL = standard (or straight) length, measured at the straight distance from the tip of the nose to the tip of the tail; CL = curvilinear length, measured along the animal's back from tip of nose to tip of tail; AG = axillary girth, measured around the animal's torso at the armpits, underneath the flippers. Bold indicates measurements with significant differences between males and females ($p<0.5$).

Year	All Weanlings					Female Weanlings					Male Weanlings				
	N	Mass	SL	CL	AG	N	Mass	SL	CL	AG	N	Mass	SL	CL	AG
1984	80	134.0 ± 19.8	--	--	--	37	130.1 ± 15.8	--	--	--	41	137.9 ± 22.4	--	--	--
1985	85	136.7 ± 23.5	147.3 ± 8.0	--	--	34	134.7 ± 19.1	145.4 ± 7.0	--	--	51	138.1 ± 26.1	148.4 ± 8.5	--	--
1987	81	127.1 ± 25.3	148.0 ± 8.7	--	135.6 ± 13.4	49	123.6 ± 25.4	*146.4 ± 9.1	--	134.6 ± 14.7	32	132.6 ± 24.6	*150.3 ± 7.8	--	137.1 ± 11.1
1988	207	133.1 ± 27.8	145.4 ± 9.0	--	139.7 ± 12.8	102	*129.2 ± 29.5	144.1 ± 9.6	--	138.1 ± 13.0	105	***137.0 ± 25.7**	146.7 ± 8.3	--	141.1 ± 12.5
1989	206	131.3 ± 25.0	146.2 ± 8.1	--	136.9 ± 13.1	110	130.3 ± 24.2	146.1 ± 8.2	--	136.5 ± 13.9	96	132.5 ± 26.0	146.3 ± 8.1	--	137.4 ± 12.3
1990	88	124.8 ± 25.4	143.6 ± 7.2	--	131.4 ± 11.5	46	123.9 ± 24.7	142.6 ± 7.5	--	131.0 ± 10.9	42	125.7 ± 26.3	144.8 ± 6.7	--	131.7 ± 12.3
1991	55	130.0 ± 22.1	145.6 ± 8.7	--	135.6 ± 14.0	29	127.4 ± 20.9	145.0 ± 9.9	--	133.0 ± 12.8	25	132.9 ± 23.8	146.0 ± 7.2	--	138.3 ± 15.2
1992	102	125.0 ± 21.3	141.8 ± 6.7	--	137.2 ± 12.2	51	123.0 ± 22.3	141.2 ± 6.6	--	136.6 ± 12.4	51	127.0 ± 20.4	142.5 ±6.8	--	138.0 ± 12.1
1993	54	117.4 ± 20.8	142.5 ± 9.8	--	131.8 ± 15.1	27	115.7 ± 17.4	142.7 ± 10.8	--	131.3 ± 16.5	27	119.0 ± 24.0	142.3 ± 8.8	--	132.3 ± 13.8
1994	83	128.7 ± 22.2	142.4 ± 8.1	--	135.4 ± 13.1	43	130.0 ± 23.1	141.3 ± 7.8	--	134.9 ± 13.6	40	127.4 ± 21.5	143.6 ± 8.3	--	135.9 ± 12.7
1995	105	118.5 ± 20.2	142.7 ± 8.6	--	132.3 ± 10.2	53	*113.4 ± 20.1	*140.5 ± 8.8	--	130.5 ± 11.5	52	***123.8 ± 19.1**	*144.9 ± 8.0	--	134.2 ± 8.4
1996	187	124.7 ± 21.0	142.1 ± 9.2	--	135.2 ± 11.9	84	121.5 ± 18.9	*139.7 ± 9.4	--	133.7 ± 10.7	103	127.2 ± 22.3	*144.1 ± 8.6	--	136.4 ± 12.8
1997	97	123.3 ± 23.3	139.2 ± 9.5	--	136.3 ± 12.4	50	*114.8 ± 22.7	*136.4 ± 8.8	--	134.2 ± 13.4	47	***132.4 ± 20.6**	8142.1 ± 9.5	--	138.6 ± 11.0
1998	175	127.6 ± 19.1	141.5 ± 7.8	--	133.9 ± 8.7	82	125.2 ± 17.4	141.1 ± 7.7	--	132.8 ± 8.0	93	129.8 ± 20.3	141.7 ± 7.8	--	134.8 ± 9.3
1999	86	120.4 ± 22.9	141.0 ± 8.0	--	130.8 ± 11.5	40	117.7 ± 18.0	140.6 ± 8.1	--	130.9 ± 11.9	46	122.7 ± 26.4	141.3 ± 8.1	--	130.8 ± 11.2
2000	82	123.7 ± 25.4	142.6 ± 9.8	--	133.6 ± 12.5	41	***114.5 ± 22.4**	140.9 ± 9.8	--	*129.7 ± 1.8	41	***132.9 ± 25.2**	144.4 ± 9.6	--	***137.5 ± 13.1**
2001	92	130.1 ± 21.1	146.3 ± 7.4	--	132.8 ± 10.1	42	127.0 ± 20.0	***144.4 ± 6.2**	--	131.2 ± 10.1	50	132.7 ± 21.9	***147.7 ± 8.0**	--	134.0 ± 10.0
2002	113	130.0 ± 22.3	147.5 ± 7.0	--	131.6 ± 11.1	56	130.5 ± 18.4	147.7 ± 7.0	--	133.2 ± 9.7	57	129.4 ± 25.8	147.3 ± 6.9	--	130.1 ± 12.2

Table S3.9 con't – Annual average (± standard deviation) measurements of weanlings on the mainland breeding colony at Año Nuevo State Park during population growth (1984 – 2002). SL = standard (or straight) length, measured at the straight distance from the tip of the nose to the tip of the tail; CL = curvilinear length, measured along the animal's back from tip of nose to tip of tail; AG = axillary girth, measured around the animal's torso at the armpits, underneath the flippers. Bold indicates measurements with significant differences between males and females ($p<0.5$).

	All Weanlings					Female Weanlings					Male Weanlings				
Year	N	Mass	SL	CL	AG	N	Mass	SL	CL	AG	N	Mass	SL	CL	AG
2003	148	127.4 ± 29.6	146.0 ± 9.8	--	130.4 ± 14.2	87	125.9 ± 31.6	**144.5 ± 10.9**	--	129.9 ± 15.1	61	129.4 ± 26.6	**148.2 ± 7.4**	--	131.3 ±12.9
2004	166	125.7 ± 22.5	145.8 ± 8.0	--	129.7 ± 11.2	97	126.8 ± 22.2	145.2 ± 7.4	--	130.9 ± 11.0	69	124.2 ± 23.0	146.7 ± 8.7	--	127.9 ± 11.2
2005	135	124.0 ± 22.7	146.5 ± 7.8	159.0 ± 8.7	129.2 ± 11.2	66	122.0 ± 24.8	**145.1 ± 8.9**	**157.1 ± 9.9**	127.5 ± 12.4	69	125.9 ± 20.4	**148.0 ± 6.4**	**160.9 ± 6.9**	130.9 ± 9.8
2006	101	122.4 ± 18.6	145.3 ± 7.1	157.3 ± 6.9	127.2 ± 10.3	49	120.6 ± 19.3	145.0 ± 7.6	157.2 ± 7.3	125.9 ± 10.9	52	124.1 ± 17.9	145.7 ± 6.6	157.2 ± 6.6	128.4 ± 9.7
2007	68	124.8 ± 17.3	146.8 ± 7.8	159.4 ± 13.9	132.3 ± 8.7	34	122.4 ± 17.0	146.9 ± 7.0	156.8 ± 5.8	130.4 ± 8.8	34	127.1 ± 17.5	146.6 ± 8.7	162.0 ± 18.6	134.1 ± 8.3
2008	72	122.4 ± 18.8	145.6 ± 8.0	156.3 ± 9.0	130.9 ± 10.5	41	119.4 ± 18.7	144.3 ± 7.2	155.0 ± 9.0	129.9 ± 10.6	31	126.3 ± 18.5	147.3 ± 8.6	157.9 ± 8.8	132.2 ± 10.5
2009	99	124.2 ± 18.9	141.7 ± 10.4	157.6 ± 10.2	130.9 ± 9.9	45	**119.8 ± 21.5**	141.0 ± 10.4	155.2 ± 9.8	129.6 ± 11.0	54	**127.9 ± 15.6**	142.4 ± 10.4	160.2 ± 10.2	132.0 ± 8.8
2010	119	121.0 ± 20.8	142.9 ± 8.0	154.8 ± 7.5	127.5 ± 12.6	60	121.1 ± 19.9	143.2 ± 8.8	155.7 ± 7.3	126.9 ± 13.2	59	120.9 ± 21.8	142.7 ± 7.1	154.0 ± 7.6	128.2 ± 12.1
2011	183	128.5 ± 21.3	144.7 ± 8.6	156.5 ± 9.5	130.0 ± 10.8	93	126.4 ± 18.3	143.5 ± 7.8	155.5 ± 8.8	129.4 ± 4.4	90	130.7 ± 23.9	146.0 ± 9.2	157.6 ± 10.1	130.6 ± 12.5
2012	203	128.4 ± 21.8	145.6 ± 8.3	155.9 ± 8.3	132.4 ± 11.2	108	127.0 ± 18.2	144.7 ± 10.6	154.9 ± 7.8	132.5 ± 9.7	95	130.0 ± 25.3	146.5 ± 8.8	157.2 ± 8.8	132.3 ± 12.9
2013	239	132.2 ± 22.6	147.9 ± 7.9	158.4 ± 11.7	129.7 ± 12.1	129	131.7 ± 21.1	147.6 ± 7.2	158.2 ± 7.2	129.3 ± 11.3	110	132.8 ± 24.1	148.2 ± 8.6	158.7 ± 15.1	130.2 ± 13.1
2014	86	127.9 ± 20.8	144.8 ± 7.8	155.8 ± 8.1	131.4 ± 10.6	40	126.5 ± 18.4	143.8 ± 7.7	155.3 ± 7.7	130.2 ± 8.0	46	129.1 ± 22.9	145.6 ± 7.8	156.3 ± 8.4	132.5 ± 12.5
2015	95	120.9 ± 21.5	146.3 ± 9.3	155.9 ± 9.1	125.2 ± 12.7	42	116.5 ± 22.9	144.7 ± 10.6	154.1 ± 10.8	123.5 ± 14.4	53	124.4 ± 19.8	147.6 ± 8.0	157.4 ± 7.3	126.6 ± 11.2
2016	184	121.8 ± 21.4	144.0 ± 8.3	156.5 ± 8.7	125.1 ± 11.8	99	119.9 ± 19.2	143.7 ± 7.7	156.3 ± 8.1	124.0 ± 11.4	85	124.0 ± 23.6	144.5 ± 9.0	156.8 ± 9.4	126.4 ± 12.2
2017	269	123.3 ± 20.9	141.2 ± 9.2	151.8 ± 9.5	130.9 ± 11.8	118	**120.1 ± 18.9**	**139.8 ± 8.7**	150.5 ± 8.9	**129.0 ± 12.2**	151	**125.8 ± 22.2**	**142.3 ± 9.5**	152.8 ± 9.8	**132.3 ± 11.3**
2018	274	121.9 ± 20.0	143.6 ± 7.3	155.5 ± 7.8	131.7 ± 11.6	133	120.6 ± 19.9	143.0 ± 7.2	154.7 ± 7.9	131.2 ± 11.9	140	123.1 ± 20.2	144.1 ± 7.3	156.2 ± 7.8	132.2 ± 11.2
2019	250	124.7 ± 20.	141.9 ± 8.3	154.0 ± 8.9	130.8 ± 10.7	116	122.9 ± 18.9	**140.4 ± 8.6**	152.2 ± 9.2	130.2 ± 9.6	134	126.3 ± 21.3	**143.2 ± 7.8**	155.5 ± 8.3	131.3 ± 11.5

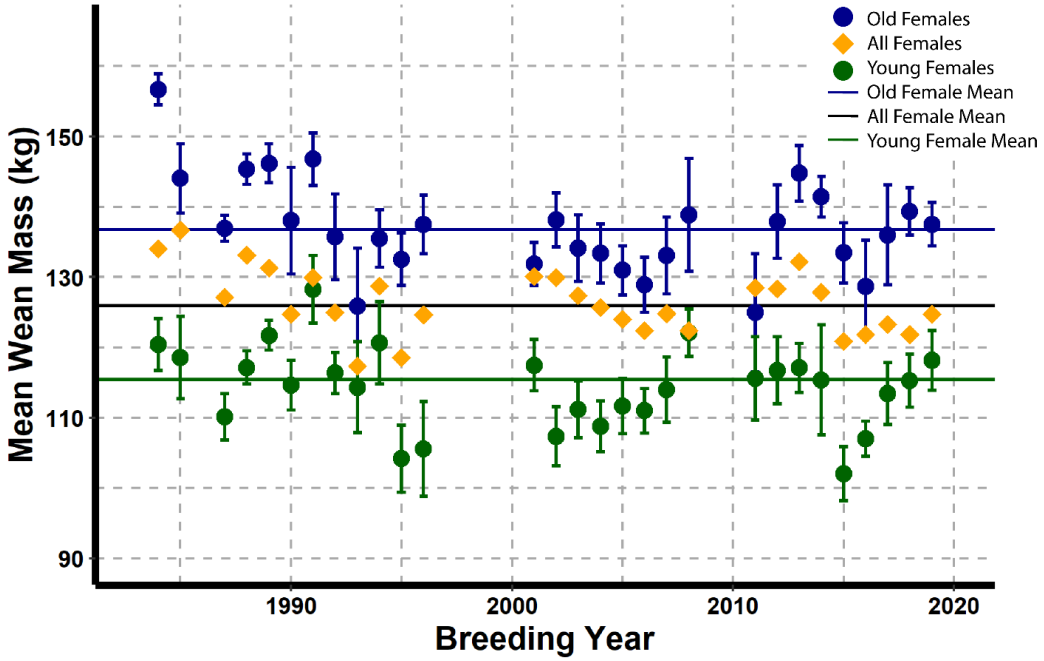

S3.10 - Average weaning masses of pups from moms of different age classes. Points in blue are the average weaning mass of females 9 years old or older. Green points represent average weaning mass of females 5 years of age or younger. Yellow points show the annual mean of all females. The means across all years are shown by solid blue, green, and black lines, respectively.

Table S3.11 – Average (± standard deviation) values of age and mass gain for adult females that returned during the breeding season in 2005-2019. These data exclude both skip breeding individuals and individuals that were lost at sea (# Bred indicates sample size for all calculated values).

Breed Year	# Deploy	# Bred	Age	Depart Mass (kg)	Arrival Mass (kg)	Arrival Mass Range (kg)	Mass Gain (kg)	% Mass Gain
2005	25	22	7.22± 1.99	270±23.9	545±14.7	473 - 630	275± 33.0	1.02±. 096
2006	25	19	8.45± 2.25	272±32.3	564±10.3	549 - 639	292± 21.4	1.09±. 165
2007	22	17	8.00± 2.53	282±37.2	567±16.8	486 - 624	258± 49.3	1.03±. 247
2008	20	15	8.56± 3.42	267±24.7	544±12.1	456 - 624	277± 30.0	1.04±. 090
2009	20	12	8.40± 2.41	279±45.2	567±26.6	474 - 619	288± 17.6	1.05±. 135
2010	7	6	6.67± 1.53	268±53.1	558±24.4	501 - 645	291± 40.4	1.14±. 392
2011	20	13	10.12 ±3.27	291±44.9	572±17.2	485 - 660	281± 38.7	0.99±. 200
2012	20	15	7.67± 2.29	275±27.4	560±12.9	466 - 657	285± 39.1	1.05±. 170
2013	22	17	7.33± 2.57	289±43.0	575±14.7	484 - 687	287± 27.7	1.01±. 153
2014	22	13	7.00± 2.00	286±24.8	597±12.5	542 - 680	311± 24.5	1.09±. 101
2015	20	10	8.50± 1.76	293±27.1	592±7.4	558 - 623	298± 19.7	1.03±. 141
2016	20	14	7.33± 2.15	285±47.2	565±14.8	467 - 638	280± 29.0	1.01±. 216
2017	20	13	8.00± 2.92	285±37.1	543±14.9	480 - 617	264± 28.4	0.95±. 133
2018	10	5	6.40± 0.89	260±28.4	526±21.1	467 - 579	265± 21.2	1.02±. 066
2019	14	9	7.50± 1.60	303±20.2	598±13.3	529 - 634	296± 23.7	0.98±. 061